DNA DAMAGE SIGNALING ORCHESTRATES SV40 CHROMATIN REPLICATION

By

Gregory A. Sowd

Dissertation

Submitted to the Faculty of the

Graduate School of Vanderbilt University

in partial fulfillment of the requirements

for the degree of

DOCTOR OF PHILOSOPHY

in

Biological Sciences

December, 2013

Nashville, Tennessee

Approved:

Katherine L. Friedman

David Cortez

Terence S. Dermody

Ellen H. Fanning

Ryoma Ohi

ACKNOWLEDGMENTS

I would first like to thank everyone who has supported me during my time as both a technician and as a graduate student. With regards to my scientific career, I am most indebted to two people: Ellen Fanning and Patricia Opresko. Both of them have been great friends to me as I have advanced as a scientist. Throughout my tenure as a graduate student at Vanderbilt Ellen has provided me with a tremendous amount of freedom of experimental direction and trust in my abilities as a scientist. Therefore, I have been allowed to grow academically, technically, as a mentor, and to have confidence in myself. Ellen's encouragement to try new techniques and give scientific talks has aided greatly aided my development. She has such creative ways of making things understandable, and I always enjoy her insight. Ellen has always provided me with enthusiastic aid as a mentor and her experience is invaluable to me. Our conversations are fun, and I am ecstatic and proud to have been her mentee.

Patty Opresko, my mentor as a technician at the University of Pittsburgh, showed me what it was to be to be a technically adept, troubleshooting, adaptable scientist. The way I was taken under her wing as a technician made me feel special. As a result of her mentorship, I came to graduate school ready for the challenges that would follow. Patty had demonstrated to me how to figure out what technique was appropriate and why I need to use said technique. Patty is a wonderful person, was/ still is a great mentor, and, like Ellen, is always there for me when I need help.

I would like to thank my committee for helping me during my graduate career. Kathy Friedman has been tremendously helpful as my committee Chair. Kathy helped me learn how to perform 2d gel electrophoresis and analyze the southern blots generated from those gels. Kathy's ability to ask thoughtful questions is admirable, and I am always thankful for her aid.

Dave Cortez has been an amazing source of knowledge and expertise during my graduate career. Dave is always willing to provide me resources or any technical aid for experiments. Furthermore, Dave has a critical eye that has been useful as I have navigated through graduate school. Due to both Dave and Ellen, I have been allowed to meet some titans of DNA repair and DNA replication. I cannot thank him and Ellen enough for this. Dave is an all around good guy whose dry sense of humor always makes me laugh. I am especially grateful to Dave for inviting Patty to Vanderbilt for a seminar. Familiar faces can make a world of a difference sometimes. Thank you Dave!

Ryoma (Puck) Ohi has been very accommodating as a committee member. Puck has been a pleasure to know and brings a much different scientific repertoire than myself. Due to this, Puck has been very useful because he has the ability to bring an outside opinion to the committee and might see things that I have overlooked. I always enjoy Puck's questions; they are always well meaning and useful. I am very appreciative of Puck for his aid throughout graduate school.

Terry Dermody was not just a member of my committee; he was a fantastic teacher to me. Chris Aiken and Terry taught what was by far my favorite class in graduate school, molecular virology. Terry is a bundle of energy and excitement, both of which always make me smile. His skill set and knowledge as both a medical doctor and principal investigator are exceptional. For some reason during committee meetings, Terry was always apologizing for asking questions pertaining to my research. I am grateful for those questions as it showed me he was interested in my research, which means a lot. Terry always has good intentions, and I have been privileged to have gotten to know him while at Vanderbilt.

I would like to thank the NIH, the Vanderbilt University biological sciences department, Vanderbilt University, Vanderbilt BRET, James Crowe for T32 grant

support, and the Vanderbilt University Medical Center for funding my research and education.

A great many of thanks goes out to my friends and family for their support. Thank you Mom and Dad for always telling me how proud you are of me and my efforts in graduate school. This has meant a lot to me. Both of my parents instilled a hard work ethic in me that I still follow to this day. My love for science comes from my mom. She set me on the right path when I was young. Thank you mom and dad for always being there for me.

My friends are the best. They always stick by me. Thank you lab mates for your conversations.

I would especially like to thank my undergraduate research assistants Nancy Li and Josh Eggold. Nancy and Josh are exceptional, detail oriented people. Both of them were a pleasure to mentor and watching them grow was/ has been a delight. Nancy is a positive all around good person, and I was so elated to have helped her. Josh is a very hard worker. He is technically excellent. It has been most enjoyable to get to know him and mentor him. Things in the Fanning lab are not the same when Nancy and Josh are not around. Thank you mentees!

Lastly, I would like to thank my wife Ashley. Ashley is always there for me. She brings a smile to my face every day and is my rock. She puts up with all my imperfections and has stuck with me no matter how tired or frustrating I am. I do not think I would have made it through graduate school as quickly without her love and ability to take care of me. Ashley is my greatest supporter and is always there for me. Thank you Ashley!

TABLE OF CONTENTS

Page

ACKNOWLEDGMENTS ii

LIST OF TABLES v

LIST OF FIGURES ix

LIST OF ABBREVIATIONS xi

Chapter

I. SIMIAN VIRUS 40: A PARADIGM FOR METAZOAN DNA TRANSACTIONS 1

- DNA replication: the duplication of genetic information 1
- Primate DNA replication: origins ready, set, fire 2
- DNA repair: safeguarding the genome 7
- DSB repair: strength in redundancy 10
  - NHEJ 11
  - MMEJ 15
  - 5' to 3' end resection: initiation of homology dependent repair 16
  - SSA 19
  - HR 19
- DNA damage signaling: big kinases for a complex job 21
- ATM: ataxia telangiectasia and beyond 22
- Replication stress: ATR and the S phase checkpoint 25
- The DNA damage checkpoint: a niche for small DNA tumor viruses 29
- Simian virus 40: elegantly small 31
- Large T antigen: the Swiss army knife of proteins 34
- SV40 chromatin replication: a platform for discovery 37
- SV40 DNA replication *in cellulo*: not as simple as expected 40
- Hypotheses for the role of DNA damage signaling during SV40 infection 43
- Experimental rationale and summary 45

II. ATM AND ATR ACTIVITIES MAINTAIN REPLICATION FORK INTEGRITY DURING SV40 CHROMATIN REPLICATION 47

- Introduction 47
- Results 49
  - SV40 chromatin replication activates DNA damage signaling 49
  - Inhibition of ATM disrupts viral DNA replication centers 57
  - Inhibition of ATM activity reduces the quantity and quality of viral replication products 59
  - ATM inhibition increases rolling circle DNA replication and strand invasion 64
  - Caffeine inhibits SV40 chromatin replication 67
  - DNA-PK_{cs} activity is dispensable for SV40 chromatin replication 69

Inhibition of ATR decreases SV40 DNA replication 69
Chk1 inhibition decreases viral DNA replication....72
Broken and/ or stalled forks accumulate in ATR inhibited SV40-infected cells....76
Chk1-inhibited cells amass broken and/ or stalled forks 79
DNA-PK_{cs}, ATM, and ATR activities can partially compensate for each other in SV40 DNA replication 82
Discussion 85
DNA damage signaling nucleates the assembly of SV40 replication centers 87
ATM signaling orchestrates reassembly of viral replication forks, reducing unidirectional replication forks 88
How does ATR-Chk1 signaling orchestrate SV40 replication fork convergence?....90
ATM, ATR, and DNA-PK_{cs}: Collaborating for genome maintenance....91

III. ATM AND ATR KINASES PROMOTE S PHASE ARREST DURING SV40 INFECTION....94

Introduction....94
Results....95
ATM kinase activity contributes to S phase arrest in the early phase of infection....95
ATR enforces S phase arrest during all phases of SV40 infection....97
Discussion....98
The SV40 pseudo-S phase: an ATM/ ATR collaboration....98

IV. ATM ACTIVITY INHIBITS DNA-PK_{CS} ACTIVATION AND LOCALIZATION TO VIRAL REPLICATION CENTERS DURING SV40 INFECTION....100

Introduction....100
Results....102
Viral DNA replication centers colocalize with homology directed repair....102
NHEJ proteins do not localize to Tag foci in SV40-infected cells....103
ATR inhibition does not disrupt viral DNA replication centers....110
Inhibition of ATM or ATR kinase activity increases DNA-PK activation....111
ATM kinase activity prevents DNA-PK activation at the viral replication centers....113
Discussion....117
ATM activation blocks DNA-PK_{cs} function at viral DNA replication centers....117

V. PERSPECTIVES AND FUTURE DIRECTIONS....120

Introduction....120
DNA damage signaling induction by viral DNA replication....121
The DNA damage checkpoint and SV40....122

ATR and ATM function: insights from a virus 124
Models for ATR and ATM prevention of replication-associated breaks 125
Viral replication centers: hubs of homology-directed DNA repair 129
Are ATM and ATR good drug targets for anti-virals and chemotherapeutics? 131

VI. MATERIALS AND METHODS 131

Cells and SV40 infection 134
WST-1 viability assay 134
Plasmids and transfection 134
Low molecular weight DNA extraction 135
DNA Isolation 136
Immunoblots 136
Immunofluorescence microscopy 137
Use of PIKK Inhibitors 138
Agarose gel electrophoresis 139
Southern blotting analysis 139
Statistics 140

Appendix

A. ATM AND ATR KINASE ACTIVITIES IMPEDE LINEAR PRODUCT FORMATION DURING SV40 DNA REPLICATION 141

B. ELICITATION OF SV40 PSEUDO-S PHASE IS NOT MEDIATED BY P21 DEGRADATION 147

C. SV40 LARGE T ANTIGEN IS PHOSPHORYLATED BY ATM AND ATR 151

REFERENCES 154

LIST OF TABLES

Table Page

1. DNA modifications stemming from endogenous and exogenous sources....8

2. Proteins sufficient to replicate SV40 genome *in vitro*....41

LIST OF FIGURES

Figure		Page
1	Eukaryotic replisome formation	3
2	Cellular DNA polymerization	5
3	Models of NHEJ and MMEJ	12
4	Homology-directed repair model	17
5	ATM DSB signaling	23
6	ATR DNA damage signaling	26
7	SV40 genome map	32
8	Large T antigen: master of viral DNA replication	35
9	Models of DNA polymerase function at the viral replication fork	39
10	SV40 chromatin replication results in DNA damage signaling	51
11	Viral replication centers co-localize with host DNA replication factors in SV40-infected BSC40 cells	53
12	Host DNA replication proteins co-localize with Tag in SV40-infected U2OS cells	55
13	ATM inhibition during viral DNA replication disrupts viral replication centers	58
14	Ku-55933 treatment during viral DNA replication increases aberrant DNA structures	60
15	Aberrant DNA structures accumulate in ATM-inhibited SV40-infected U2OS cells	63
16	ATM inhibition increases recombination and unidirectional replication	65
17	Caffeine inhibits ATM and ATR activities in SV40-infected BSC40 cells	68
18	ATM and ATR inhibition increases aberrant DNA product accumulation	70
19	DNA-PK_{cs} activity is dispensable in unperturbed SV40 infection	71
20	ATRi inhibits ATR activity in SV40-infected BSC40 cells	73

Figure Page

21 ATR is crucial for SV40 chromatin replication 74

22 ATR is needed for efficient viral DNA replication in U2OS cells....75

23 Chk1 is crucial for SV40 DNA replication *in cellulo*....77

24 ATR or Chk1 inhibition results in fork stalling and breakage of converging forks 78

25 ATR inhibition results in replication fork stalling and breakage....80

26 ATM, ATR, and DNA-PK_{cs} have partially overlapping functions in SV40 DNA replication 84

27 Model of ATM and ATR functions in SV40 DNA replication....86

28 ATM and ATR contribute to S phase arrest during SV40 infection in BSC40 cells 96

29 SV40 DNA replication centers colocalize with HR proteins 104

30 BLM colocalization with Tag correlates with SV40 DNA replication....105

31 DNA-PK components are stable throughout SV40 infection....107

32 Factors that promote NHEJ do not co-localize with Tag in SV40-infected BSC40 cells 108

33 NHEJ proteins are not localized to viral replication centers in SV40-infected U2OS cells....109

34 Unlike Ku-55933, the presence of ATRi does not affect viral DNA replication centers....112

35 ATM inhibition affects the localization of DNA repair proteins during SV40 chromatin replication 115

36 ATM or ATR inhibition increases unidirectional replication forks and large linear viral replication products 143

37 p21 is not induced by SV40 infection 149

38 ATM and ATR phosphorylate residue S120 of SV40 Tag....152

LIST OF ABBREVIATIONS

9-1-1 ..... Rad9-Hus1-Rad1

ATM ..... Ataxia telangiectasia-mutated

ATMIN ..... ATM interactor

ATR ..... ATM and Rad3-related

ATRIP ..... ATR-interacting protein

BER ..... Base excision repair

BKV ..... BK virus

BLM ..... Bloom syndrome helicase

bps ..... Basepairs

Brca2 ..... Breast cancer associated gene 2

CDK ..... Cyclin dependent kinase

cm ..... Centimeter

CMG ..... Cdc45-MCM(2-7)-GINS

CO_2 ..... Carbon dioxide

CtIP ..... CtBP-interacting protein

°C ..... Degrees Celsius

D-loop ..... displacement loop

DMEM ..... Dulbecco's modified Eagle's medium

DMSO ..... Dimethyl sulfoxide

DNA ..... Deoxyribonucleic acid

DNA-PK_{cs} ..... DNA dependent protein kinase catalytic subunit

dHJ ..... Double Holliday junction

DSB ..... Double strand breaks

dsDNA ..... Double stranded DNA

EDTA..... Ethylenediaminetetraacetic Acid

EdU ..... 5-ethynyl-2'-deoxyuridine

γH2AX H2AX pS139

HPV.....Human papillomavirus

HR.....Homologous recombination

IC_{50} ..... Half maximal inhibitory concentration

ICL ..... Interstrand crosslink repair

JCV .....JC virus

kb ..... Kilobases

K_i .....Inhibitor constant

Ku..... Ku70/ Ku80 heterodimer

mg ..... Milligram

mL .....Milliliter

mM .....Millimolar

µg .....Microgram

µL ..... Microliter

µM ..... Micromolar

MCV ..... Merkel cell virus

MDC1 ..... Mediator of checkpoint1

MMEJ ..... Microhomology-mediated end joining

MMR .....Mismatch repair

MRN Mre11-Rad50-Nbs1

NaCl ..... Sodium chloride

NCS ..... Neocarzinostatin

ng ..... Nanogram

NER ..... Nucleotide excision repair

NHEJ.....Non-homologous end joining

OBD ..... Origin binding domain

ORC .....Origin recognition complex

Ori ..... Origin of replication

PARP1 ..... Poly-ADP polymerase 1

PARP2 ..... Poly-ADP polymerase 2

PARylation ..... Poly-ADP-ribosylation

PBS.....Phosphate buffered saline

PIKK.....PI3K-related kinase

PML.....Progressive multifocal leukoencephalopathy

PVAN .....Polyomavirus-associated nephropathy

Rb ..... Retinoblastoma protein

RFC.....Replication factor C

RMI .....RecQ Mediated Genome Instability

RNA .....Ribonucleic acid

RPA.....Replication protein A

RS-SCID .....Radiosensitive-severe combined immunodeficiency disorder

SDS.....Sodium dodecyl sulfate

SDSA .....Synthesis dependent strand annealing

SSA.....Single-strand annealing

SSB..... Single strand break

ssDNA.....Single stranded DNA

SV40 ..... Simian virus 40

Tag.....Large T antigen

TBS .....Tris buffered saline

Tris .....Tris-(hydroxymethyl)-aminomethane

U ..... Unit

UV ..... Ultraviolet light

V.....Volt

VP2/3 ..... VP2 or VP3

xg .....Times gravity

CHAPTER I

SIMIAN VIRUS 40: A PARADIGM FOR METAZOAN DNA TRANSACTIONS

DNA replication: the duplication of genetic information

To facilitate passage of genetic information from generation to generation, cellular DNA must be duplicated once during the S phase of each cell cycle. The process of DNA replication takes place in multiple steps. First, the origin of replication (ori), an element of the DNA, is bound by a complex of proteins that mark origins to be replicated. The protein-bound origin then recruits additional replication licensing factors creating a pre-replication complex that melts a small region of the DNA. The initial melting of the origin allows a DNA helicase to unwind the double stranded DNA (dsDNA) duplex into single stranded DNA (ssDNA) thereby exposing the template bases of the DNA. A complementary RNA primer is synthesized in the 5' to 3' direction onto the exposed ssDNA by a primase creating a RNA/DNA heteroduplex. The 3' hydroxyl group of the RNA primer is then extended by DNA polymerases utilizing deoxyribonucleoside triphosphates to synthesize a nascent double strand DNA (dsDNA). Torsional stress resulting from the unwinding of the DNA by the helicase is removed by type I topoisomerases, enzymes that transiently nick one strand of DNA and pass the second strand through the nick. The complex of proteins that collectively replicate DNA is termed the replisome. Replisomes moving away from the origin eventually converge with a second replisome replicating in the opposing direction, creating two identical copies of DNA, each containing a template and nascent strand. The fully replicated DNA is entangled or knotted upon replisome convergence and is subsequently untangled by

type II topoisomerases in a process termed decatenation. Thus, DNA replication takes one DNA template and generates two identical copies of the template DNA.

Primate DNA replication: origins ready, set, fire

Control of DNA replication timing and fidelity is essential. One duplication of the genomic content occurs during each S phase of the cell cycle through an ordered series of events. During late M or early G1 phases, cellular origins of DNA replication are bound by the origin recognition complex (ORC) (Figure 1A) (Mechali, 2010). Binding of the ORC heterohexamer recruits cdc6 and cdt1 to replication origins (Figure 1B, C) (Bell and Dutta, 2002). A pre-replication complex is finally formed when the MCM (2-7) heterohexamer ATPase is loaded at the origin bound by ORC, cdc6, and cdt1 (Bell et al., 2002) (Figure 1C). After the MCM complex is bound, cdt1 and cdc6 leave the complex (Figure 1D, E). To prevent reloading of MCM (2-7) onto ORC and re-replication of the genome during the subsequent phases of the cell cycle, cdt1 is either degraded or sequestered by its inhibitor geminin (Masai, Matsumoto et al., 2010) (Figure 1D).

At the G1 to S phase transition, retinoblastoma (Rb) family proteins are degraded to release E2F family transcription factors that promote the transcription of several critical S phase proteins including cdc45, ribonucleotide reductase, and DNA polymerases (Cam and Dynlacht, 2003). The subsequent high levels of cyclin dependent kinase (CDK) and cdc7-dbf4 kinase activities that propel the G1 to S transition result in the binding of cdc45 and the GINS heterotetramer to the pre-replication complex on the origin (Figure 1F) creating an active cdc45-MCM(2-7)-GINS (CMG) helicase (Masai et al., 2010). Furthermore, phosphorylation events catalyzed by CDK and cdc7-dbf4 promote further binding of several replication factors including

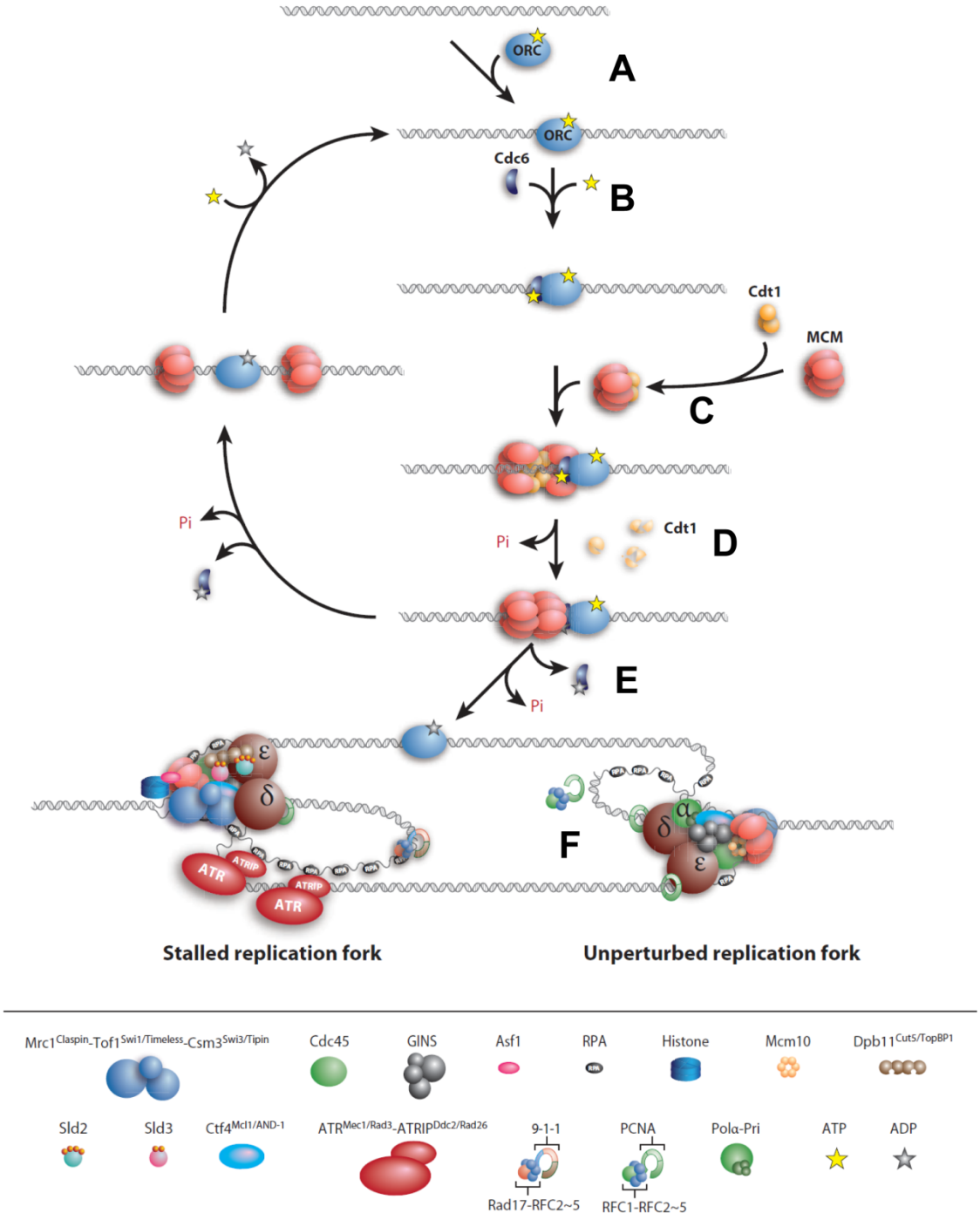

Figure 1. Eukaryotic replisome formation.
(A) Cellular oris are bound by ORC. (B, C) Cdc6 binds to ORC and recruits Cdt1 and MCM2-7. (D, E) Cdt1 and Cdc6 leave the pre-replication complex bound to the origin. (F) Phosphorylation of the pre-replication complex promotes binding of Cdc45, GINS, and other replisome factors. Adapted from Masai et al., 2010. Annu Rev Biochem. 79: 89-130.

TopBP1, CTF-4/AND-1, timeless, tipin, and MCM10 that link the CMG helicase to polymerase α/primase and polymerase ε (Figure 1F) (Masai et al., 2010).

The culmination of these biochemical events creates a fully functional replisome containing a multitude of activities at the ori. The CMG helicase translocates 3' to 5' along ssDNA to unwind DNA (Figure 2A) (Kang, Galal et al., 2012). Following unwinding, the ssDNA binding protein replication protein A (RPA) binds to the exposed ssDNA and protects it from endonucleolytic digestion by nucleases (Figure 2A). In addition, the RPA bound ssDNA prevents reannealing of unwound DNA behind the helicase, thereby presenting the template ssDNA for DNA polymerase α/primase to synthesize an RNA primer and initial nascent DNA (Figure 2B) (Waga and Stillman, 1998). High-fidelity, processive DNA synthesis is performed by DNA polymerases ε and δ on the leading and lagging strands, respectively (Figure 2C) (Pursell and Kunkel, 2008; Kunkel and Burgers, 2008). The RNA primer and DNA synthesized by polymerase α/primase are removed from nascent DNA by the combined strand displacement activity of polymerase δ and 5' ssDNA flap endonucleolytic activity of FEN1 (Figure 2C) (Balakrishnan and Bambara, 2011). The RNA-free nascent DNA strands are then ligated together by DNA ligase I and untangled by topoisomerase I and topoisomerase IIα.

Another hurdle that the replisome must overcome is the higher-order compacted structure of eukaryotic genomes termed chromatin. To compress the large eukaryotic genome into chromatin, DNA is wrapped around proteinaceous histone octamers composed of two molecules each of histones H2A, H2AB, H3, and H4 or their respective histone variants (Ruthenburg, Li et al., 2007). The histones and their post-translational modifications must also be replicated during DNA replication. For this function, chromatin remodeling and modifying factors that remove and replace histones are also contained in the replisome. Thus, a functional replisome is capable of creating

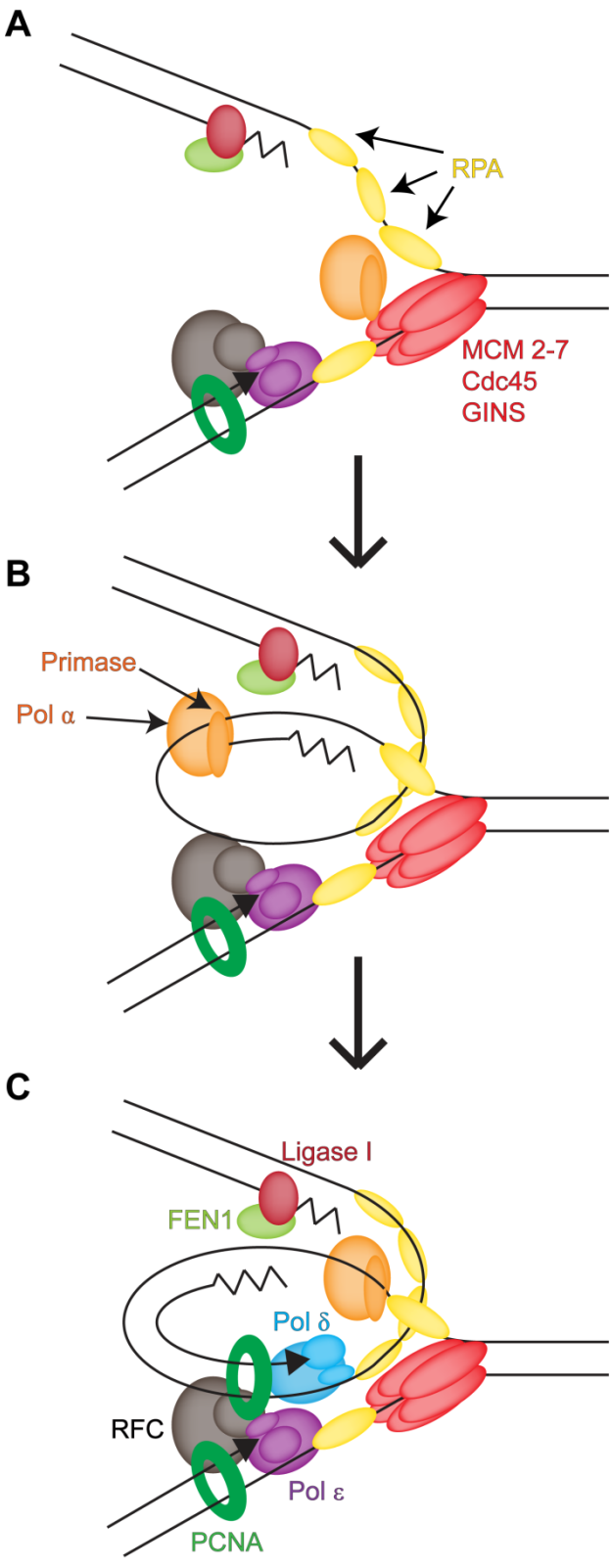
A
RPA
MCM 2-7
Cdc45
GINS
B
Primase
Pol α
C
Ligase I
FEN1
Pol δ
RFC
Pol ε
PCNA

Figure 2.

Figure 2. Cellular DNA polymerization.
(A) CMG unwinds DNA and loads RPA onto ssDNA. (B) Bound RPA on the lagging strand is removed from the ssDNA by CMG and polymerase α / primase creates an RNA (zig zag) / DNA (smooth line) primer. (C) Polymerase α / primase is displaced by RFC. RFC loads PCNA at the ssDNA / dsDNA junction. Polymerase δ binds to PCNA at the ssDNA / dsDNA junction and polymerizes the lagging strand. On the leading strand Polymerase ε synthesizes the nascent DNA.

continuous strands of chromatinized DNA that are topologically separated from one another.

DNA repair: safeguarding the genome

Although replicative DNA polymerases exhibit extreme accuracy (around 1 base substitution per 10^6 to 10^8 basepairs (bps) (Kunkel, 2004)), DNA is constantly subject to damage from both endogenous and exogenous sources with several consequences. Various modifications to DNA including base adducts, DNA inter- and intra-strand crosslinks, and both single and double strand breaks (SSB and DSB, respectively) (Table 1) (Ciccia and Elledge, 2010) are repaired by a multitude of mechanisms that prevent accumulation of mutations and chromosome translocations during DNA replication. Thus, DNA repair provides a safety net to prevent adverse cellular consequences, such as cellular senescence, cell death, or unregulated cell division, that are associated with increased mutation frequency in the genome.

A general theme in DNA repair is that DNA damage is detected by protein sensors. Each sensor directs repair towards specific pathways that are able to remove or correct the type of damage on the DNA. Although some proteins of a pathway or an entire pathway can be used in the repair of multiple types of DNA damage, DNA repair can be divided into six major branches: mismatch repair (MMR), base excision repair (BER), nucleotide excision repair (NER), SSB repair, interstrand crosslink (ICL) repair, and DSB repair. MMR removes DNA replication associated errors. Since polymerase α lacks proofreading exonuclease activity and polymerizes DNA at a much lower fidelity than do polymerases ε and δ, MMR provides a backup mechanism to remove errors created by this polymerase (Crouse, 2010). This pathway is estimated to increase DNA replication fidelity by orders of magnitude to around 1 base substitution per 10^{10} bps

Table 1: DNA modifications stemming from endogenous and exogenous sources
(Adapted from Ciccia et al., (2010). Mol Cell. 40: 179-204.)

Endogenous DNA Damage	DNA Lesions Generated	Number Lesions/Cell/Day	
Depurination	AP site	10000[a]	
Cytosine deamination	Base transition	100–500[a]	
SAM-induced methylation	3meA	600[a]	
	7meG	4000[a]	
	O^6meG	10–30[b]	
Oxidation	8oxoG	400–1500[c]	
Exogenous DNA Damage	**Dose Exposure (mSv)**	**DNA Lesions Generated**	**Estimated Number Lesions/Cell**
Peak hr sunlight	—	Pyrimidine dimers, (6–4) photoproducts	100,000/day[d]
Cigarette smoke	—	aromatic DNA adducts	45–1029[e]
Chest X-rays	0.02[f,g,h]	DSBs	0.0008[i]
Dental X-rays	0.005[f,g,h]	DSBs	0.0002[i]
Mammography	0.4[f,g,h]	DSBs	0.016[i]
Body CT	7[f]	DSBs	0.28[i]
Head CT	2[f,g]	DSBs	0.08[i]
Coronary angioplasty	22[h]	DSBs	0.88[i]
Tumor PET scan (^{18}F)	10[h]	DSBs	0.4[i]
^{131}I treatment	70–150[h]	DSBs	2.8–6[i]
External beam therapy	1800–2000[j]	DSBs	72–80
Airline travel	0.005/hr[f]	DSBs	0.0002/hr[j]
Space mission (60 days)	50[k]	DSBs	2[i]
Chernobyl accident	300[l]	DSBs	12[i]
Hiroshima and Nagasaki atomic bombs	5–4000[k]	DSBs	0.2–160[i]

Type and number of DNA lesions are indicated. The number of lesions/cell has been estimated as described.
[a] Lindahl and Barnes (2000)
[b] Rydberg and Lindahl (1982)
[c] Klungland et al. (1999)
[d] Hoeijmakers (2009)

(Crouse, 2010) and is thus crucial for the prevention of nucleotide misincorporation by DNA polymerases.

On the DNA, base modifications can result from exogenous agents such as methyl methanesulfonate or reactive oxygen species emitted from the mitochondria. These lesions are removed by BER. The oxidized base modification 8-oxo-dG has been estimated to occur at numbers ranging from 180 (Iyama and Wilson, 2013) to 400-1500 (Ciccia et al., 2010) lesions per cell per day (Table 1). Such base lesions can be removed through the action of one of several DNA glycosylases. In doing so, BER leaves abasic sites in the DNA that are subsequently repaired by the combined actions of AP endonuclease, a DNA lyase, DNA polymerase β, and DNA ligase III (Iyama et al., 2013). Failure to repair base adducts by BER can result in nucleotide misincorporation across from the modified base or increased polymerase stalling. Polymerase stalling can be particularly toxic as this event can coincide with replication fork breakage which is a DSB that is quite toxic to the cell.

NER repairs bulkier DNA lesions that distort the DNA helix. These lesions are exemplified by intrastrand crosslinked thymidine dimers introduced by ultraviolet light (UV) irradiation. Like modified bases, bulky nucleotide lesions need to be excised from the DNA and repaired. Like the base modifications repaired by BER, these bulkier adducts can also arrest the DNA polymerase or cause nucleotide misincorporation across from the crosslinked DNA. Thus, it is crucial that NER repairs these lesions prior to and during DNA replication. NER can be elicited by two pathways. The first, global genome NER, utilizes proteins that recognize the lesion in dsDNA, whereas the second utilizes stalling of transcriptional machinery to activate NER, termed transcription-coupled NER (Hoeijmakers, 2009). Both pathways funnel repair toward a mechanism in which the DNA around the lesion is unwound by the TFIIH DNA helicase. The bubble is then cleaved by ERCC1-XPF and XPG endonucleases leading to the selective removal

of the DNA strand containing the intrastrand crosslink (Hoeijmakers, 2009). The resulting gap is filled by a DNA polymerase and the DNA is ligated. Null or inactivating mutations to proteins that contribute to NER causes the UV sensitivity disorder xeroderma pigmentosum. This disorder is characterized by high rates of skin cancer and developmental abnormalities.

An important byproduct of both the BER and NER pathways is the generation of nicked or gapped DNA. This nicked or gapped DNA, a type of SSB, is actually the substrate for which SSB repair is elicited. The SSB is initially recognized by poly-ADP polymerase 1 (PARP1) and poly-ADP polymerase 2 (PARP2). PARP1 and PARP2 subsequently ribosylate numerous substrates at the SSB including themselves and nearby histones in a process termed poly-ADP-ribosylation (PARylation) (Rouleau, Patel et al., 2010). PARylation recruits factors including polymerases, nucleases, and ligases that can fill the DNA gap and repair the SSB (Rouleau et al., 2010). Failure to repair a SSB can lead to the conversion of the SSB at the replication fork to a DSB when the replicative helicase unwinds the SSB. This mechanism of DSB formation is similar to that observed when the replisome encounters a topoisomerase I cleavage complex caused by the topoisomerase inhibitor camptothecin, a common chemotherapeutic agent. Furthermore, SSB repair is currently the target of several recent novel chemotherapeutics that target the initial step of the pathway, PARylation (Wang, Wang et al., 2012). Hence, this pathway is highly relevant to cancer.

DSB repair: strength in redundancy

Unlike the aforementioned pathways, DSB repair cannot be categorized into one catch-all pathway. Multiple mechanisms are able to repair this type of damage. This likely results from the numerous distinct ways that both strands of the DNA double helix

can be broken. Several common cancer therapies that induce DSBs include ionizing radiation (X and gamma rays), topoisomerase I inhibitors (e.g., camptothecin), or topoisomerase II inhibitors (e.g., etoposide and teniposide). Additionally, DNA replication itself can create a DSB when the replisome replicates through a SSB, with the separation of the DNA into individual strands generating an one-ended DSB. DSBs are an extremely toxic type of damage to the cells as they can result in many types of mutation and chromosomal translocations. Therefore to combat this type of damage, metazoan cells have evolved many mechanisms to repair DSBs.

Non-homologous end joining (NHEJ), homologous recombination (HR), microhomology-mediated end joining (MMEJ), and single-strand annealing (SSA) are independent pathways used by primate cells to repair DSBs (Ciccia et al., 2010). Despite having many DSB repair pathways, not each DSB repair pathway is created equal, with different pathways varying in repair efficiency and accuracy. Furthermore, the preference for one pathway or another is tightly regulated by cell cycle dependent post translational modifications, chromatin state, and DNA substrate preferences. Thus, multiple complex factors influence the outcome of repair and which pathway is used to repair a given DSB.

NHEJ

NHEJ can be considered the work horse of DSB repair and functions to directly fuse the broken DNA ends (Figure 3) (Neal and Meek, 2011). Although NHEJ is more prone to errors, often resulting in substitutions, small insertions, or small deletions at the site of DNA breakage, this pathway repairs the majority of DSBs during G1 and G2 and is active throughout the cell cycle (Shibata, Conrad et al., 2011; Jeggo, Geuting et al., 2011). Upon DSB formation, the abundant Ku70/Ku80 heterodimer (Ku) recognizes the broken DNA end with high affinity. Binding of Ku protects the DNA end from processing

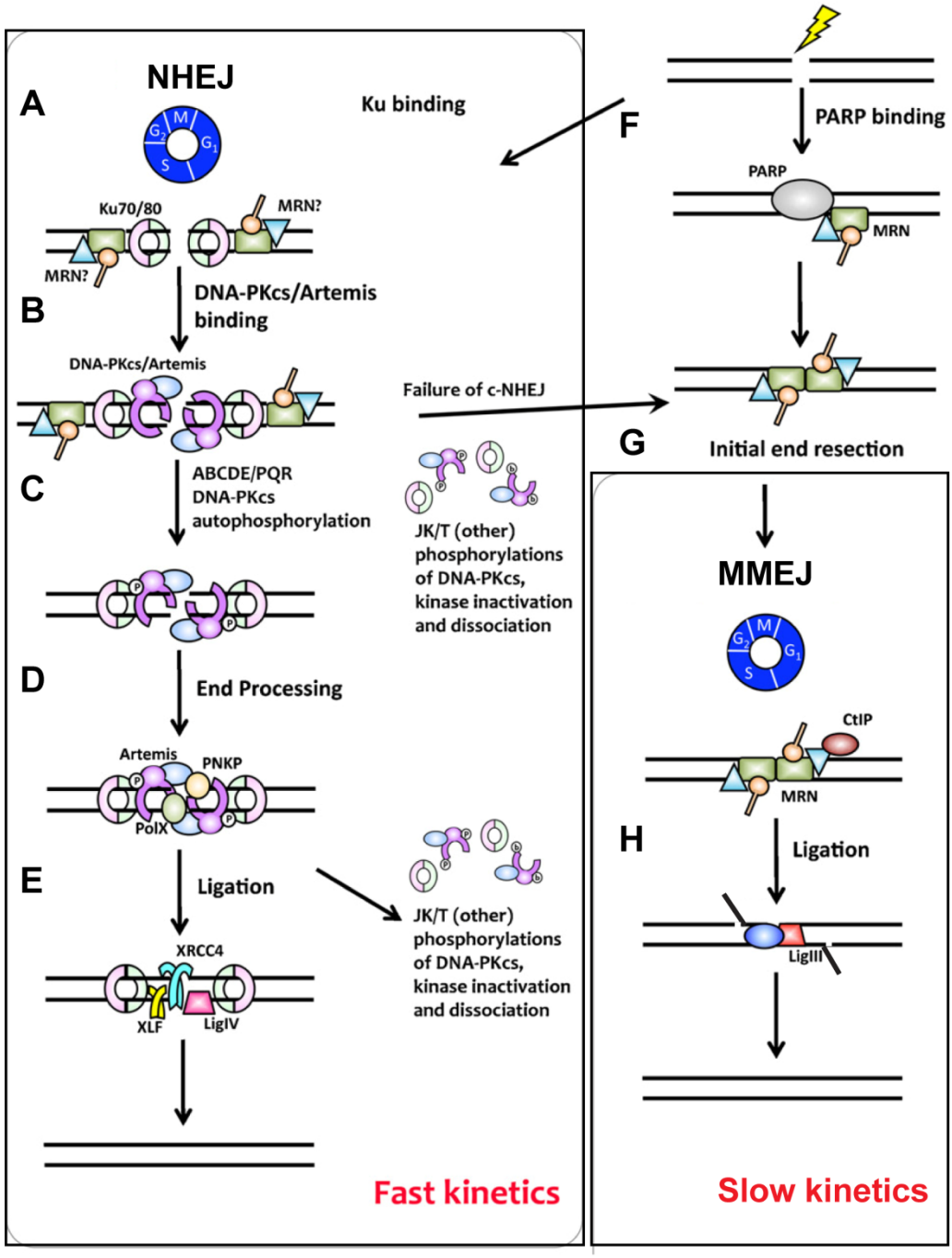
NHEJ
A
Ku binding
Ku70/80
MRN?
MRN?
B
DNA-PKcs/Artemis binding
DNA-PKcs/Artemis
C
ABCDE/PQR DNA-PKcs autophosphorylation
D
End Processing
Artemis
PNKP
PolX
E
Ligation
XRCC4
XLF
LigIV
Failure of c-NHEJ
JK/T (other) phosphorylations of DNA-PKcs, kinase inactivation and dissociation
JK/T (other) phosphorylations of DNA-PKcs, kinase inactivation and dissociation
Fast kinetics
F
PARP binding
PARP
MRN
G
Initial end resection
MMEJ
CtIP
MRN
H
Ligation
LigIII
Slow kinetics

Figure 3.

Figure 3. Models of NHEJ and MMEJ.
(A) Ku binds to termini of DSB protecting them from nuclease digestion. (B) DNA-PK_{cs} binds to Ku80 and Ku moves away from DSB termini. (C) The kinase activity of DNA-PK_{cs} auto-phosphorylates itself thereby exposing DSB termini. (D) DSB ends are processed to remove base adducts by the 5' to 3' exonuclease Artemis and lyase activity of Ku. DNA polymerases lambda and mu (Pol X) fill in any gaps that are created. (E) XLF, XRCC4, and Ligase VI ligate the broken DNA repairing the DSB. (F) PARP1 or PARP2 promote PARylation of chromatin at DSB termini enhancing MRN binding to the end of the DSB. The nuclease activities of Mre11 begin 5' to 3' end resection. (G) CtIP binds to MRN promoting more processive 5' to 3' end resection creating a 3' tail at the DSB termini. (H) Small tracts of complementary sequence are annealed. Unannealed DNA is cleaved by nucleases, and DNA is ligated by Ligase III. Adapted from Neal et al., 2011. Mutat Res. 711: 73-86.

by nucleases (Figure 3A) and recruits DNA-dependent protein kinase catalytic subunit (DNA-PK_{cs}), a member of the PI3K-related kinase (PIKK) family. The binding of DNA-PK_{cs} to Ku forms the DNA-PK holoenzyme and results in the movement of Ku away from the DSB ends allowing DNA-PK_{cs} to contact them (Figure 3B) (Meek, Dang et al., 2008). Importantly, Ku binding to DNA-PK_{cs} activates the kinase activity of DNA-PK_{cs}, thereby promoting NHEJ (Figure 3B) (Meek et al., 2008).

DNA-PK_{cs} phosphorylates a multitude of substrates at the site of the DSB and is essential for NHEJ (Meek et al., 2008). DNA-PK_{cs} also is the primary target of its kinase activity (Meek, Douglas et al., 2007; Neal, Dang et al., 2011). With its kinase activity, DNA-PK determines whether NHEJ or another pathway repairs the DSB (Neal et al., 2011). This function is thought to occur through the auto-phosphorylation of multiple patches of residues on DNA-PK_{cs} in trans that results in distinct outcomes of repair (Weterings and Chen, 2007; Neal et al., 2011). The best characterized of these autophosphorylation patches on DNA-PK_{cs} is the ABCDE cluster (residues from 2609-2657 of DNA-PK_{cs}) and PQR cluster (residues lying around 2023-2056 of DNA-PK_{cs}) (Chen, Chan et al., 2005; Chen, Uematsu et al., 2007; Meek et al., 2007). The ABCDE cluster is a substrate of ATM, ATR, and DNA-PK_{cs} (Chen et al., 2007; Meek et al., 2007; Yajima, Lee et al., 2006). Phosphorylation of DNA-PK_{cs} at the ABCDE cluster causes a conformational change in DNA-PK that allows DNA end processing by endo- and exonucleases such as Artemis (Figure 3C) (Uematsu, Weterings et al., 2007; Meek et al., 2007; Shibata et al., 2011). On the other hand, the PQR cluster is phosphorylated only by DNA-PK_{cs} *in vivo* (Chen et al., 2007). Auto-phosphorylation at the PQR cluster is hypothesized to protect the broken DNA end from nucleolytic processing (Uematsu et al., 2007; Meek et al., 2007). Thus, DNA-PK is thought to function as a gatekeeper to the termini of DSBs.

After DNA-PK activation, the break can be processed by Ku, polynucleotide kinase/ phosphatase, and the Artemis endonuclease to remove modifications from the break site (Figure 3D) (Neal et al., 2011). Gaps in the DNA left after end processing are then filled utilizing DNA polymerases lambda and mu (Figure 3D), and the DNA is ligated together by XRCC4/ligase VI with the aid of NHEJ accessory factor XLF (Figure 3E) (Neal et al., 2011). Like other DNA repair pathways, mutations inactivating components of NHEJ results in human disease, with mutations to DNA-PK_{cs}, XLF, Artemis, or XRCC4/ligase VI causing radiosensitive-severe combined immunodeficiency disorder (RS-SCID) (Goodarzi and Jeggo, 2013). The SCID phenotype is a result of the failure of essential functions of the NHEJ pathway in V-D-J recombination used to re-arrange antigen receptor genes. Collectively, NHEJ is crucial to the repair of DSBs.

MMEJ

During G1, an alternative pathway to NHEJ can also be used to repair DSBs and is termed MMEJ, also known as alternative-NHEJ. MMEJ functions primarily in the absence of Ku, is even more error prone than NHEJ, and can generate large deletions at the site of breakage (Goodarzi et al., 2013). Although much less is known about the proteins contributing to MMEJ, a subset of proteins that contribute to this pathway have been defined. Similar to SSB repair, PARP1 and PARP2 can recognize and PARylate DSBs (Figure 3F). PARylation at the DSB is hypothesized to promote decomposition of chromatin at the DSB site (Ciccia et al., 2010) and contribute to the recruitment of a complex containing Mre11-Rad50-Nbs1 (MRN) and CtBP-interacting protein (CtIP) to break sites (Figure 3G) (Haince, McDonald et al., 2008). Upon MRN/CtIP binding to the DSB, the nuclease activities of this complex digest the 5' end of the broken DNA (Stracker and Petrini, 2011), creating a short 3' tail in a process termed end resection (Figure 3G). Using unknown factors, the 3' tail is then annealed using small regions of

homology, creating 5' flaps. The un-annealed 5' flaps are excised from the DNA, and the annealed regions are ligated by ligase III to repair the DSB (Figure 3H) (Goodarzi et al., 2013). This pathway is seldom used by the cell when NHEJ is functional and can generate large or small deletions due to the excision of the 5' flaps. Therefore, the circumstances in which MMEJ is used in favor of NHEJ are not well understood.

5' to 3' end resection: initiation of homology dependent repair

Unlike NHEJ and MMEJ, homology-directed repair by HR and SSA requires an intact sister chromatid to repair DSBs and is therefore only active during the S and G2 phases of the cell cycle. The ability of HR and SSA to utilize the replicated sister chromatid to repair DSBs endows these pathways with the unique ability to repair one-ended breaks created by broken DNA replication forks. Homology-directed repair commences with the MRN/CtIP complex binding to the DSB, a process that may be linked to PARylation at the DSB by PARP1 and PARP2 (Figure 4A) (Haince et al., 2008). Processive 5' to 3' end resection that generates long 3' tails at the site of the DSB is a strict requirement for HR and SSA and is limited to S and G2 phases by CDK-dependent phosphorylation of CtIP at multiple residues (Sartori, Lukas et al., 2007; Huertas and Jackson, 2009; Yun and Hiom, 2009). The phosphorylation of CtIP residue 847 by S phase CDK/Cyclin kinase activities increases the nuclease activities of the MRN/CtIP complex, thereby restricting processive end resection to S and G2 (Figure 4B) (Huertas et al., 2009). Initiation of resection *in vitro* utilizes the endonuclease activity of Mre11 to nick the DNA, creating a substrate for the 3' to 5' exonuclease of Mre11 (Garcia, Phelps et al., 2011). This initial 3' tail can be resected more vigorously by Exo1, a 5' to 3' exonculease, or the combined actions of the Bloom syndrome helicase (BLM) and endonuclease Dna2, which can cleave 5' flaps (Figure 4C)

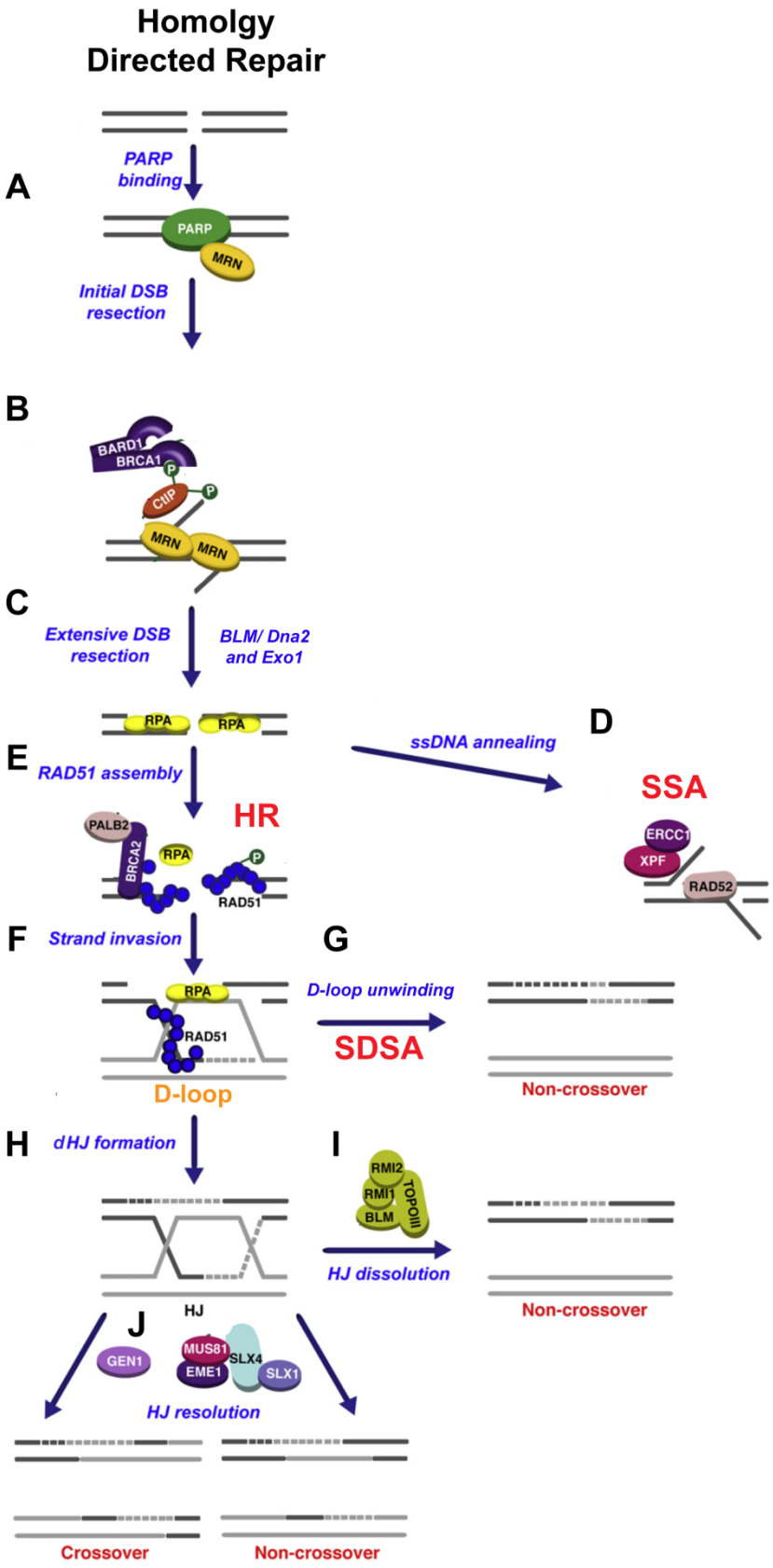
Homolgy
Directed Repair
A
PARP
binding
PARP
MRN
Initial DSB
resection
B
BARD1
BRCA1
P
CHIP
P
MRN
MRN
C
Extensive DSB
resection
BLM/ Dna2
and Exo1
RPA
RPA
D
ssDNA annealing
SSA
ERCC1
XPF
RAD52
E
RAD51 assembly
HR
PALB2
BRCA2
RPA
P
RAD51
F
Strand invasion
G
RPA
RAD51
D-loop
D-loop unwinding
SDSA
Non-crossover
H
dHJ formation
I
RMI2
RMI1
BLM
TOPOIII
HJ dissolution
HJ
Non-crossover
J
GEN1
MUS81
EME1
SLX4
SLX1
HJ resolution
Crossover
Non-crossover

Figure 4.

Figure 4. Homology-directed repair model.
(A) PARylation at DSB termini enhanced MRN binding. Initial 5' to 3' end resection. (B) The CtIP/ MRN complex processively digests 5' strand of DSB creating a short 3' tail. The interaction of Brca1 and CtIP during S and G2 phases may enhance end resection processivity by CtIP/MRN (Chapman, Taylor et al., 2012). (C) The 5' to 3' exonuclease Exo1 and BLM/ Dna2 complex promote the generation of lengthy 3' ssDNA tails at the DSB. RPA protects 3' tails from nucleases. (D) Rad52 binds to RPA bound ssDNA and anneals complementary DNA sequences thereby displacing RPA. Non-complementary 3' tails are excised and the DNA is ligated by ligase III. (E) Brca2 displaces RPA by loading Rad51 onto 3' tails. (F) Rad51 searches for homologous sequence and promotes strand invasion. (G) SDSA - DNA polymerase(s) extend the invaded strand. DNA helicases or dsDNA translocases including BLM (Bachrati, Borts et al., 2006), WRN (Opresko, Sowd et al., 2009), or Rad54 (Bugreev, Hanaoka et al., 2007) are able to processively resolve the D-loop releasing the strand invasion event. Complementary sequences of the newly polymerized DNA is annealed by Rad52. The gaps are filled by polymerases, and the DNA is ligated. (H, I, J) HR - (H) Rad52 anneals non-invaded 3' tail to the displaced strand of the D-loop. Extension and ligation of the annealed strands creates a dHJ. (I) dHJ dissolution by BTR resulting in exclusively non-crossover repair products. (J) dHJ resolution by Mus81/Eme1/Slx4/Slx1 or Gen1 generates a mix of both crossover and non-crossover repaired products. Adapted from Ciccia et al., 2010. Mol Cell. 40: 179-204.

(Nimonkar, Genschel et al., 2011). The combined actions of all these nucleases create an extensively resected 3' tail that is the substrate for homology-directed repair.

SSA

Following end resection, either HR or SSA can commence. As 5' to 3' end resection progresses, the exposed 3' ssDNA tail is bound by the ssDNA binding protein RPA. The RPA-bound ssDNA is the platform for numerous interactions with DNA replication and repair proteins (Figure 4C). SSA is able to repair long 3' tails that have large amounts of sequence complementarity such as those found in repetitive DNA sequences (Ciccia et al., 2010). Rad52 is able to anneal ssDNA in the presence of RPA (Figure 4D). This activity of Rad52 allows it to anneal complementary sequence at the DSB to generate annealed 3' tails. Similar to MMEJ, the 5' non-complementary flaps, if they exist, or other non-complementary DNA are removed by endonucleases, and any remaining gaps are filled and ligated, fully repairing the DNA. This process can be deleterious on a fully replicated chromosome during G2 since non-complementary sequences between DNA repeats can be lost. However, since the lagging strand can contain up to 100 bps of ssDNA behind the replication fork (Hashimoto, Puddu et al., 2012), a one-ended DSB found on the leading strand of a replication fork might be able to be efficiently repaired by SSA. Thus, SSA might be a relevant mechanism to repair replication associated DSBs.

HR

Akin to the way RPA-bound ssDNA can be used to elicit SSA, RPA-bound ssDNA at a DSB also serves as the binding partner for breast cancer associated gene 2 (Brca2) to transfer the recombinase Rad51 onto the 3' overhang (Figure 4E) (Moynahan and Jasin, 2010). Upon Rad51 binding, Rad51 forms nucleoprotein filaments on the

ssDNA and, similar to RPA, is able to protect the ssDNA (Schlacher, Christ et al., 2011). Utilizing the bound ssDNA, Rad51 catalyzes a search for complementary sequences on the sister chromatid. When these sequences are found, Rad51 catalyzes strand invasion, creating a displacement loop (D-loop) (Figure 4F), and hydrolyzes ATP. ATP hydrolysis by Rad51 causes the disassembly of the Rad51 filament (Holloman, 2011). The resulting D-loop can be extended by polymerases, creating complementary DNA sequences between the broken ends of the DSB (Figure 4F). At this junction the D-loop can be dissociated by numerous DNA helicases and translocases, funneling homology-directed repair towards synthesis dependent strand annealing (SDSA) (Figure 4G). When the D-loop is resolved, annealed, and re-ligated, SDSA creates exclusively non-crossover products with gene conversion in the sequence extended by the DNA polymerase. Therefore, SDSA is considered to be an extremely accurate type of homology-directed repair.

Alternatively, the second end of the DSB can be captured by utilizing the ssDNA annealing activity of Rad52. When the annealed DNA is extended by a DNA polymerases and ligated, this process results in the in the creation of a double Holliday junction (dHJ) (Figure 4H). A dHJ represents a topologically constrained, entangled molecule, and its resolution can generate both crossover and non-crossover gene conversion products. Three distinct mechanisms are capable of resolving a dHJ in primates (Wechsler, Newman et al., 2011). The first utilizes a complex of proteins termed BTR that can resolve dHJs into exclusively non-crossover products in a process termed dissolution (Figure 4I) (Wu and Hickson, 2003). BTR consists of a helicase (BLM), a type I topoisomerase (topoisomerase IIIα), and two accessory factors (RecQ Mediated Genome Instability (RMI) 1, and RMI2) (Yin, Sobeck et al., 2005; Xu, Guo et al., 2008; Singh, Ali et al., 2008). dHJs can also be resolved by the actions of Holliday junction resolvases, types of specialized endonucleases that nick opposing strands on

both Holliday junctions, thereby generating crossover and non-crossover products (Figure 4J). Two separate dHJ resolvases exist in primates, one is composed of the Mus81/Eme1/Slx4/Slx1 heterotetramer and the other, Gen1, functions alone to resolve dHJs (Wechsler et al., 2011).

Classic HR, through the formation of a dHJ, is very accurate, and thus unlike NHEJ, does not lead to base substitutions, insertions, or deletions at the site of the DSB. In spite of this, HR can still lead to deletions and translocations in repetitive DNA sequences, so no DSB repair pathway is perfect. With all the distinct ways to repair a DSB and the ubiquitous amounts of Ku in the nucleoplasm, a critical question begins to emerge: how does the cell know which DSB repair pathway to use at a given DSB? Perhaps, the answer lies in the immense cascade of DNA damage signaling that is elicited upon DNA breakage and replication stress.

DNA damage signaling: big kinases for a complex job

DNA damage signaling is relayed by three kinases from the PIKK family: ataxia telangiectasia-mutated (ATM), ATM and Rad3-related (ATR), and DNA-PK_{cs}. These kinases share common features. Each PIKK utilizes a sensor protein to recognize DNA damage. DNA-PK_{cs} utilizes Ku to identify DSBs, ATM utilizes the MRN complex bound to the DSB termini (Derheimer and Kastan, 2010), and ATR identifies ssDNA via ATR-interacting protein (ATRIP) (Zou and Elledge, 2003). Additionally, these kinases can phosphorylate many of the same substrates (Matsuoka, Ballif et al., 2007) due to their shared consensus phosphorylation sequence, S/T-Q.

The best characterized example of a common substrate among these kinases is S129 of histone H2AX which can be phosphorylated by ATM, ATR, or DNA-PK_{cs} to a form known as γH2AX (Lobrich, Shibata et al., 2010). However, even with some

similarities, ATM, ATR, and DNA-PK_{cs} have unique substrates that define and dictate the outcome of their activation. Unlike the previously discussed DNA-PK_{cs}, whose kinase action promotes only NHEJ, the series of events promoted by ATM and ATR kinase activation do not fall into one pathway of DNA repair. ATM and ATR proteins have a central role in orchestrating repair and eliciting the cell cycle arrest known as a the DNA damage checkpoint during all phases of the cell cycle in response to DSBs and replication stress. Due to this, ATM and ATR can be considered as conductors of DNA repair.

ATM: ataxia telangiectasia and beyond

Loss of the ATM protein results in the genetic disorder ataxia telangiectasia (McKinnon, 2012). Ataxia telangiectasia patients display pronounced ataxia and are prone to lymphomas and leukemia. Cells from patients with this disorder exhibit increased sensitivity to ionizing radiation (McKinnon, 2012), radio-resistant DNA synthesis (Painter and Young, 1980), slowed DSB repair (Berkovich, Monnat et al., 2007), and some DNA replication associated defects (Cohen and Simpson, 1980; Murnane and Painter, 1982). ATM can be activated by oxidation (Guo, Kozlov et al., 2010), MRN binding to DSBs (Falck, Coates et al., 2005), or changes in chromatin conformation, the latter of which is modulated by ATM interactor (ATMIN) (Bakkenist and Kastan, 2003; Kanu and Behrens, 2007). In spite of the multitude of ways to activate ATM, DSB induction is the most well studied and is required for timely repair of DSBs (Berkovich et al., 2007).

Upon DNA breakage, MRN binds to DSBs (Figure 5A) and recruits ATM through an interaction of ATM with Nbs1 (Figure 5B). The interaction of MRN with ATM at the DSB activates the kinase activity of ATM triggering auto-phosphorylation in-trans at

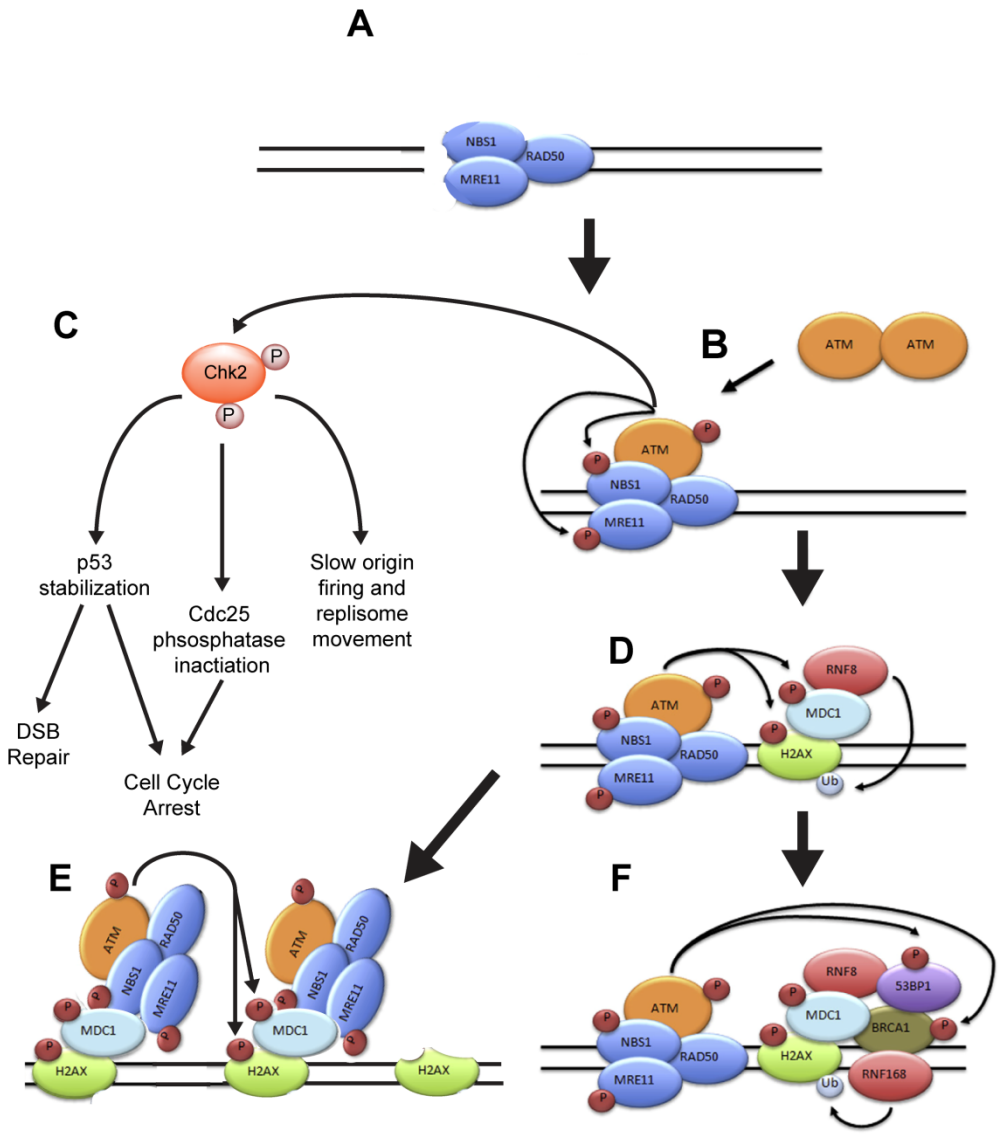

Figure 5. ATM DSB signaling.
(A, B) MRN binds to DSB termini and recruits ATM to DSB. (B) ATM kinase is activated. ATM dimers dissociate into monomers (Bakkenist et al., 2003). (C) ATM mediated phosphorylation activates Chk2. Chk2 phosphorylations promote cell cycle arrest and slowing of DNA replication. (D) ATM phosphorylates histone H2AX at replication fork. γH2AX binds to MDC1. ATM phosphorylates MDC1 creating a binding site for RNF8. RNF8 ubiquitinates H2AX, H2A, and numerous other factors at the DSB. (E) γH2AX bound MDC1 interacts with Nbs1 and recruits more ATM to sites proximal to the DSB. ATM bound to MDC1 spreads ATM dependent phosphorylations on the chromatin creating more γH2AX-MDC1-ATM-RNF8 complexes on the chromatin. (F) Ubiquitinated H2A and H2AX is bound by RNF168. RNF168 further ubiquitinates chromatin resulting in binding sites for Brca1 and exposing 53BP1 binding sites. Adapted from Derheimer et al., 2010. FEBS Lett. 584: 3675-81.

S1981, resulting in monomerization of ATM dimers (Figure 5B) (Bakkenist et al., 2003). Following the initial activation, evidence from *Xenopus laevis* egg extracts suggests that ATM can be further activated by nucleolytic digestion at the DSB termini by Mre11 (Jazayeri, Balestrini et al., 2008). ATM then phosphorylates the effector kinase Chk2 on residue T68 (Figure 5C). This phosphorylation event on Chk2 coincides with its activation. Chk2 is able to phosphorylate numerous substrates with the end results of cycle arrest, slowed DNA replication, and DSB repair.

At the DSB site, ATM phosphorylates numerous proteins, including Kap1, resulting in opening of heterochromatin structure (Ziv, Bielopolski et al., 2006) and the histone variant H2AX (Lukas, Lukas et al., 2011). Phosphorylated residue S129 of H2AX binds to mediator of checkpoint1 (MDC1) (Stucki, Clapperton et al., 2005). MDC1 is able to directly bind Nbs1 and thusly indirectly recruit more ATM to chromatin proximal to the DSB (Figure 5E) (Lukas et al., 2011). At these proximal chromatin sites, ATM further phosphorylates H2AX, spreading the γH2AX mark (You, Bailis et al., 2007). γH2AX expansion creates multiple binding sites adjacent and proximal to the break for MDC1 on the chromatin (Figure 5E). ATM phosphorylation of MDC1 enables the ordered recruitment of the E3 ubiquitin ligase RNF8 (Kolas, Chapman et al., 2007) followed by a second E3 ubiquitin ligase, RNF168 (Figure 5D) (Lukas et al., 2011). RNF8 and RNF168 promote the lysine 63-linked polyubiquitination of histones H2A and H2AX, further opening the chromatin structure (Figure 5D) (Lukas et al., 2011).

The ubiquitin modification directly recruits a complex containing Brca1 and Rap80 to DSBs (Figure 5F) (Chapman et al., 2012). On the other hand, the opening of the chromatin structure by K63-linked polyubiquitination has been hypothesized to allow binding of 53BP1 to dimethylated histone H3 at lysine 79 (Figure 5F) (Chapman et al., 2012). 53BP1 and Brca1 chromatin binding promotes antagonistic DSB repair pathways. 53BP1 promotes NHEJ, and Brca1 promotes homology-directed repair

(Chapman et al., 2012). However, what aspects of 53BP1 and Brca1 mediate this antagonism are not fully understood. Additionally, ATM is able to phosphorylate numerous DNA repair proteins in both NHEJ and homology-directed repair (Ciccia et al., 2010). Thus, ATM is able to promote several major DSB repair pathways through its kinase activation, yet it is not required per se for either NHEJ or HR activity to occur (Rass, Chandramouly et al., 2013).

Replication stress: ATR and the S phase checkpoint

Similar to ATM kinase signaling, the kinase activity of ATR has a wide variety of substrates and mechanisms to activate it. Yet unlike ATM, null mutations in the ATR protein are lethal (Brown and Baltimore, 2000) and hypomorphic mutations in ATR cause the rare disorder Seckel syndrome, which is characterized by reduced head size and growth retardation (Nam and Cortez, 2011). Supporting the role of ATR in directing the repair of stalled and broken DNA replication forks, Seckel syndrome cells demonstrate sensitivity to agents causing DNA replication stress (O'Driscoll, Ruiz-Perez et al., 2003), failed S phase checkpoint following DNA replication stress (Alderton, Joenje et al., 2004), and increased gapping and breakage at common fragile sites, loci in the genome prone to gaps and breaks on metaphase spreads (Casper, Nghiem et al., 2002; Casper, Durkin et al., 2004). ATR is primarily activated by accumulation of ssDNA in the genome; a circumstance that can occur due to DNA polymerase stalling or end resection during homology-directed repair of DSBs (Figure 6A-C).

ATR signaling is elicited by both replication stress and by DSBs. Replication stress can be induced in many ways including nucleotide depletion with ribonucleotide reductase inhibitors (e.g., hydroxyurea), UV irradiation, or polymerase inhibition (aphidicolin). A main contributor to ATR activation in response to replication stress is

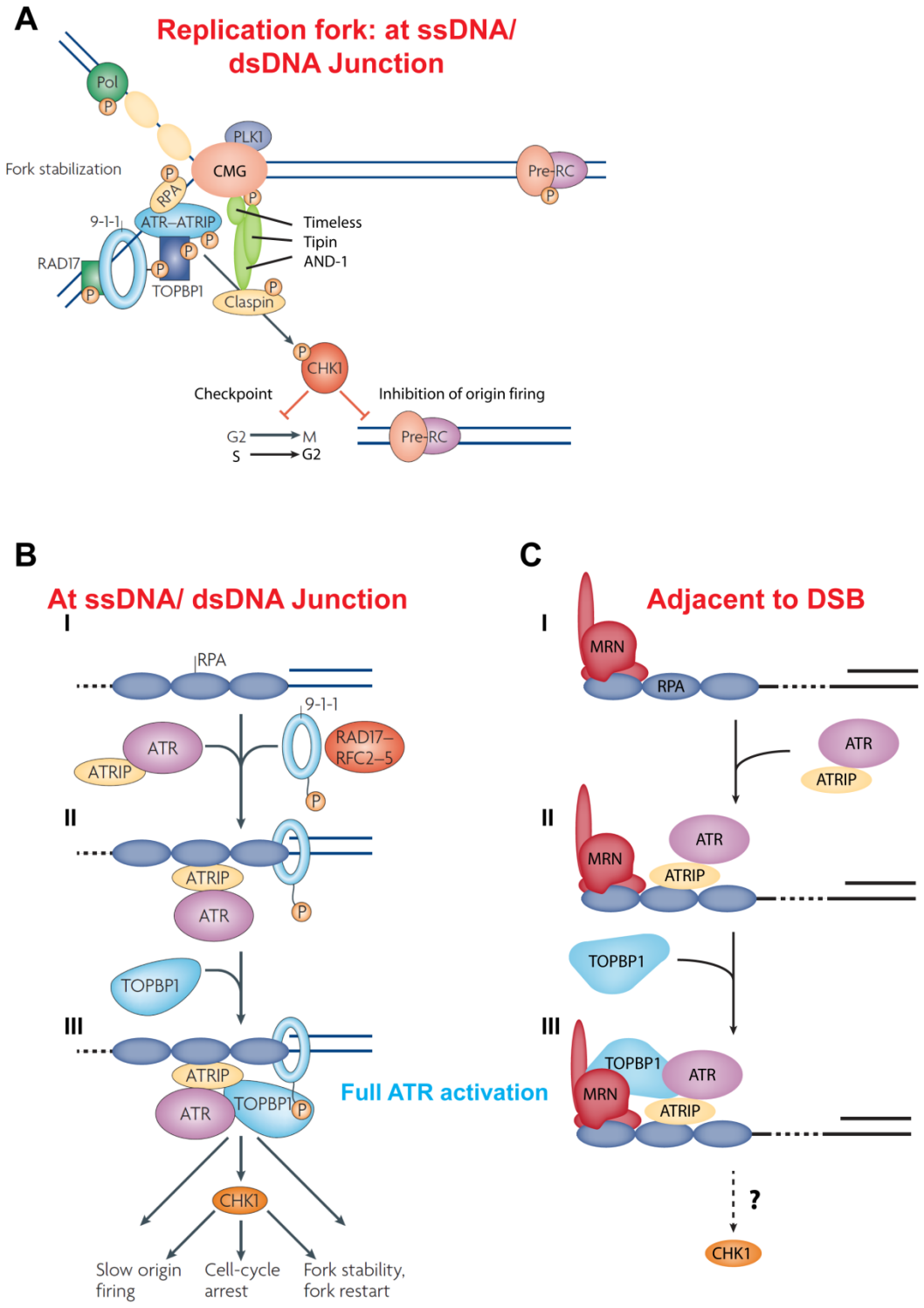
A
Replication fork: at ssDNA/ dsDNA Junction
Pol
PLK1
Fork stabilization
CMG
Pre-RC
RPA
9-1-1
ATR–ATRIP
Timeless
Tipin
AND-1
RAD17
TOPBP1
Claspin
CHK1
Checkpoint
Inhibition of origin firing
G2 → M
S → G2
B
At ssDNA/ dsDNA Junction
I
RPA
9-1-1
ATR
ATRIP
RAD17–RFC2–5
II
ATRIP
ATR
TOPBP1
III
ATRIP
ATR
TOPBP1
Full ATR activation
CHK1
Slow origin firing
Cell-cycle arrest
Fork stability, fork restart
C
Adjacent to DSB
I
MRN
RPA
ATR
ATRIP
II
MRN
ATR
ATRIP
TOPBP1
III
TOPBP1
ATR
MRN
ATRIP
?
CHK1

Figure 6.

Figure 6. ATR DNA damage signaling.
(A) Model of ATR activation at a stalled DNA replication fork. (B, C) Models of ATR activation adjacent to a ssDNA / dsDNA junction (B) or near the termini of a resected DSB (C). (B I) RPA bound ssDNA recruits ATR / ATRIP to ssDNA. Rad17 loads 9-1-1 onto the ssDNA / dsDNA junction. (B II) TopBP1 interacts with 9-1-1 and activates ATR kinase activity. (B III) ATR kinase phosphorylates numerous substrates including H2AX, MDC1, DNA polymerases, CMG, and Chk1. Similar to ATM activation, ATR activation creates DNA damage repair centers that bind to RNF8, RNF168, Brca1, and 53BP1. Chk1 kinase activity is directly activated by ATR phosphorylations. Chk1 kinase activities promote cell cycle arrest, DNA replication arrest, and DNA repair. (C I) MRN and ATR-ATRIP bind to RPA bound ssDNA. (C II) MRN recruits TopBP1 to ATR. (C III) ATR kinase activity becomes activated with similar consequences to (B). Panels (A) and (B) were adapted from Cimprich et al,. 2008. Nat Rev Mol Cell Biol. 9: 616-27.

stalling of a replicative DNA polymerase on the leading strand (Figure 6A). Under replication stress conditions, the CMG replicative helicase will continue to unwind the dsDNA. The combined contributions of continued helicase activity and a stalled polymerase leaves a tract of ssDNA bound by RPA (Figure 6A). RPA-bound ssDNA is the primary mechanism of recruitment of the ATR-ATRIP heterodimer to DNA (Zou et al., 2003) at both the DNA replication fork (Figure 6BI and BII) and 5' to 3' resected DSBs (Figure 6CII). ATRIP directly interacts with RPA and ATR, and is needed for ATR recruitment to ssDNA (Figure 6BII) (Ball, Myers et al., 2005; Namiki and Zou, 2006). Although ATR is recruited to ssDNA, several more factors that bind independently of ATR are needed to fully activate ATR.

Prior to full ATR activation, the ATR activating protein TopBP1 must bind nearby the RPA-associated ATRIP/ATR hetero-dimer. There are two mechanisms to accomplish TopBP1 binding nearby ATR at damaged DNA have been defined experimentally. In the first, RPA near the ssDNA/dsDNA junction binds to the repair clamp loader Rad17. Rad17 facilitates loading of the ring-shaped Rad9-Hus1-Rad1 (9-1-1) repair clamp at the ssDNA/dsDNA junction (Figure 6BI and II) (Zou, Cortez et al., 2002). 9-1-1 directly interacts with TopBP1 and recruits TopBP1 to ATR where the ATR-activating domain of TopBP1 activates the kinase activity of ATR (Figure 6BIII) (Kumagai, Lee et al., 2006; Mordes, Glick et al., 2008). Alternatively, ATR activation can occur at regions adjacent to a DSB and far away from a ssDNA/dsDNA junction. This mode of activation first requires 5' to 3' resection of the DSB to generate a 3' ssDNA tail that can be bound by RPA and subsequently bind to ATR (Figure 6CI and II). MRN bound to the DSB is then able to recruit TopBP1 to ATR by using a TopBP1-interacting module in Nbs1 (Figure 6CIII) (Shiotani, Nguyen et al., 2013; Duursma, Driscoll et al., 2013), thus activating ATR (Stiff, Reis et al., 2005).

Activation of ATR kinase activity enables it to phosphorylate numerous substrates that arrest DNA replication, prevent late DNA replication origin firing, and facilitate DNA repair (Figure 6A and B) (Cimprich and Cortez, 2008). One of these substrates is the checkpoint kinase Chk1. Analogous to the manner in which ATM activates Chk2, phosphorylation of Chk1 by ATR activates the kinase activity of Chk1. However, unlike Chk2, Chk1 is an essential protein (Liu, Guntuku et al., 2000) that is required for normal G2/M checkpoint function (Antoni, Sodha et al., 2007). Chk1 phosphorylates the Cdc25 phosphatases and p53 to enforce the S phase checkpoint (Figure 6A and B) (Toledo, Murga et al., 2011) and regulate the activity of several DNA repair proteins (Bunz, 2011), replisome factors, and origin firing upon checkpoint activation (Cimprich et al., 2008). Thus, the ATR-Chk1 pathway is a key contributor to genome stability.

The DNA damage checkpoint: a niche for small DNA tumor viruses

The S and G2/M checkpoints elicited by ATM and ATR signaling, collectively called the DNA damage checkpoint, provide the time needed to repair DNA. This arrest prevents the cell from taking un-replicated or damaged DNA into mitosis, and, therefore, is able to prevent loss of genetic information or further breakage of the genome. Although the DNA damage checkpoint protects the host genome, it may present an opportunity for foreign DNA.

Viruses that require the host cell to enter S phase to replicate commonly have small genomes (typically <10 kilobases (kb)) and encode a limited number of proteins needed to encapsidate their genome and manipulate the cell (Levine, 2009). Due to the limited genomic information carried by these viruses, they heavily rely upon host transcription and DNA replication factors to facilitate their own replication (DeCaprio and

Garcea, 2013). The small DNA tumor viruses are a group of viruses associated with cancer in their hosts (Levine, 2009). This group consists of several virus families including *Papillomaviridae* and *Polyomaviridae* (Levine, 2009). These viruses have circular dsDNA genomes ranging from 5 to 8 kb (DeCaprio et al., 2013; DiMaio and Miller, 2006). *Papillomaviridae* contains several important human pathogens including high risk human papillomaviruses (HPV) 16 and 18 associated with cervical cancer and head and neck cancer (Psyrri and DiMaio, 2008). Similarly, *Polyomaviridae* also contains several members that cause disease (DeCaprio et al., 2013). Notably, Merkel cell virus (MCV) is associated with Merkel cell carcinoma, whereas two other members, JC virus (JCV) and BK virus (BKV), are associated with progressive multifocal leukoencephalopathy (PML) and polyomavirus-associated nephropathy (PVAN), respectively, in immunocompromised patients (Gjoerup and Chang, 2010). PML and PVAN cause severe complications and commonly result in death. Collectively, the severe consequences that are associated with infection of several small DNA tumor viruses illustrate the need for a better understanding of the mechanisms by which these viruses replicate.

Although use of cellular machinery has its benefits, the reliance on cellular machinery by small DNA tumor viruses makes them subject to the rules that normally govern the cell, including cell cycle timing and cell death programs. Therefore, these viruses have evolved to disrupt normal cell programming to enhance their own propagation. To accomplish this, small DNA tumor viruses must first encourage the cell to enter S phase, a highly regulated process, and then arrest the cell in S phase. Polyoma- and papillomaviruses encode proteins that over-ride growth-dependent control of the G1 to S transition through Rb proteins to promote premature S phase entry (Levine, 2009). S phase arrest or the viral pseudo-S phase is accomplished through activation of the DNA damage checkpoint (Weitzman, Lilley et al., 2010). However,

checkpoint activation provokes its own set of problems, including inhibition of cellular replication machinery and eventual cell death. To prevent the ill effects of prolonged DNA damage checkpoint, these viruses inactivate the tumor suppressor p53 to disrupt the normal cellular stress programming (Levine and Oren, 2009) and utilize a subset of DNA replication proteins that are checkpoint resistant (Sowd and Fanning, 2012).

Simian Virus 40: elegantly small

To control and disrupt the complex mechanisms of the cell cycle, polyomaviruses deploy one master protein, large T antigen (Tag). The archetype Tag was initially discovered from tumors of rodents injected with the polyomavirus simian virus 40 (SV40) (Fanning and Zhao, 2009). Originally identified as a contaminant in the cells used to produce the polio virus vaccine, SV40 natively infects the Rhesus macaque without overt disease or cytopathic effect. In contrast, kidney cells of African Green Monkey display cytopathic effects when infected by SV40 (Levine, 2009). SV40 is able to cause tumors in young hamsters infected with the virus (Fanning et al., 2009). However, cellular transformation by the virus can only be elicited in an abortive infection in nonpermissive hosts (Fanning and Knippers, 1992). Thus, unlike high risk HPVs and MCV, SV40 appears to cause cancer only in nonpermissive hosts.

SV40 consists of a 5,243 basepair (bp) circular dsDNA genome with a genetically encoded discrete viral origin of DNA replication (Figure 7A). Transcription of the viral genome emanates from a bidirectional promoter/enhancer from which all viral proteins are transcribed (Figure 7A). Based on the direction of transcription and with reference to the order by which viral transcripts arise during infection, the genome can be divided into early and late regions. The virion consists of a chromatinized viral genome encased in a non-enveloped proteinaceous capsid (Gjoerup et al., 2010). The icosahedral capsid

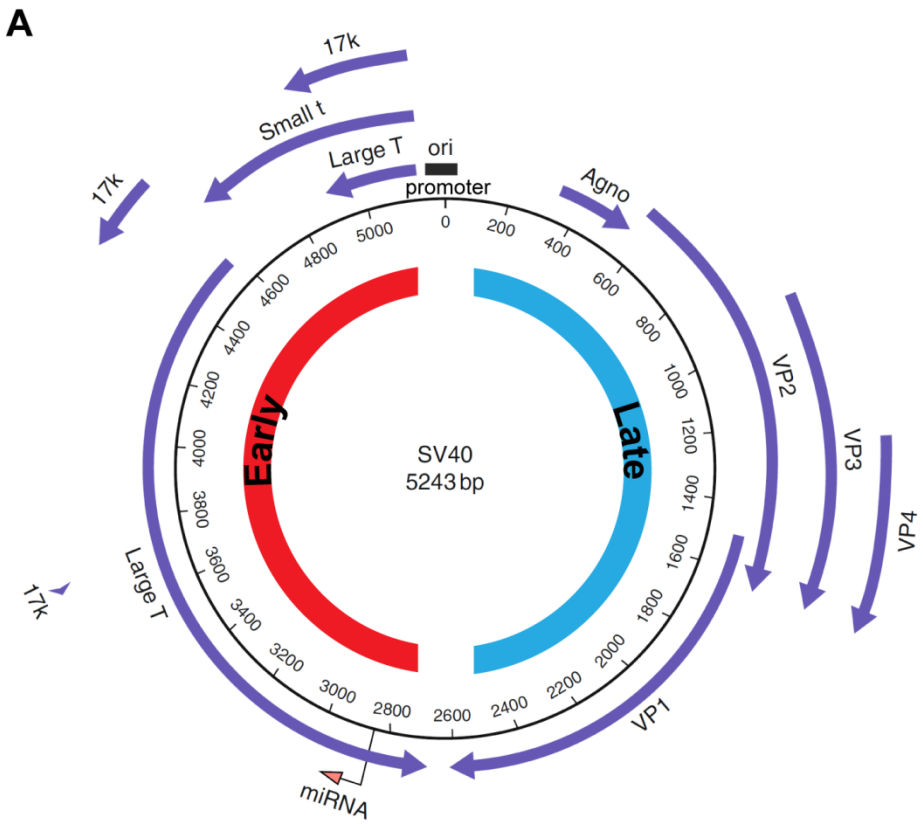

Figure 7. SV40 genome map.
(A) Genome features are marked with thick arrows for transcripts encoding proteins. Early and late refer to the time during infection when the transcripts are heavily transcribed. Adapted from Gjoerup et al., 2010. Adv Cancer Res. 106: 1-51.

consists of VP1, VP2, and VP3. Seventy-two pentamers of VP1 form the outer capsid, with each pentamer interacting with one internal VP2 or VP3 (VP2/3) (Liddington, Yan et al., 1991). The internal VP2/3 makes contact with the viral genome (Stehle, Gamblin et al., 1996).

To enter the cell, VP1 on the viral capsid binds to glycan GM1 (monosialotetrahexosylganglioside) and is endocytosed into the caveosome (Neu, Stehle et al., 2009). The capsid is then trafficked to the endoplasmic reticulum where protein disulfide isomerases rearrange disulfide bonds on VP1 leading to partial disassembly of the capsid (Neu et al., 2009). This series of events leads to release of the partially disassembled capsid into the cytoplasm where the newly exposed nuclear localization signal (NLS) of VP1 likely promotes nuclear entry (Neu et al., 2009).

Inside the nucleus the remaining capsid is hypothesized to be fully removed allowing transcription to occur on the chromatinized viral genome. Chromatin remodeling generates a nucleosome-free region, allowing host proteins to bind the enhancer/promoter (Yaniv, 2009). The early region of the viral genome is first transcribed into three differentially spliced transcripts that encode Tag, small t antigen, and 17k (Figure 7A). These gene products collectively function to manipulate the cell and promote viral genome amplification. Large amounts of early transcripts are made during the first 24 hours of infection after which Tag modulates a switch to robust genome amplification and increased transcription from the late region of the genome (Fanning et al., 1992). Transcripts from the late region of the genome encode proteins that promote viral egress (Agno and VP4) and the viral capsid proteins (VP1, VP2, and VP3) (Figure 7A). Collectively, transcription of the viral genome primes the cell for viral take over and ultimately its own demise.

Large T antigen: the Swiss army knife of proteins

Translation of the early transcripts encoding Tag drives viral infection forward toward viral DNA replication. Tag is a modular phospho-protein that functions as the lynchpin of viral DNA replication (Figure 8A). The N-terminal region contains a DnaJ domain that associates with Hsc70 to enable protein chaperone function implicated in viral DNA replication (Campbell, Mullane et al., 1997). The linker between the DnaJ domain and origin binding domain (OBD) contains an LxCxE motif required to bind to Rb family proteins (Gjoerup et al., 2010). The binding of the LxCxE within Tag to Rb, p130, and p107 in cooperation with the DnaJ domain disrupts Rb/E2F complexes, freeing E2F to function as a transcription factor (DeCaprio, 2009). The E2F promoter complexes lacking Rb are actively transcribed, thus promoting the G1 to S transition (Cam et al., 2003). Several E2F-driven genes encode DNA replication and repair factors that are required for both cellular (Cam et al., 2003) and viral DNA replication. Thus, the Rb-Tag interaction is crucial for viral DNA replication as it allows the virus to replicate even in quiescent or senescent cells (DeCaprio, 2009).

In addition to the LxCxE motif, numerous phosphorylation sites lie between the DnaJ domain and the OBD. Residues 130 to 250 of Tag constitute the OBD. This region specifically binds to the pentanucleotide repeats within the central palindrome of viral origin (Figure 8B) (Sowd et al., 2012). The domain directly C terminal of the OBD is a helicase domain containing a AAA+ ATPase and zinc finger sub-domains (Sowd et al., 2012). Nested within the helicase domain of Tag is the binding site for p53 (Gjoerup et al., 2010). Binding of Tag to p53 prevents p53 from functioning as a transcriptional activator following cellular stress and stabilizes p53 levels inside the cell (Levine et al., 2009). The interaction of p53 and Tag is thought to prevent many of the ill effects that are associated with prolonged checkpoint signaling and unscheduled S phase entry.

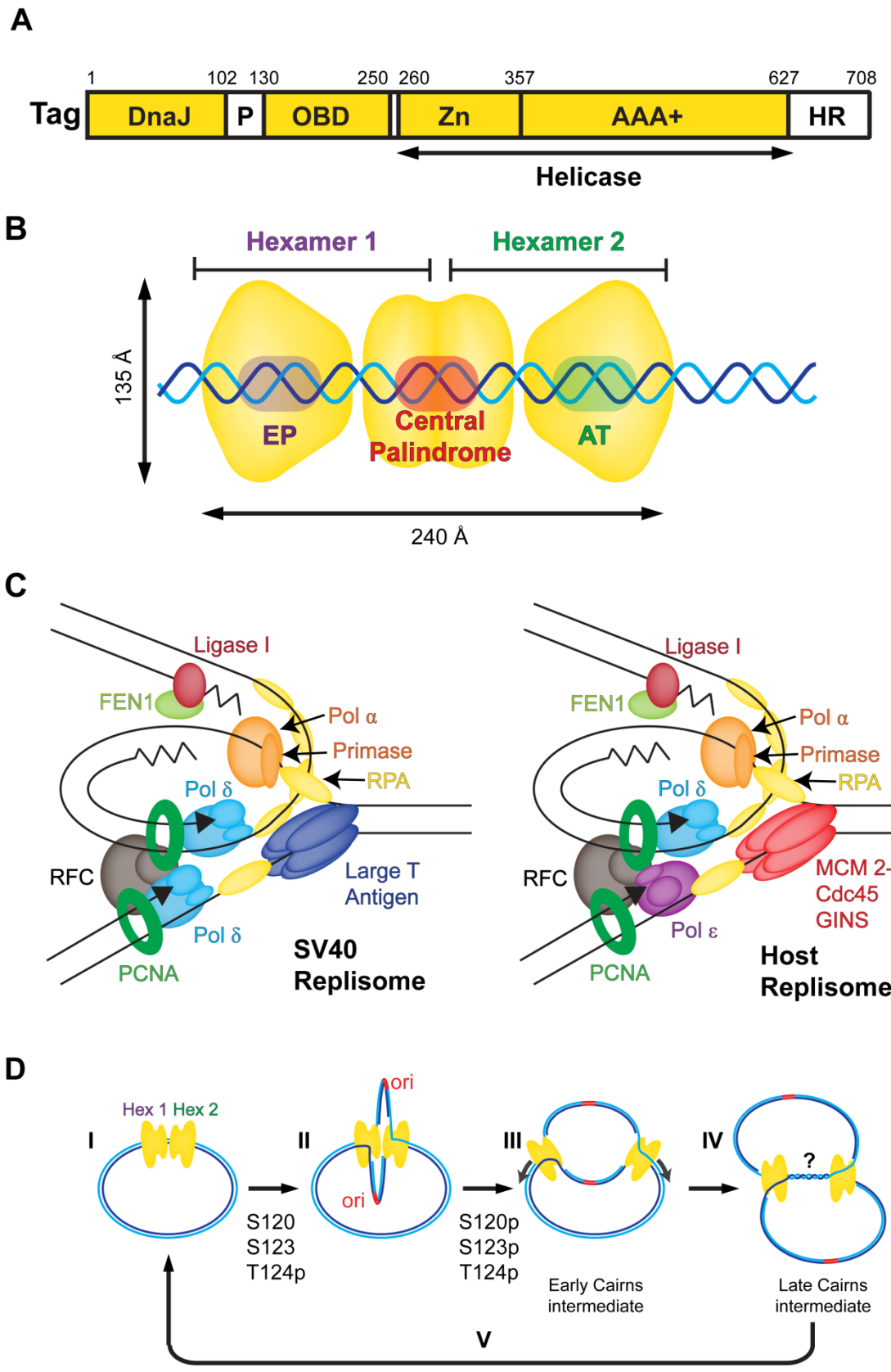
A
1
102
130
250
260
357
627
708
Tag
DnaJ
P
OBD
Zn
AAA+
HR
Helicase
B
Hexamer 1
Hexamer 2
135 Å
EP
Central
Palindrome
AT
240 Å
C
Ligase I
FEN1
Pol α
Primase
RPA
Pol δ
RFC
Large T
Antigen
Pol δ
PCNA
SV40
Replisome
Ligase I
FEN1
Pol α
Primase
RPA
Pol δ
RFC
MCM 2-7
Cdc45
GINS
Pol ε
PCNA
Host
Replisome
D
Hex 1 Hex 2
I
II
ori
ori
III
IV
?
S120
S123
T124p
S120p
S123p
T124p
Early Cairns
intermediate
Late Cairns
intermediate
V

Figure 8.

Figure 8. Large T antigen: master of viral DNA replication.
(A) Domains of Tag. Structured and unstructured domains are shown in yellow and white, respectively. (B) Model of Tag double hexamer bound to the viral ori. (C) Diagram showing the factors used by the viral and host replisomes. (D) Model of SV40 replication. (D I) Hypophosphorylated Tag double hexamer bound to the origin initiates DNA replication. (D II) Hypophosphorylated, coupled double hexamer initiates DNA unwinding. (D III) Residues S120 and S123 become phosphorylated and double hexamer uncouples. (D IV) Tag hexamers converge and replicated genomes are decatenated (D V). Figure adapted from Sowd et al., 2012. PLoS Pathog. 9: e1003283.

SV40 Chromatin Replication: a platform for discovery

SV40 can replace host ORC, Cdt1, Cdc6, Mcm2-7, Cdc45, GINS, AND-1, and Mcm10 cellular functions with one protein, Tag (Figure 8C). Whereas the cell utilizes these 21 proteins and kinases that regulate them to create an ordered DNA replication cycle that prevents genome re-duplication, the deployment of Tag by SV40 as an origin recognition complex and replicative helicase (Figure 8C) circumvents several cellular limitations. The limitations of S phase machinery include an inability of cellular machinery to re-duplicate the genome during S phase, to re-license origins during S phase (Bell et al., 2002), and to replicate large amounts of DNA during checkpoint signaling (Cimprich et al., 2008).

Similar to cellular replicative helicases, Tag replicative DNA helicase function is restricted to S phase by putative CDK2-cyclin A dependent phosphorylation on T124 (Fotedar and Roberts, 1991; Moarefi, Small et al., 1993; Weisshart, Taneja et al., 1999; Adamczewski, Gannon et al., 1993). To initiate viral genome replication, the OBD of one Tag monomer binds to the cis-acting pentanucleotide repeat within the central palindrome of the viral ori (Chang, Xu et al., 2013). This interaction is followed by the helicase domain binding to the AT rich or EP element within the ori (Figure 8B). Crystallographic data suggest that the interactions of the Tag monomer with the viral ori result in the binding of another monomer of Tag forming a dimer on the origin wherein the second monomer interacts with a hidden site GC site within the central palindrome (Chang et al., 2013). Dimer bound to the origin is hypothesized to stimulate binding of four more molecules on the central palindrome, EP site, and AT sites forming a double hexamer on the origin (Figure 8B and D). The interactions between opposing OBD interfaces of the double hexamer (Figure 8B) are essential for viral DNA replication and are dictated by the phosphorylation state of Tag (Fanning, 1994). Residues S120, S123,

and T124 of the linker between the DnaJ and OBD domains all lie in this interface and are phosphorylated at some point after initiation of viral DNA replication (Figure 8A) (Fanning et al., 1992). However, only residue T124 of Tag can be phosphorylated on the viral origin to form a pre-replicative Tag double hexamer complex (Figure 8D) (Schneider and Fanning, 1988; Moarefi et al., 1993; Fanning, 1994; Weisshart et al., 1999; Sowd et al., 2012) analogous to ORC/CMG bound eukaryotic origins.

Following initial origin melting by Tag, which is an ATPase independent event, Tag facilitates RPA binding to the ssDNA created at the melted origin of replication. This process is performed through specific interactions of Tag and RPA mediated through the OBD and helicase domains of Tag and the RPA70 and RPA32 subunits of the RPA heterotrimer (Figure 9AI) (Jiang, Klimovich et al., 2006; Dornreiter, Erdile et al., 1992). Tag unwinds the DNA in an ATP-dependent manner creating more binding sites for the active loading of RPA. Subsequently, through interactions of Tag with polymerase α/ primase (Huang, Weiner et al., 2010; Huang, Zhao et al., 2010; Zhou, Arnett et al., 2012) and RPA (Jiang et al., 2006), RPA is removed from the ssDNA (Figure 9AII and AIII) enabling pol/prim to create a RNA primer on the melted DNA, which is extended by polymerase α (Figure 9AIII and B2). PCNA is loaded onto the RNA/DNA primer by RFC and in so doing displaces polymerase α (Figure 9B3 and B4) (Waga et al., 1998). The homotrimeric ring PCNA bound to the ssDNA/dsDNA junction interacts with polymerase δ allowing processive DNA synthesis (Figure 9B4). After initial DNA synthesis, the Tag double hexamer is hypothesized to become further phosphorylated at S120, a PIKK kinase consensus site (Shi, Dodson et al., 2005), and S123, allowing the double hexamers to become uncoupled (Figure 8DIII) and creating a classical bidirectional replication bubble containing both leading an lagging strands (termed early Cairns intermediate, Figure 8DIII) (Sowd et al., 2012).

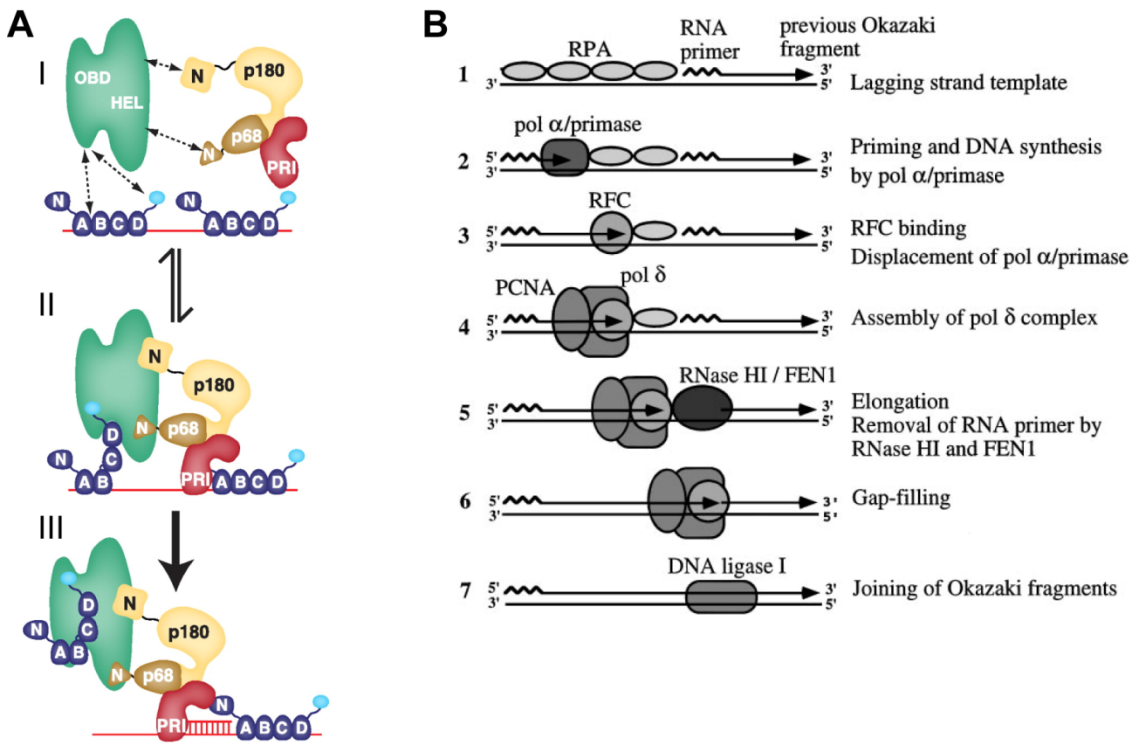

Figure 9. Models of DNA polymerase function at the viral replication fork.
(A) Model of viral primosome function adapted from Huang et al., 2010. J Biol Chem. 285: 17112-22. (A I) Arrows show direct interactions between Tag and polymerase α / primase and RPA that contribute to primosome function. (A II) Tag removes RPA and positions polymerase α / primase onto ssDNA. (A III) Polymerase α / primase makes a primer. (B) Model of lagging strand maturation. (B 1, 2) Described above. (B 3, 4) RFC displaces polymerase α / primase and load PCNA. PCNA binds to polymerase δ. (B 5, 6, 7) Polymerase δ synthesizes DNA. DNA synthesized by polymerase α / primase is displaced by the strand displacement activity of polymerase δ creating a 5' flap. This flap is removed by FEN1 and remaining RNA primer is degraded by RNAse H. Model in (B) adapted from Waga et al., 1998. Annu Rev Biochem. 67: 721-51.

Similar to cellular DNA replication, DNA entanglements behind the replication fork known as pre-catenanes are removed by topoisomerase IIα and prevented by topoisomerase I (Nitiss, 2009). Thus, the combined topoisomerase activities of topoisomerase I and IIα allow continuous replisome function. The viral replisomes replicate around the viral genome and meet at a region opposing the viral ori creating a late Cairns intermediate (Figure 8DIV) (Tapper, Anderson et al., 1979). At this point, the molecules are decatenated by topoisomerase IIα generating two topologically distinct, chromatinized dsDNA molecules (Figure 8DV) (Sundin and Varshavsky, 1981; Sundin and Varshavsky, 1980; Yang, Wold et al., 1987) that can be re-replicated by subsequent Tag binding cycles. This process can generate hundreds of thousands of viral genomes during one prolonged S phase in a SV40-infected cell (Rigby and Berg, 1978).

The re-replication characteristic of SV40 DNA replication was previously exploited to replicate viral origin containing plasmid DNA in primate cellular extracts (Li and Kelly, 1985; Li and Kelly, 1984; Stillman and Gluzman, 1985). Thereafter, these extracts were used to identify and purify human proteins whose functions were needed to replicate the viral origin *in vitro* (Waga, Bauer et al., 1994; Waga and Stillman, 1994). From these experiments, a set of 10 human proteins whose activities are necessary and sufficient to replicate naked supercoiled viral origin containing DNA into supercoiled DNA product were identified (Table 2).

SV40 DNA replication *in cellulo*: not as simple as expected

Despite the simplicity of viral DNA replication *in vitro*, DNA replication presents additional obstacles to viral propagation, including a necessity to arrest the cell cycle in S phase. Thus, the proteins that were originally identified to replicate the viral ori *in vitro* might only represent a subset of those actually needed to replicate the chromatinized

Table 2: Proteins sufficient to replicate SV40 genome *in vitro*.
Adapted from Hassell et al., (1996). SV40 and Polyomavirus DNA Replication. DNA Replication in Eukaryotic Cells. M. L. DePamphilis. Plainview, NY, Cold Spring Harbor Press: 639-677.

Factor	Molecular mass (kD)	Function
Large T antigen	90	origin recognition protein; unwinds DNA; helicase; primosome loading protein
RP-A	70 32 14	binds single-stranded DNA; promotes origin unwinding; stimulates DNA polymerase-α:primase; cooperates with RF-C and PCNA to stimulate DNA polymerase-δ
DNA polymerase-α:primase	180 68 58 48	initiates leading- and lagging-strand synthesis
DNA polymerase-δ	125 66 50 12	completes leading- and lagging-strand synthesis
RF-C	140 40 38 37 36.5	auxiliary factor for DNA polymerase-δ and ε; loads PCNA onto DNA; DNA-dependent ATPase
PCNA	36	auxiliary factor for DNA polymerase-δ and ε, increases processivity
Topoisomerase I	110	relieves torsional strain in front of replication forks
Topoisomerase IIa	170	segregates progeny strands by removing catenated intertwines behind forks
MF-I (FEN-1)	45	5′→3′ exonuclease removes terminal monoribonucleotide from Okazaki fragments
RNase H1	68	endonuclease; cleaves RNA primer
DNA ligase I	125	ligates Okazaki fragments

viral genome *in cellulo*. As such, it is highly likely that several other factors are still needed to achieve maximal replication efficiency inside the cell. DNA-PK_{cs} and ATM can phosphorylate Tag (Wang, Zhou et al., 1999; Shi et al., 2005). ATM and ATR are strongly activated inside SV40-infected cells (Shi et al., 2005; Zhao, Madden-Fuentes et al., 2008; Rohaly, Korf et al., 2010). Perhaps through the DNA damage checkpoint, such DNA damage signaling is able to elicit an indefinite S phase inside SV40 infected cells (Sowd et al., 2012). Thus, a role for checkpoint signaling in cell cycle arrest inside SV40-infected cells seems probable.

S120 Tag is targeted for phosphorylation in an ATM dependent manner *in cellulo* (Shi et al., 2005), and phosphorylation at this site is crucial for viral DNA replication (Schneider et al., 1988; Virshup, Russo et al., 1992; Cegielska, Moarefi et al., 1994) . Yet *in vitro*, a strict requirement for dephosphorylated Tag at S120 is necessary for proper double hexamer activation (Cegielska et al., 1994; Virshup et al., 1992; Fanning, 1994), and only the purified hypophosphorylated Tag (S120, S123, p124) with 10 purified human DNA replication factors can generate supercoiled product (Waga et al., 1994). Collectively, these data imply that the hypophosphorylated version of Tag is competent to replicate viral DNA, but the regulation of phosphorylation at S120 by ATM or other PIKKs is crucial *in cellulo.* How these two opposing mechanisms interact in cells remains unknown.

Beyond the phosphorylation of Tag, several studies have demonstrated that Tag foci co-localize with the foci of several proteins localizing to damaged DNA inside SV40-infected cells. One repair pathway, HR, seems to have an abundance of proteins recruited to Tag foci. MRN (Zhao et al., 2008) and Rad51 (Boichuk, Hu et al., 2010) colocalize with Tag during SV40 infection, implying that homology-directed repair might be used during viral replication. Furthermore, 53BP1 (Boichuk et al., 2010), Brca1 (Boichuk et al., 2010), and γH2AX (Zhao et al., 2008) all localize to Tag foci inside

SV40-infected nuclei, suggesting that DNA damage signaling is induced by viral DNA replication. These same Tag foci inside SV40-infected cells also co-localize with polymerase α/ primase (Zhao et al., 2008), RPA (Zhao et al., 2008), and EdU (Rohaly et al., 2010), indicating that they may be areas of active viral DNA replication. Hence, SV40 might also be using other pathways to maximize viral DNA replication *in cellulo* beyond the 10 factors identified *in vitro*. However, it remains unclear how the virus actually induces ATM and ATR activation. Additionally, the substrate of the DNA repair proteins at viral DNA replication centers is not clear. Furthermore, whether the recruitment of the repair and signaling proteins is actually a result of viral DNA replication is the subject of debate.

Hypotheses for the role of DNA damage signaling during SV40 infection

Several possible mechanisms have been suggested to activate ATM or ATR during small DNA tumor virus infection. Based on the correlated timing of viral DNA replication, formation of Tag foci that colocalize with DNA damage signaling proteins, and activation of ATM and ATR during infection, an initial model proposed that viral DNA replication is associated with DNA damage and subsequent DNA damage signaling (Zhao et al., 2008). In spite of the close relation of viral DNA replication and DNA damage signaling, this model had not been thoroughly tested using either polyomaviruses or papillomaviruses.

Another model for the activation of DNA damage signaling by SV40 is based on the finding that ectopically expressed Tag associates with Bub1, a protein required for the anaphase checkpoint (Lara-Gonzalez, Westhorpe et al., 2012), and leads to its degradation (Cotsiki, Lock et al., 2004; Hein, Boichuk et al., 2009). Degradation of Bub1 in Tag-overexpressing cells increased polyploidy, and the loss of the anaphase

checkpoint inside SV40-infected cells causes chromosomal DNA damage through chromosomal breakage during mitosis (Cotsiki et al., 2004). However, the plasmids used in one of these studies to overexpress Tag contained the viral origin (Cotsiki et al., 2004), raising the possibility that the increased DNA content observed might have stemmed from Tag mediated origin dependent DNA replication rather than from abrogation of the anaphase checkpoint.

Subsequent studies by the same group using CMV based overexpression of Tag from a retroviral system that lacked the viral origin of replication found that DNA damage signaling is activated following a week of selection for stable transductants that express Tag (Hein et al., 2009; Boichuk et al., 2010). Contrary to Cotsiki et al., Hein et al., found a more subtle induction of polyploidy upon Tag overexpression (Hein et al., 2009). Given these results, the timepoints examined by these studies (168 h) do not correlate well with actual SV40 infection (72 h) (Boichuk et al., 2010; Hein et al., 2009). Another consideration arguing against the relevance of the Tag-Bub1 findings is the fact that activation of ATM and ATR by SV40 infection would prevent mitotic entry. As such, how an SV40 infected cell would enter mitosis is difficult to imagine. Collectively, it is difficult to determine from these results how the abrogation of the anaphase checkpoint contributes to DNA damage during actual SV40 infection.

A final proposal for the activation of DNA damage signaling during small DNA tumor virus infection is based on the observation that overexpression of helicases is able to elicit DNA damage signaling through the creation of large amounts of ssDNA. Again, this model primarily stems from data gained using transfection or transduction to ectopically express viral replicative helicases, HPV E1 or Tag (Sakakibara, Mitra et al., 2011; Boichuk et al., 2010). Wild-type HPV E1 expression, without the viral ORC E2, activated the DNA damage response, but E1 that lacked ATPase or DNA binding activity did not (Sakakibara et al., 2011). However, unlike singular E1 expression, co-

expression of E1 and E2 results in DNA damage signaling that is localized to a viral replication center, suggesting that in infected permissive cells, E1 and E2 elicit damage specifically at the viral replication center (Sakakibara et al., 2011).

Similarly, transduction of Tag expression vectors lacking the SV40 origin into cells suggested Tag activates ATM and ATR signals, generates DNA repair foci that colocalize with Tag foci, and induces genomic DNA damage (Boichuk et al., 2010). However, the timeline of the experiments (168 h) was again not relevant to SV40 infection (72 h) (Boichuk et al., 2010). Additionally, these experiments did not test the contribution of the viral origin to the timing of damage and damage to the host genome. In spite of this, both sets of experiments indicate that unregulated expression of a viral replicative DNA helicase elicits DNA damage signaling emanating from damage to the host chromosome. The damage sustained by the host genome upon ectopic viral helicase expression is likely due to deregulated helicase unwinding in the absence of the viral ori at ssDNA/dsDNA junctions. Deregulated helicase activity would generate substantial amounts of ssDNA that would be the substrate for ATR signaling and nucleases. Yet, what aspects of helicase overexpression in the absence of the viral origin are relevant to permissive SV40 infection have not been determined.

Experimental rationale and summary

Given that multiple mechanisms might contribute to the activation of DNA damage signaling during SV40 infection, I felt it was prudent to first study what aspect of infection is necessary to induce DNA damage signaling and determine if DNA damage signaling through ATM and ATR directly affects viral DNA replication. This investigation was published in *PLoS Pathogens* (Sowd, Li et al., 2013) and immediately follows as chapter II. In addition to Chapter II containing the *PLoS Pathogens* manuscript, I also

added the supporting figures from the manuscript to the main text and two figures of unpublished results. The two unpublished figures contain experiments that directly support and build upon the conclusions of the *PLoS Pathogens* paper.

Chapters III and IV contain unpublished results that will be used to construct two papers. A brief examination of how ATM and ATR influence the viral pseudo-S phase is presented in Chapter III. Chapter IV explores what components of DSB repair localize to viral DNA replication centers. Additionally, the impact of ATM and ATR kinase activities on the localization DSB repair proteins inside SV40-infected cells is tested in Chapter IV. This chapter contains a fairly comprehensive amount of unpublished data.

Thus as a whole, the dissertation chapters that follow are an attempt to address two questions: 1. How DNA damage signaling is activated during a permissive SV40 infection? 2. What activities promote accurate replication of the viral genome? While reading these chapters, it is important to keep in mind a few key points. First, ATR functions during each cellular S phase to promote genome stability (Toledo et al., 2011). Second, ATM-deficient cells display some DNA replication abnormalities that may stem from interactions of ATM with replication factors (Gamper, Choi et al., 2012). Third, ATM and ATR are conductors of DNA damage signaling and have widespread effects on the cell (Ciccia et al., 2010). After the presentation of the results in chapters II-IV, I speculate in chapter V how the collective results of chapters II, III, and IV fit together.

CHAPTER II

ATM AND ATR ACTIVITIES MAINTAIN REPLICATION FORK INTEGRITY DURING SV40 CHROMATIN REPLICATION

Portions of chapter II were previously published in (Sowd et al., 2013).

Introduction

Faithful duplication of the genome is vital for cell proliferation. In metazoans, the consequences of inaccurate genome replication include cell death, premature aging syndromes, neuro-degeneration disorders, and susceptibility to cancer (Ciccia et al., 2010; Chu and Hickson, 2009). The DNA damage signaling protein kinases ATM and ATR, members of the PIKK family, act to ensure that cells with incompletely replicated or damaged DNA do not progress through the cell cycle (Ciccia et al., 2010). ATM and DNA-PK_{cs} respond primarily to DNA DSBs that are associated with either MRN (Stracker et al., 2011) or Ku70/80 (Meek et al., 2008), respectively. Additionally, intracellular oxidation or alterations in chromatin structure can activate ATM kinase (Guo et al., 2010; Bakkenist et al., 2003). In contrast, single-stranded DNA (ssDNA) bound by RPA activate ATR (Zou et al., 2003; Cimprich et al., 2008). When activated, ATM and ATR phosphorylate consensus SQ/TQ motifs in target proteins at sites of damage, e.g., the histone H2AX, which facilitates recruitment of repair proteins and activation of downstream kinases Chk1 and Chk2 that enforce the checkpoint (Cimprich et al., 2008; Matsuoka et al., 2007).

Failure to activate DNA damage checkpoints results in genome instability syndromes. Mutations in the human ATM gene can cause the cancer-prone disorder

ataxia telangiectasia. Hypomorphic mutations in the ATR gene can cause the genomic instability disorder Seckel Syndrome, but complete loss of ATR results in cell death (Brown et al., 2000; Casper et al., 2002). The central roles of ATM and ATR in genome maintenance suggest the potential to manipulate their activity for cancer chemotherapy, fueling the development of potent small molecules that specifically inhibit ATM and ATR activities *in cellulo* (Hickson, Zhao et al., 2004; Reaper, Griffiths et al., 2011).

Interestingly, multiple animal viruses have evolved to manipulate DNA damage signaling pathways to facilitate viral propagation (Weitzman et al., 2010). Some viruses, e.g., herpes simplex virus, evade or disable DNA damage response pathways that result in inappropriate processing of viral DNA (Weitzman, Lilley et al., 2011; Weller, 2010). In other cases, viral infection appears to activate checkpoint signaling and harness it to promote the infection. HIV, papillomaviruses, and polyomaviruses induce and depend on ATM signaling for viral propagation (Lau, Swinbank et al., 2005; Moody and Laimins, 2009; Sakakibara et al., 2011; Wallace, Robinson et al., 2012; Dahl, You et al., 2005; Jiang, Zhao et al., 2012). However, mechanistic understanding of how these viruses activate damage signaling and exploit it for viral propagation is limited.

SV40, a polyomavirus that propagates in monkey kidney cells, has served as a powerful model to study eukaryotic replication proteins and mechanisms *in vivo* and *in vitro* (Bullock, 1997; Borowiec, Dean et al., 1990; Waga et al., 1994; Sowd et al., 2012; Fanning et al., 2009). Checkpoint signaling proteins are dispensable for SV40 DNA replication *in vitro*, yet in infected cells, ATM or ATR knockdown, over-expression of kinase-dead variant proteins, or chemical inhibition of checkpoint signaling clearly decreases or delays SV40 chromatin replication (Shi et al., 2005; Zhao et al., 2008; Rohaly et al., 2010; Sowd et al., 2012). To determine how checkpoint signaling facilitates viral replication in SV40-infected primate cells, we have utilized small molecule inhibitors of the PIKK family members ATM, ATR, and DNA-PK to suppress checkpoint signaling

in host cells during three specific time windows after SV40 infection. Characterization of the resulting viral DNA replication products reveals that inhibition of ATM or ATR, but not DNA-PK, reduced the yield of unit length viral replication products and caused accumulation of aberrant viral DNA species. ATM inhibition led to unidirectional SV40 DNA replication and concatemeric products, whereas ATR inhibition markedly increased broken SV40 DNA replication forks. Our results strongly suggest that unperturbed viral chromatin replication in infected cells results in double strand breaks, activating checkpoint signaling and fork repair to generate unit length viral replication products.

Results

SV40 chromatin replication activates DNA damage signaling

Replicating SV40 chromatin in infected cells has been visualized by fluorescence microscopy in prominent subnuclear foci that co-localize with Tag and several host proteins essential for viral DNA replication *in vitro*, suggesting that these foci may represent viral chromatin replication centers (Tang, Bell et al., 2000; Zhao et al., 2008; Sowd et al., 2012). However, SV40 infection activates ATM and ATR signaling, and several DNA damage signaling and repair proteins, e.g., MRN, γH2AX, ATRIP, Rad51, Brca1, FancD2 and 53BP1, co-localize with Tag at these foci (Zhao et al., 2008; Shi et al., 2005; Boichuk et al., 2010; Rohaly et al., 2010), implying a link between SV40 replication and damage signaling. On the other hand, interaction of ectopically expressed Tag with the spindle checkpoint protein Bub1 can induce cellular chromosome breaks (Hein et al., 2009), indicating that Tag interference with host mitotic checkpoint proteins may suffice to damage genomic DNA in uninfected cells.

As a first step to assess a potential link between SV40 chromatin replication and DNA damage signaling, viral replication centers in SV40-infected BSC40 monkey cells

were characterized in detail. Chromatin-bound Tag was visualized in subnuclear foci as expected and colocalized with newly replicated DNA that had incorporated the deoxynucleoside EdU (Figures 10A, 11A). Chromatin-bound PCNA, DNA polymerase δ, and the clamp-loader RFC, host proteins that are essential for viral DNA replication *in vitro,* colocalized with Tag foci in both BSC40 and human U2OS cells at 48 hours post infection (hpi) (Figures 10A, 11B-D and 12B-D). In contrast, Cdc45 and polymerase ε, essential components of the host replisome that colocalized with replicating chromatin in mock-infected BSC40 and U2OS cells (Figures 11E and 12C, D), were virtually excluded from viral replication centers (Figures 11F, G and 12C-E). The results strongly suggest that in infected cells, these chromatin-bound Tag foci represent sites of viral, rather than host, chromatin replication.

To determine whether SV40 DNA replication itself induces DNA damage signaling in the absence of viral infection, the plasmids pMini SV40-wt, and its replication-defective variants lacking Tag helicase activity (D474N) (Zhou et al., 2012), or containing a single base pair insertion that inactivates the viral origin (In-1) (Cohen, Wright et al., 1984), were transfected into BSC40 monkey cells (Figure 10B). As expected, all three plasmids expressed Tag, but only the SV40-wt plasmid replicated (Figure 10C, D). SV40-wt elicited phosphorylation of Chk1 and Chk2 more robustly than either of the replication-defective constructs (Figure 10D, compare lane 1 to lanes 2-3). Moreover, prominent γH2AX foci, a marker of DNA damage signaling in chromatin (Lobrich et al., 2010), colocalized with chromatin-bound Tag in viral replication centers in SV40-wt transfected cells (Figure 10E). In contrast, the few γH2AX foci detected in cells transfected with the replication defective plasmids did not colocalize with Tag (Figure 12E). Thus, in the context of transfected cells, viral DNA replication, but not SV40-driven Tag expression, is sufficient to induce DNA damage signaling, suggesting that DNA breaks in replicating viral chromatin may activate checkpoint signaling.

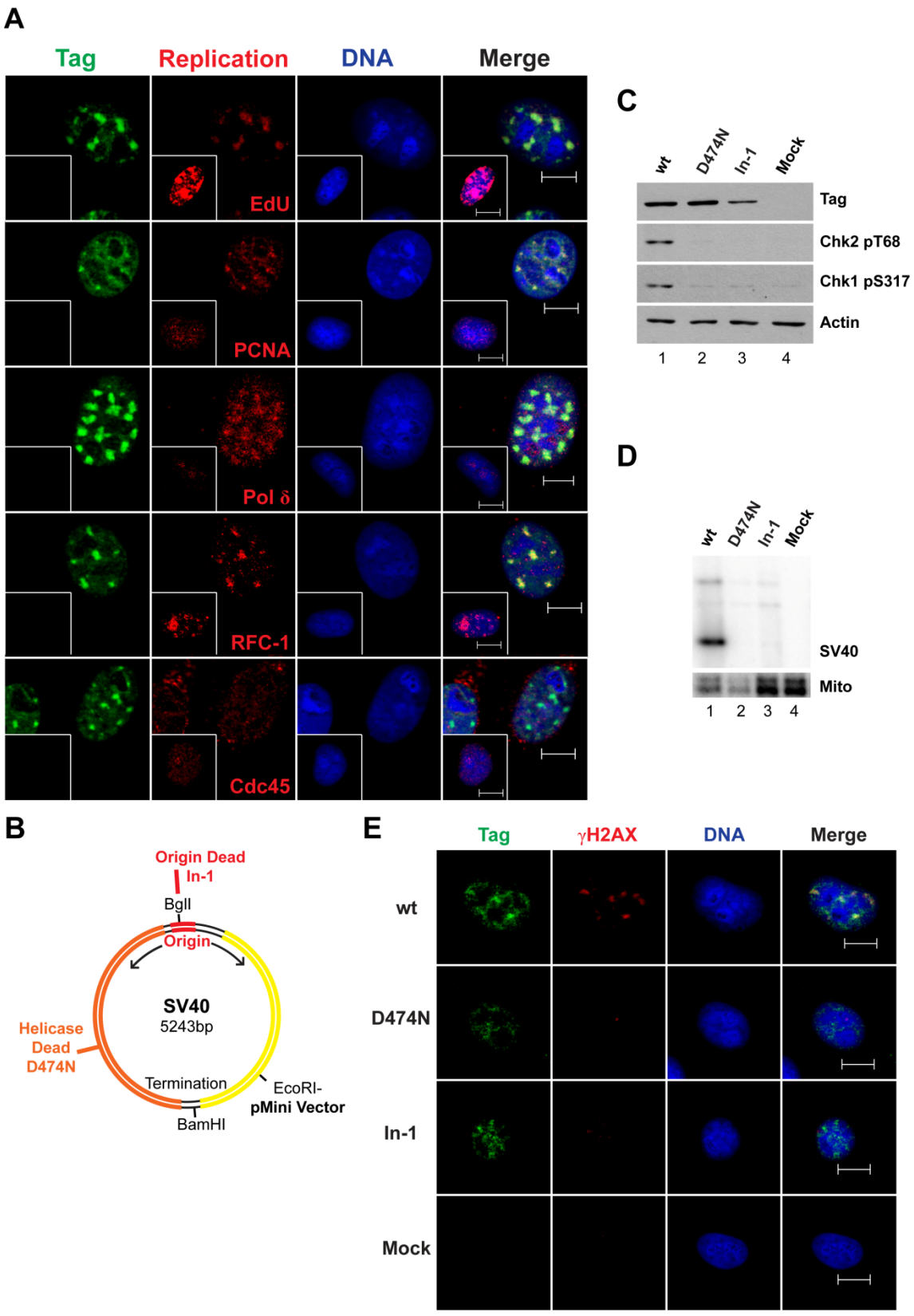
A
Tag
Replication
DNA
Merge
EdU
PCNA
Pol δ
RFC-1
Cdc45
C
wt
D474N
In-1
Mock
Tag
Chk2 pT68
Chk1 pS317
Actin
1 2 3 4
D
wt
D474N
In-1
Mock
SV40
Mito
1 2 3 4
B
Origin Dead
In-1
BglI
Origin
SV40
5243bp
Helicase
Dead
D474N
Termination
BamHI
EcoRI-
pMini Vector
E
Tag
γH2AX
DNA
Merge
wt
D474N
In-1
Mock

Figure 10.

Figure 10. SV40 chromatin replication results in DNA damage signaling.
(A) Representative images of chromatin-bound Tag and host DNA replication proteins in SV40- and mock-infected (inset) BSC40 cells at 48 hpi. (B) Features of the SV40 genome and the insertion site of pMini vector (Zhou et al., 2012). Mutation of Tag residue 474 from D to N abrogates helicase activity (Zhou et al., 2012). The defective SV40 origin mutant, In-1, features an insertion of a single GC bp in the center of the viral origin allowing Tag binding, but not origin activation (Cohen et al., 1984). (C, D, E) BSC40 cells transfected with the indicated pMini SV40 plasmids were analyzed by (C) western blot after 24 h, (D) Southern blot of low molecular weight DNA after 48 h (Hirt, 1967; Zhou et al., 2012), or (E) immunofluorescence microscopy of chromatin-bound proteins. In (D), SV40 or Mitochondrial probe signal is denoted by SV40 or Mito, respectively. Scale bars in (E), 10 μm.

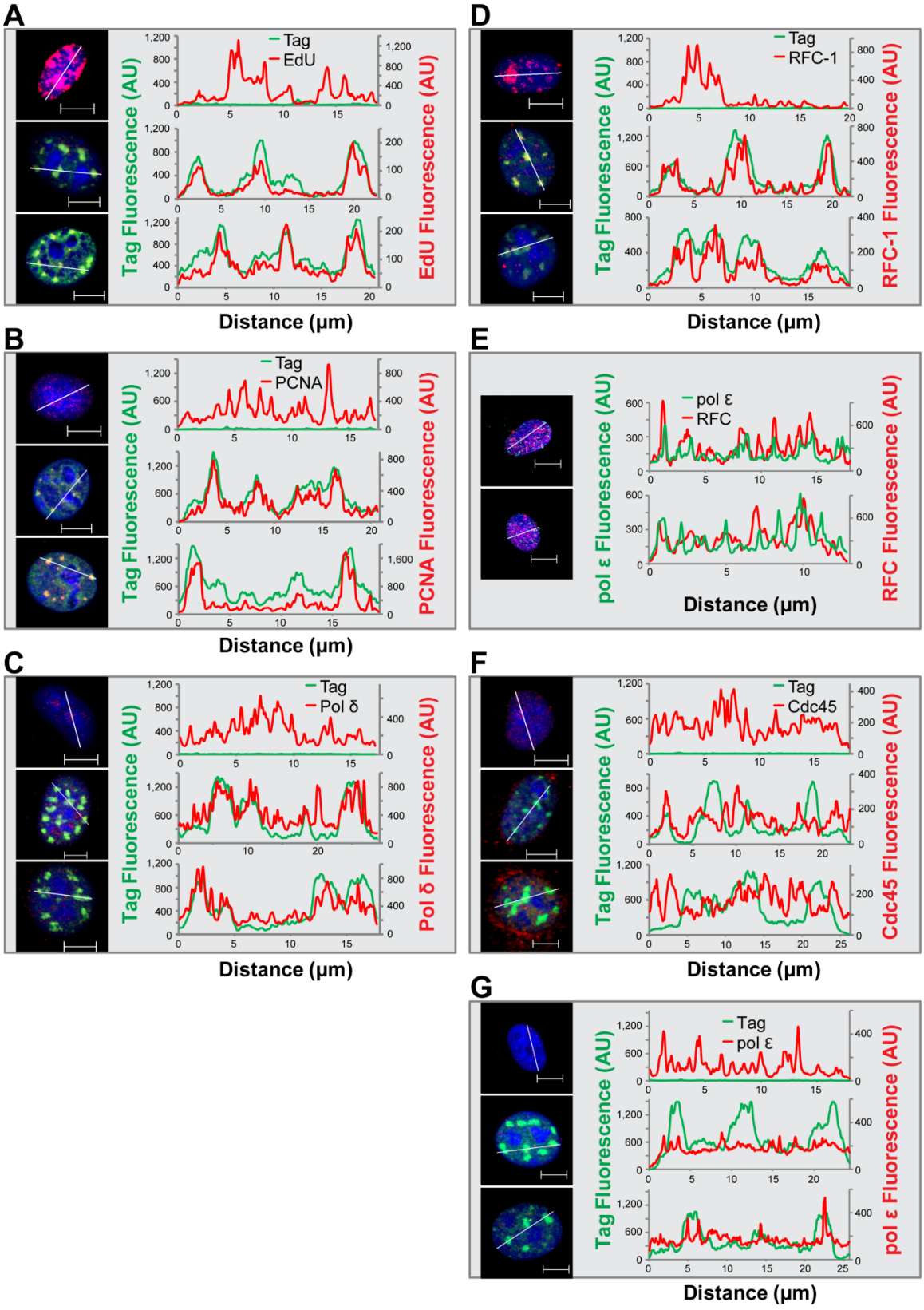
A
Tag
EdU
Tag Fluorescence (AU)
EdU Fluorescence (AU)
Distance (μm)
B
Tag
PCNA
Tag Fluorescence (AU)
PCNA Fluorescence (AU)
Distance (μm)
C
Tag
Pol δ
Tag Fluorescence (AU)
Pol δ Fluorescence (AU)
Distance (μm)
D
Tag
RFC-1
Tag Fluorescence (AU)
RFC-1 Fluorescence (AU)
Distance (μm)
E
pol ε
RFC
pol ε Fluorescence (AU)
RFC Fluorescence (AU)
Distance (μm)
F
Tag
Cdc45
Tag Fluorescence (AU)
Cdc45 Fluorescence (AU)
Distance (μm)
G
Tag
pol ε
Tag Fluorescence (AU)
pol ε Fluorescence (AU)
Distance (μm)

Figure 11.

Figure 11. Viral replication centers co-localize with host DNA replication factors in SV40-infected BSC40 cells.

(A - G) Merged images of chromatin-bound Tag and the indicated host DNA replication factors from mock- or SV40-infected BSC40 cells at 48 hpi. Top image for each replication protein is a mock-infected cell. Both images in (E.) are mock-infected cells. The fluorescence intensity in arbitrary units (AU) along the line shown in the merged image is graphed in the right panel. Scale bars, 10 μm.

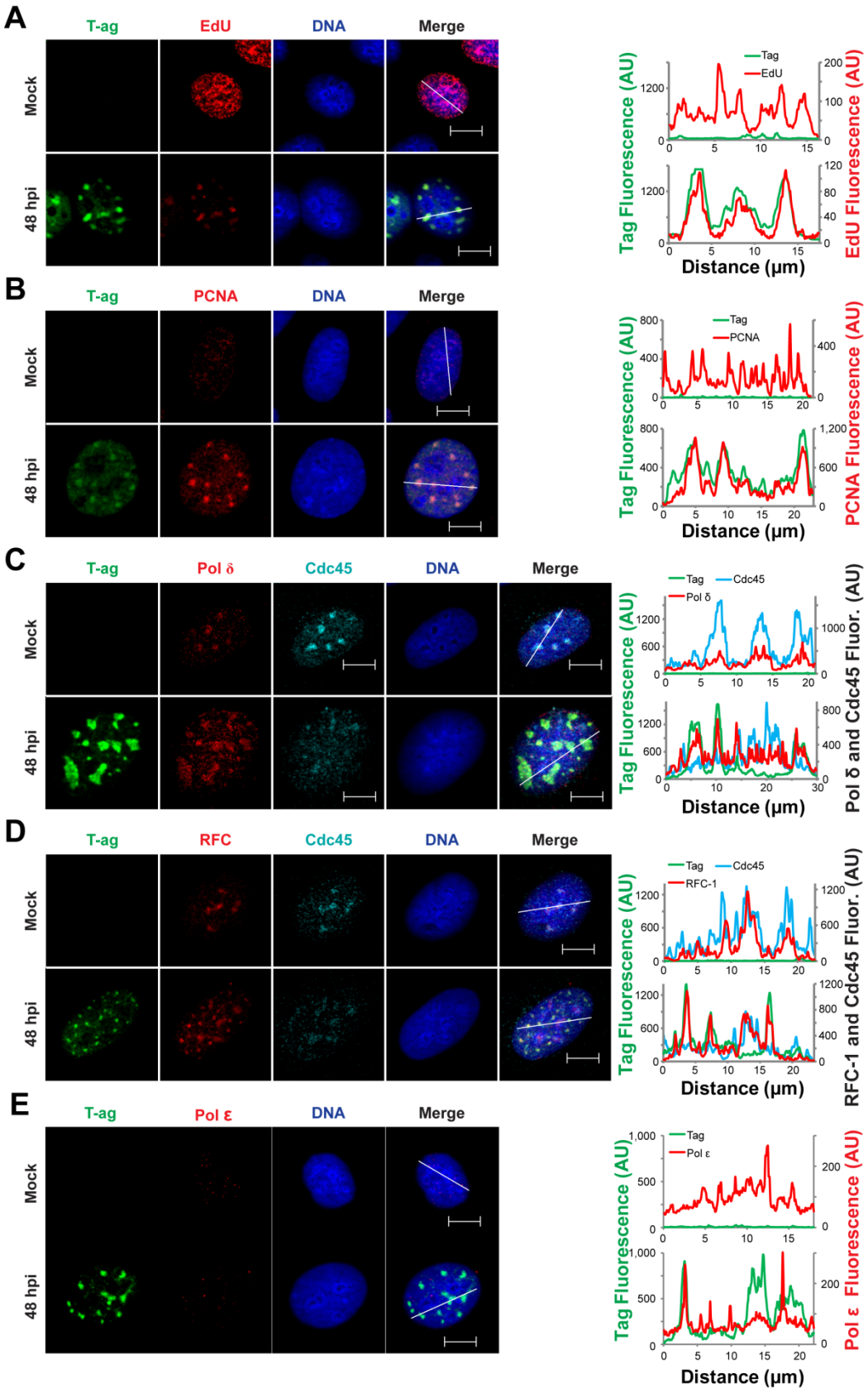
A
T-ag
EdU
DNA
Merge
Mock
48 hpi
Tag
EdU
Tag Fluorescence (AU)
EdU Fluorescence (AU)
Distance (μm)
B
T-ag
PCNA
DNA
Merge
Mock
48 hpi
Tag
PCNA
Tag Fluorescence (AU)
PCNA Fluorescence (AU)
Distance (μm)
C
T-ag
Pol δ
Cdc45
DNA
Merge
Mock
48 hpi
Tag
Cdc45
Pol δ
Tag Fluorescence (AU)
Pol δ and Cdc45 Fluor. (AU)
Distance (μm)
D
T-ag
RFC
Cdc45
DNA
Merge
Mock
48 hpi
Tag
Cdc45
RFC-1
Tag Fluorescence (AU)
RFC-1 and Cdc45 Fluor. (AU)
Distance (μm)
E
T-ag
Pol ε
DNA
Merge
Mock
48 hpi
Tag
Pol ε
Tag Fluorescence (AU)
Pol ε Fluorescence (AU)
Distance (μm)

Figure 12.

Figure 12. Host DNA replication proteins co-localize with Tag in SV40-infected U2OS cells.
(A - E) Representative images of chromatin-bound Tag and the indicated host DNA replication proteins from SV40-infected U2OS cells at 48 hpi. The fluorescence intensity in arbitrary units (AU) along the line shown in the merged image is graphed in the right panel. Scale bars, 10 μm.

Inhibition of ATM disrupts viral DNA replication centers

To determine the temporal requirements for ATM activity during infection, we exposed infected cells to the specific ATM chemical inhibitor Ku-55933 (Hickson et al., 2004) during the early phase (virus entry, Tag expression, host DNA synthesis), late phase (viral DNA replication, late gene expression, and virion assembly), or throughout a 48-hour infection (Figure 13A). Infected cells exposed to the Ku-55933 solvent, DMSO, served as a positive control. Mock-infected cells not treated with inhibitor served as a negative control. As previously observed, ATM activity was stimulated by infection, as indicated by phosphorylated Nbs1 and Chk2 in western blots (Figure 13B, compare lane 1 to lane 5), reduced by the presence of Ku-55933 in either the early or late phase of infection (Figure 13B, compare lanes 2, 3 to lane 1), and nearly abolished by the presence of Ku-55933 throughout infection (Figure 13B, lane 4). Notably, only inhibition of ATM during viral DNA replication resulted in robust DNA-PK_{cs} activation denoted by auto-phosphorylation of residue S2056 (Figure 13B, lane 3).

To assess the impact of ATM inhibition during each phase of infection on viral chromatin replication, we visualized viral replication centers and DNA damage signaling in each infected cell population using immunofluorescence microscopy (Figure 13C). In infected cells exposed to DMSO, the normal, brightly stained viral replication centers with colocalized Tag, EdU, and γH2AX were observed (Figure 13C). When Ku-55933 was present only during the early phase of infection, about half of the cells displayed normal replication centers with colocalized Tag, EdU and γH2AX foci (Figure 13C and D). However, aberrant pan-nuclear staining of Tag, EdU, and γH2AX predominated when Ku-55933 was present during the late phase or throughout infection (Figure 13C and D). Taken together, these results demonstrate that ATM activity is beneficial but not essential during the early phase of infection, whereas it is vital for the assembly and/or stability of viral replication centers during the late phase of infection.

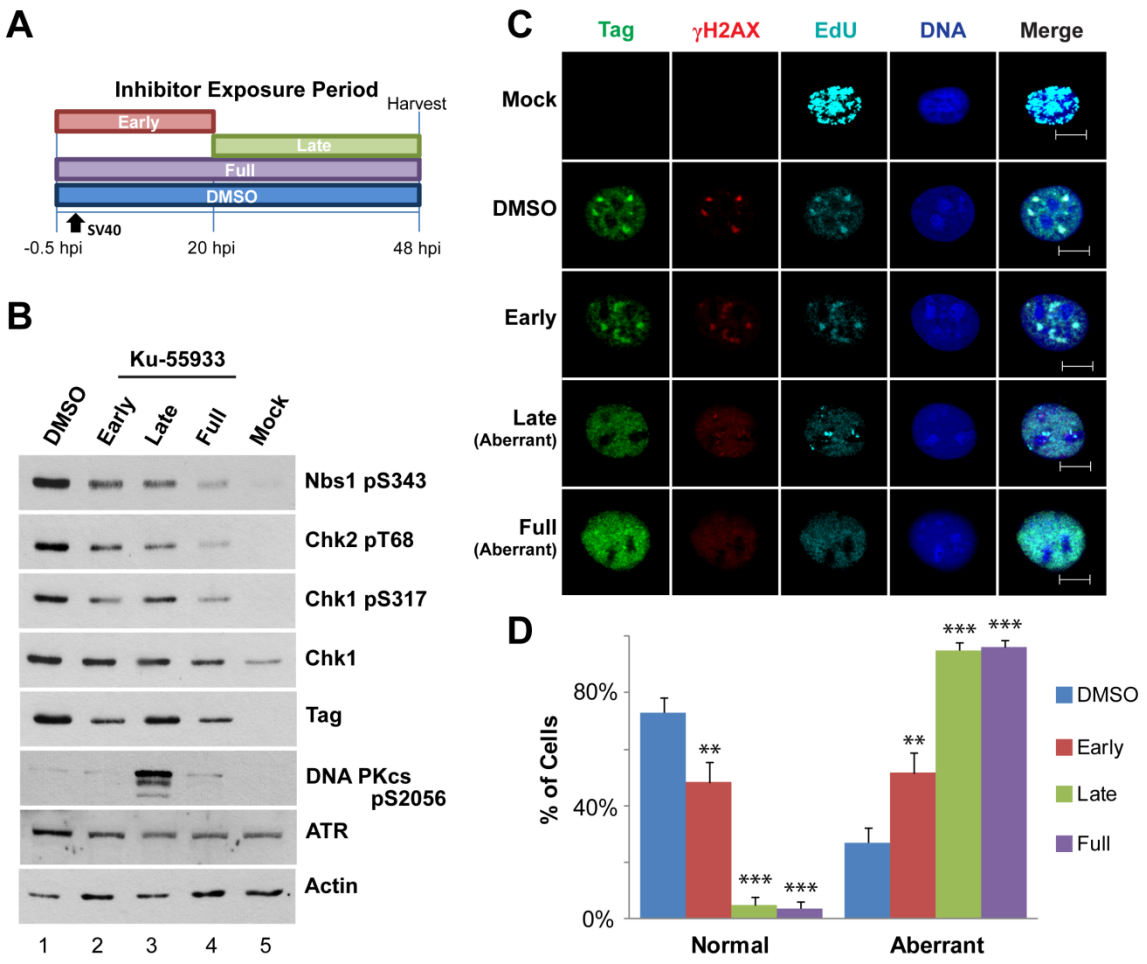

Figure 13. ATM inhibition during viral DNA replication disrupts viral replication centers.
(A) Experimental scheme for treatment of cells with inhibitor during phases of a 48 h SV40 infection. Early: inhibitor present from -0.5 to 20 hpi. Late: inhibitor present from 20 to 48hpi. DMSO and Full: solvent or inhibitor, respectively, present from -0.5 to 48 hpi. (B) Western blot of cells treated with Ku-55933 as described in (A). (C) Immunofluorescence of cells treated with Ku-55933 as described in (A) and fixed at 48 hpi. Scale bars, 10 μm. (D) Tag staining patterns, as in (C), were quantified. Graph in (D) shows the average of 3 independent experiments.

Inhibition of ATM activity reduces the quantity and quality of viral replication products

The links between ATM activity, repair protein recruitment, and SV40 replication centers led us to hypothesize that inhibition of ATM might affect not only the level, but also the nature of the viral DNA replication products. To investigate this possibility, we used southern blotting to analyze total intracellular DNA from SV40-infected BSC40 cells that had been treated with DMSO or the specific ATM inhibitor Ku-55933 (Hickson et al., 2004) throughout infection (Figure 14A). Inhibition of ATM reduced the level of 5.2 kb viral DNA products migrating as form I (supercoiled), form II (nicked), and form III (linear), relative to that in the DMSO-treated control infections (Figure 14A, compare lanes 1-4 to 5-8). However, ATM inhibition also caused accumulation of high molecular weight SV40 DNA products too large to enter the gel (Figure 14A, compare lanes 3, 4 to lanes 7, 8). These large products failed to migrate into the gel after restriction digestion with enzymes that cut host DNA but not SV40 DNA. In contrast, most of these products collapsed into unit length linear SV40 DNA after digestion with an enzyme that cleaves SV40 DNA once (Figure 15A), indicating that the large DNA products contain head-to-tail repeats of unit length viral DNA.

To quantify the data in Figure 14A, the signal in SV40 monomer bands (forms I, II, and III) in each sample was normalized to that of mitochondrial DNA (Mito) in the same sample. This normalized monomer signal in each sample was then compared to that of the normalized monomer bands in the positive control at 72 hpi. (Figure 14A, lane 4) and graphed in Figure 14B. The graph reveals that ATM inhibition reduced unit length SV40 product by at least 5-fold compared to the DMSO control infections (Figure 14B). Quantification of the concatemeric SV40 DNA in each sample relative to that of the total SV40 signal in the same sample revealed that ATM inhibition increased accumulation of viral DNA concatemers by an order of magnitude compared to that in the DMSO control

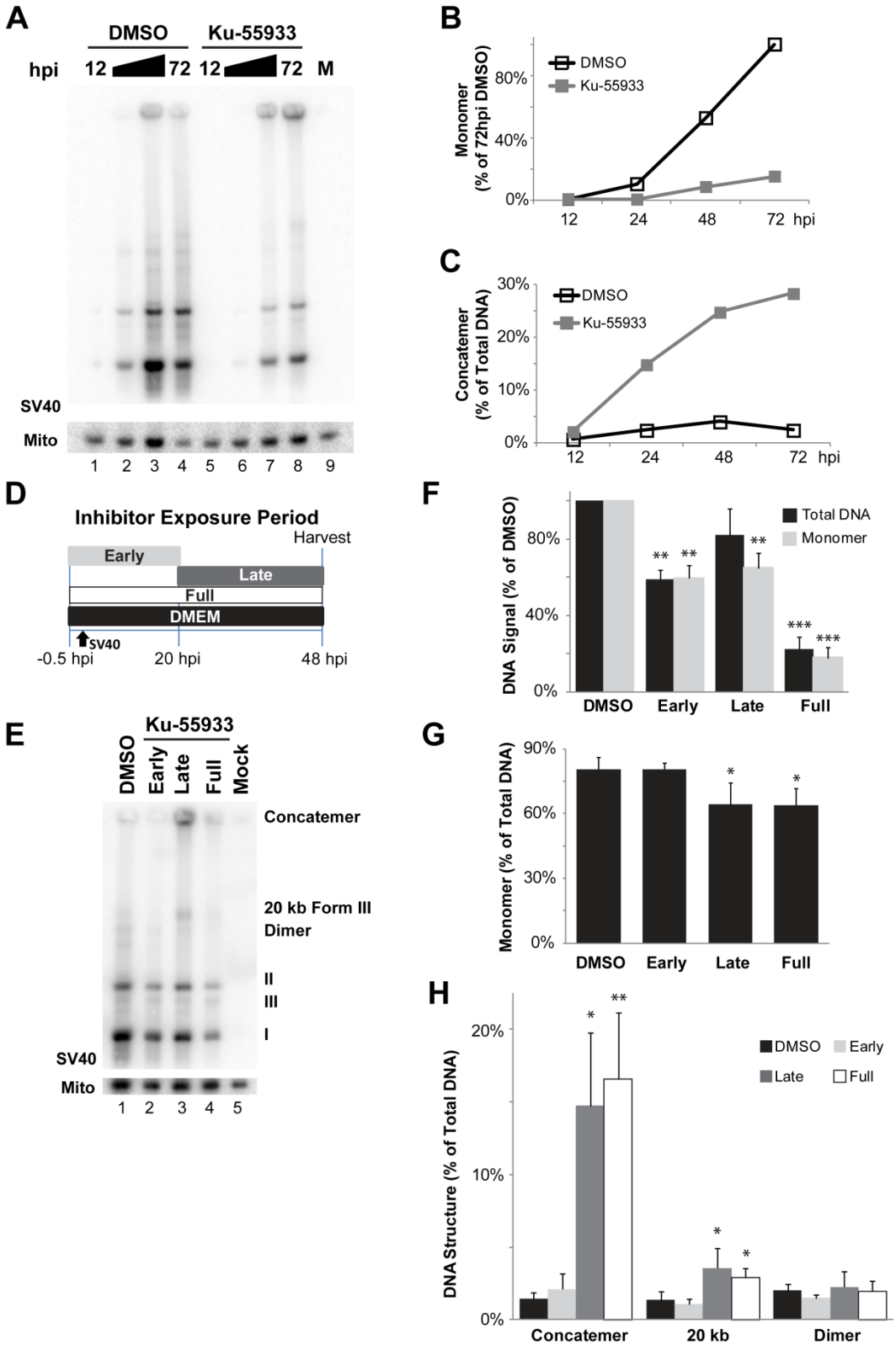
A
DMSO
Ku-55933
hpi
12
72
12
72
M
SV40
Mito
1 2 3 4 5 6 7 8 9
B
Monomer (% of 72hpi DMSO)
80%
40%
0%
DMSO
Ku-55933
12
24
48
72 hpi
C
Concatemer (% of Total DNA)
30%
20%
10%
0%
DMSO
Ku-55933
12
24
48
72 hpi
D
Inhibitor Exposure Period
Harvest
Early
Late
Full
DMEM
SV40
-0.5 hpi
20 hpi
48 hpi
E
Ku-55933
DMSO
Early
Late
Full
Mock
Concatemer
20 kb Form III
Dimer
II
III
I
SV40
Mito
1 2 3 4 5
F
DNA Signal (% of DMSO)
80%
40%
0%
Total DNA
Monomer
**
**
**
***
***
DMSO
Early
Late
Full
G
Monomer (% of Total DNA)
90%
60%
30%
0%
*
*
DMSO
Early
Late
Full
H
DNA Structure (% of Total DNA)
20%
10%
0%
*
**
*
*
DMSO
Early
Late
Full
Concatemer
20 kb
Dimer

Figure 14.

Figure 14. Ku-55933 treatment during viral DNA replication increases aberrant DNA structures. (A) Southern blot of DNA from SV40 infected BSC40 cells in the presence of DMSO or Ku-55933. DMSO or Ku-55933 was present from 30 min prior to infection until cell collection timepoint. M represents Mock-infected cells. (B) Each normalized monomer SV40 form I, II, and III product in (A) was graphed as a fraction of the corresponding normalized monomer produced at 72 hpi in the DMSO control infection. (C) Graph of the percentage of DNA products represented by concatemers in panel (A). (D) Scheme for treatment of cells with inhibitor during defined periods of a 48 h SV40 infection. Early: inhibitor present from -0.5 to 20 hpi. Late: inhibitor present from 20 to 48hpi. DMSO and Full: solvent or inhibitor, respectively, present from -0.5 to 48 hpi. (E) Southern blot of SV40 DNA replicated in the presence of Ku-55933 during phases of a 48 h infection in BSC40 cells as explained in (D). (F) Quantification of total and monomeric SV40 DNA signal normalized to DMSO control from southern blots as in (E). (G, H) Graph of DNA structures (monomer: G and DNA Structure: H) accumulating on southern blots as in (E). Graphs in (F - H) represent 3 to 4 independent experiments.

samples (Figure 14C). Thus, inhibition of ATM throughout infection reduced monomeric and increased concatemeric SV40 DNA products.

Total intracellular DNA was extracted from infected BSC40 cells exposed to Ku-55933 during the three time windows, as diagrammed in Figure 14D. The purified DNA was separated by gel electrophoresis and analyzed in southern blots (Figure 14E). Inhibition of ATM either early or throughout infection reproducibly reduced the level of total viral DNA and monomeric DNA products by 50-80% relative to that generated in the DMSO-treated control infection (Figure 14E, F). Similarly, in the late phase of infection, inhibition reduced viral DNA monomers to a level comparable to that observed when ATM was inhibited during the early phase, yet total viral DNA was only insignificantly decreased compared to DMSO-treated cells (Figure 14E, F). SV40 monomers comprised about 80% of the total viral DNA signal in samples from infected cells exposed to DMSO or Ku-55933 during early phase (Figure 14G). In contrast, monomers comprised only 64% of the total signal in samples treated with Ku-55933 late or throughout infection (Figure 14G). When Ku-55933 was applied either during the late phase or throughout infection, the fraction of total viral DNA in concatemers increased 10- and 11-fold, respectively, relative to the fraction in DMSO-treated infected cells (Figure 14H). The fraction of total SV40 DNA migrating greater than 20-kb linear (20 kb) also increased in cells treated with Ku-55933 late or throughout infection, relative to that in DMSO-treated control infections (Figure 14H).

To confirm these findings in a different cell background, the temporal requirements for ATM activity were also determined in SV40-infected human U2OS cells, with similar results (Figure 15B-E). Taking the results together, we infer that SV40-infected cells require ATM signaling, primarily during the late phase of infection, to favor production of unit-length genomes rather than aberrant products.

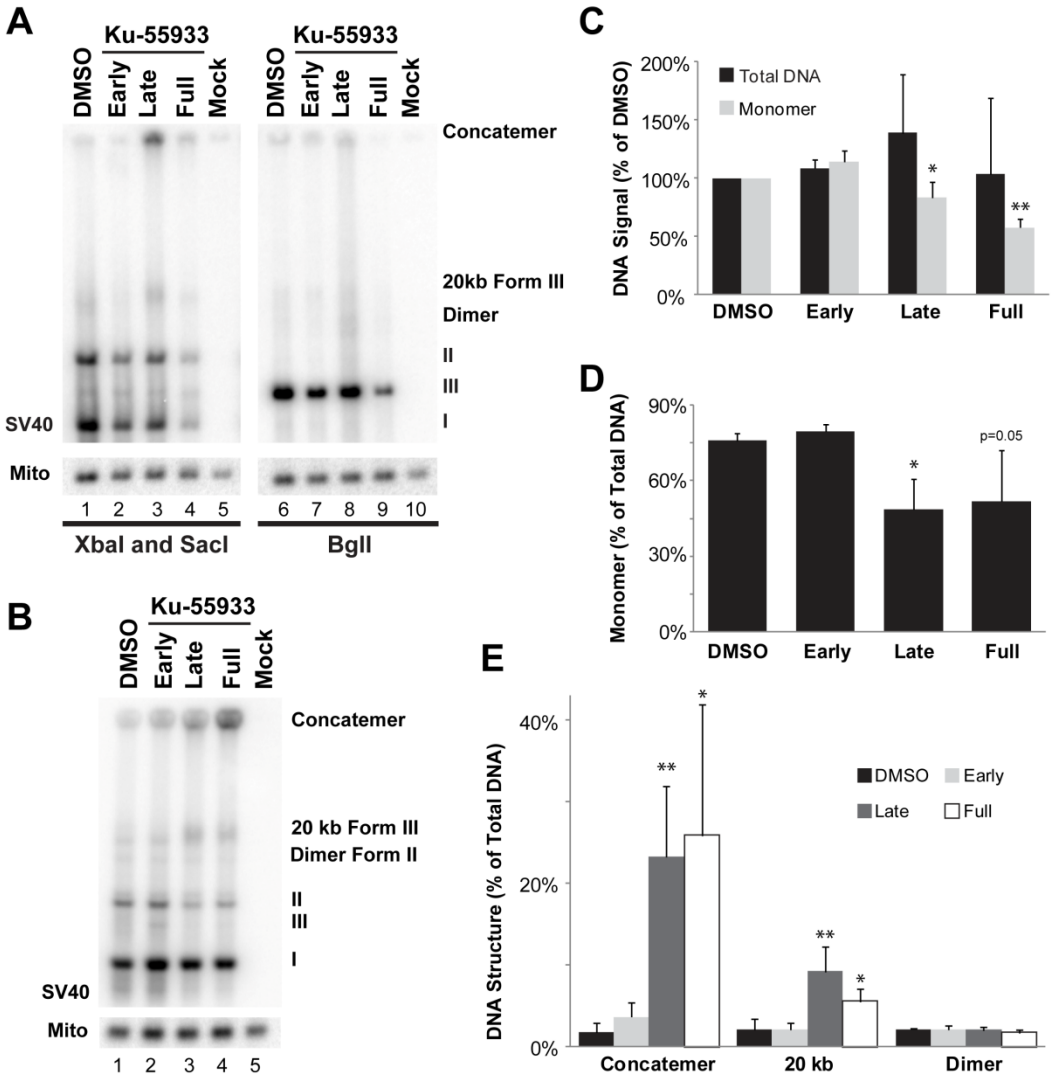

Figure 15. Aberrant DNA structures accumulate in ATM-inhibited SV40-infected U2OS cells. (A) Total DNA extracted at 48 hpi from SV40-infected BSC40 cells treated with Ku-55933 during the indicated phases of infection, as in figure 21D, was analyzed by southern blot. Lanes 1-5: DNA digested with XbaI and SacI. Lanes 6-10: DNA digested with BglI. (B) Southern blot of DNA replicated in SV40-infected U2OS cells in the presence of ATM inhibitor during the indicated phases of infection. (C) Quantification of SV40 signal in monomeric forms and the whole sample in each lane, normalized to the corresponding signals in the DMSO solvent lane as in panel B. (D, E) Fraction of signal in monomer forms (D) or in the indicated DNA structure (E) in DNA extracted at 48 hpi from cells treated with Ku-55933 during the indicated phases of infection as in panel B. Values in (C - E) represent the average of 3 to 4 independent experiments.

ATM inhibition increases rolling circle DNA replication and strand invasion

To better understand how the aberrant viral replication products arise, we compared replication intermediates generated with and without Ku-55933 during the late phase of infection. The total DNA was first digested with a restriction nuclease that cleaves SV40 once in the viral origin (BglI) or once in the region of termination (BamHI). Neutral two-dimensional (2d) gel electrophoresis was then used to separate viral replication intermediates from the accumulated non-replicating unit-mass SV40 DNA, followed by southern blotting using the whole SV40 genome as the probe (Friedman and Brewer, 1995). Replicating viral DNA is present in the form of circular, converging forks known as Cairns intermediates (Figure 16B). The digestion of Cairns intermediates with BglI or BamHI results in double Ys or bubbles, respectively (Figure 16A, B). In the BglI-cleaved DNA from DMSO-treated control infections, the bubble arc was absent and the unit-mass viral DNA migrated in the 1n spot as expected (Figure 16A-C). Also as expected, an intense double Y arc indicative of converging forks and an X structure signal indicative of hemi-catenanes or Holliday junctions were observed (Figure 16C). In addition, the simple Y arc signal revealed some unidirectional replicating forks (Figure 16C) that can be most easily explained by rolling circle replication. When BamHI-cleaved DNA from DMSO-treated infected cells was analyzed by 2d gel electrophoresis, the bubble arc was detected and the double Y arc was absent, as expected (Figure 16D). Similar to BglI digestion, both an X structure and a weaker simple Y arc were present (Figure 16D).

In contrast, the pattern of BglI-digested viral replication intermediates generated in the presence of Ku-55933 displayed a much fainter double Y arc and a more intense simple Y arc (compare Figure 16E with C). Similarly, X structures, and D-loops/complex branched intermediates (red star) were more prominent when ATM was inhibited (compare Figure 16E with C), consistent with increased Holliday junction formation

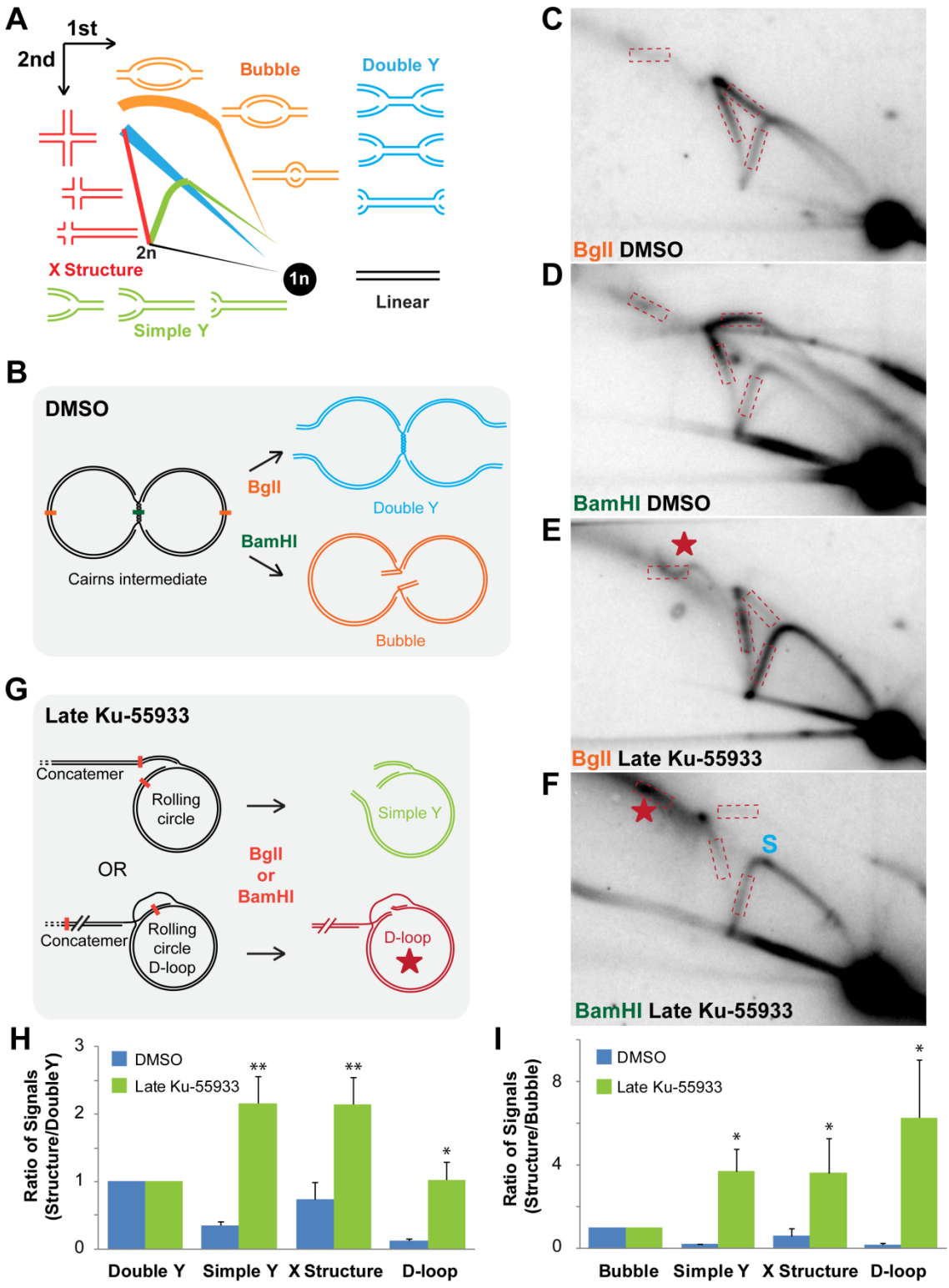
A
1st
2nd
Bubble
Double Y
X Structure
2n
1n
Linear
Simple Y
B
DMSO
BglI
Double Y
BamHI
Cairns intermediate
Bubble
C
BglI DMSO
D
BamHI DMSO
E
BglI Late Ku-55933
F
S
BamHI Late Ku-55933
G
Late Ku-55933
Concatemer
Rolling circle
Simple Y
OR
BglI or BamHI
Concatemer
Rolling circle D-loop
D-loop
H
Ratio of Signals (Structure/DoubleY)
DMSO
Late Ku-55933
Double Y
Simple Y
X Structure
D-loop
I
Ratio of Signals (Structure/Bubble)
DMSO
Late Ku-55933
Bubble
Simple Y
X Structure
D-loop

Figure 16.

Figure 16. ATM inhibition increases recombination and unidirectional replication.
(A) Diagram of neutral 2d gel electrophoresis arcs generated from digested SV40 DNA. (B) Replicating viral DNA extracted from unperturbed SV40-infected cells consists primarily of circular, late replication intermediates called late Cairns intermediates. Digestion of late Cairns intermediates with BglI yields large double Ys, whereas BamHI digestion yields large bubbles. (C, D, E, F) Southern blot of neutral 2d gel of BglI-cleaved DNA replicated in the presence of DMSO (C, D) or Ku-55933 (E, F) during the late phase of a 48h SV40 infection in BSC40 cells. DNA was cleaved within the viral origin of replication with BglI (C, E) or the region of fork convergence with BamHI (D, F). The red star denotes an arc representing strand invasion events (D-loops) or highly branched molecules (Preiser, Wilson et al., 1996; Backert, 2002). On the simple Y arc in (F), S denotes a replication stall point near the viral origin of replication. Dashed boxes denote regions of each arc quantified in (H) and (I). (G) Concatemers of SV40 DNA that accumulated when ATM was inhibited can arise by either replication- (top) or recombination- (bottom) dependent rolling circle replication. Digestion of replication-dependent rolling circles with BglI or BamHI results in simple Ys of all sizes. Digestion of recombination-dependent rolling circles creates D-loops of all sizes. (H) Graph of DNA signal present on simple Y, double Y, X structure, or D-loop arc divided by DNA signal in the double Y arc from DNA digested with BglI. (I) Graph of DNA signal from BamHI digested DNA in simple Y, bubble, X structure, or D-loop arc divided by DNA signaling in the bubble arc. Each graph in (H) and (I) represents the average of 3 to 4 independent experiments.

between replicating rolling circles (Preiser et al., 1996; Backert, 2002). Likewise, BamHI-cleaved replication intermediates from Ku-55933-treated infections displayed a robust simple Y arc and a corresponding decrease in the bubble arc (Figure 16F). Moreover, the intense X structure and D-loop arcs were retained (Figure 16F). These patterns suggest that inhibition of ATM sharply increased the frequency of rolling circle replication (Figure 16G). Quantification of the signal present in the simple Y, X structure, D-loop, and double Y arcs from BglI-digested DNA (Figure 16C, E boxes) showed that ATM inhibition increased the abundance of simple Ys, X structures, and D-loop arcs relative to the double Y arc by six, three, and eight-fold, respectively, from three to four independent experiments (Figure 16H). Analogously, quantification of BamHI-digested DNA (Figure 16D, F boxes) revealed ATM inhibition increased the quantities of simple Ys, X structures, and D-loop arcs relative to the bubble arc (Figure 16I). We conclude that the ATM inhibitor Ku-55933 increased both rolling circle replication and strand invasion events at the expense of bidirectional SV40 chromatin replication.

Caffeine inhibits SV40 chromatin replication

The importance of ATM activity in SV40 chromatin replication suggested the possibility that other checkpoint kinases might also contribute to viral infection. To further explore this question, we treated SV40-infected BSC40 cells with caffeine, a less selective inhibitor of both ATM and ATR *in vitro* and of the S/G2 checkpoints *in vivo* (Sarkaria, Busby et al., 1999). Of note, caffeine is structurally unrelated to the more potent Ku-55933 and ATR inhibitors (Hickson et al., 2004; Reaper et al., 2011). As expected, caffeine inhibited phosphorylation of Chk1 and Chk2 when present during the late phase or throughout infection (Figure 17A, B) but also hyper-activated DNA-PK (Figure 17B, compare lane 1 with lanes 2-4) (Chen et al., 2005). Caffeine reduced the level of total viral DNA products in SV40-infected BSC40 cells to less than 1% of the

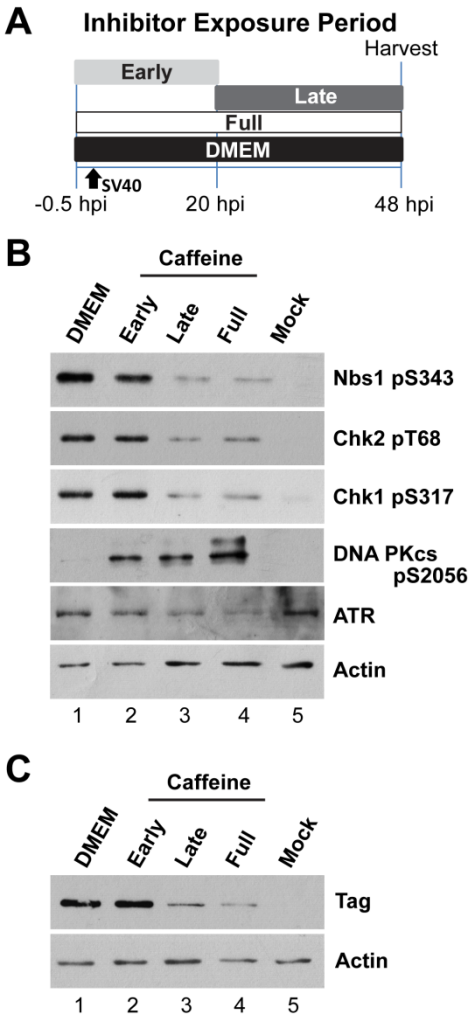

Figure 17. Caffeine inhibits ATM and ATR activities in SV40-infected BSC40 cells.
(A) BSC40 cells were treated with caffeine during the indicated phases of a 48 h SV40 infection. (B, C) Western blots of cell lysates from SV40-infected BSC40 cells exposed to caffeine as depicted in (A).

control level when caffeine was present throughout infection (Figure 18A, B). Exposure to caffeine late or throughout infection reduced the fraction of total viral DNA signal in monomers (form I, II, III) and increased the fraction in concatemers and other aberrant products (Figure 18A, C, D). Similarly, in SV40-infected U2OS cells, caffeine reduced total viral replication products and increased the fraction of aberrant products (Figure 18E-H). The results further confirm a role for ATM activity in SV40 chromatin replication in infected cells and suggest that ATR and/or DNA-PK activity may stimulate viral replication.

DNA-PK$_{cs}$ activity is dispensable for SV40 chromatin replication

Although SV40 infection did not activate DNA-PK, it was activated in infected cells exposed to Ku-55933, ATRi, or caffeine, as evidenced by DNA break-dependent auto-phosphorylation of DNA-PK at S2056 (Chen et al., 2005). To test for a potential role of DNA-PK activity in viral chromatin replication, SV40-infected BSC40 cells were exposed to small molecule inhibitors of DNA-PK during the early or late phase, or throughout infection, and total intracellular DNA was analyzed by southern blotting (Figure 19A-C). When DNA-PK was inhibited with either Nu7441 or Nu7026, the levels of viral monomer and aberrant viral DNA products closely resembled those in SV40-infected BSC40 cells (Figure 19D). Moreover, inhibition of DNA-PK had little or no effect on viral replication centers (data not shown). Thus, it is unlikely that DNA-PK has a major role in viral chromatin replication in unperturbed infected cells.

Inhibition of ATR decreases SV40 DNA replication

The role of ATR kinase activity in infection was directly examined by treating SV40-infected BSC40 cells with a specific small molecule inhibitor of ATR, VE-821 (ATRi) (Reaper et al., 2011), during three different time windows of infection (Figure

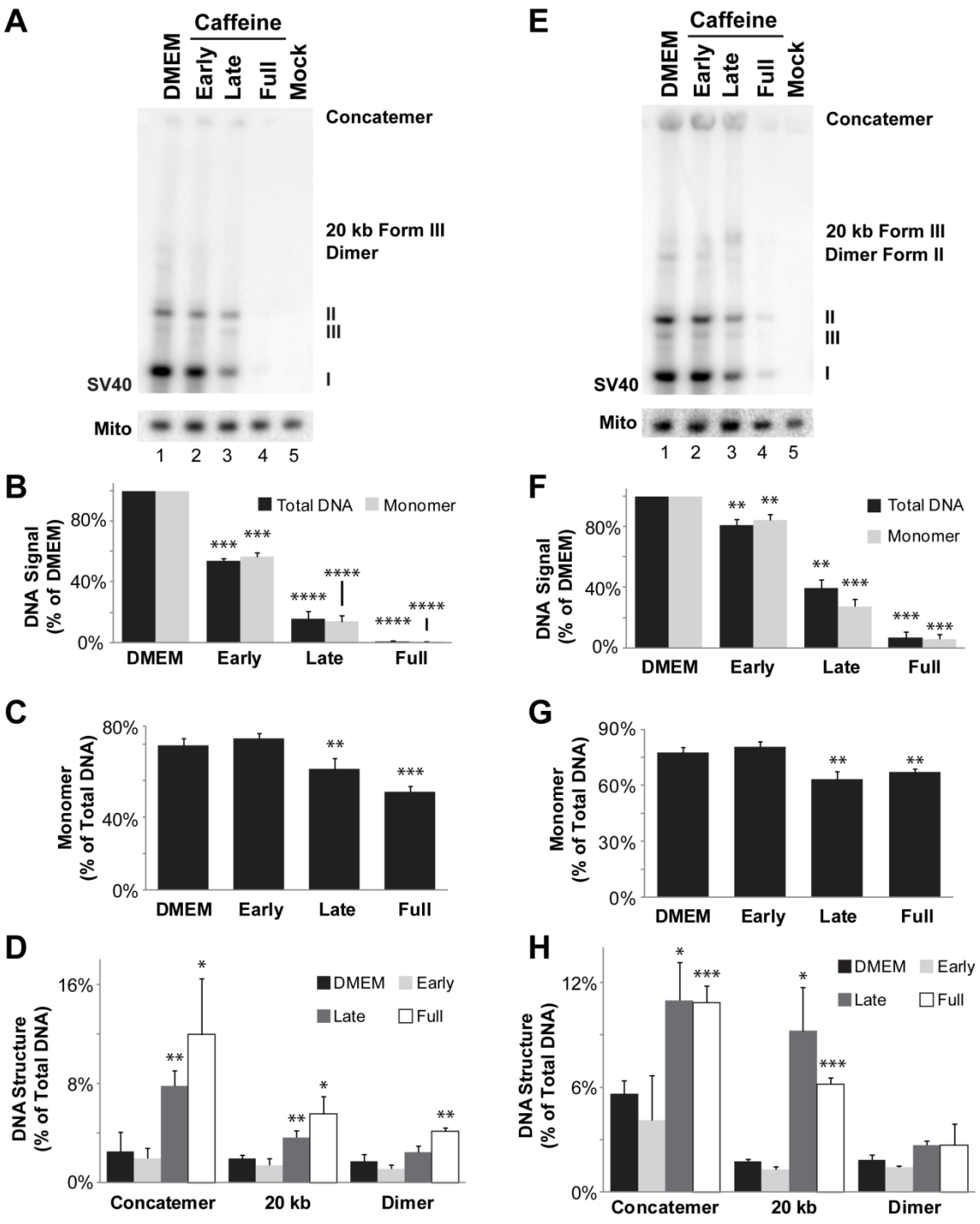

Figure 18. ATM and ATR inhibition increases aberrant DNA product accumulation.
(A, E) Southern blots of total DNA extracted from BSC40 (A) or U2OS (E) cells treated with caffeine during phases of SV40 infection as described in Figure 24A. (B, F) Quantification of signal in SV40 monomer forms or total DNA in caffeine-treated BSC40 (B) or U2OS (F) cells, normalized to that in DMEM solvent. (C, D, G, H) SV40 signal in monomer forms (C and G) or aberrant DNA structures (D and H) accumulated in caffeine-treated BSC40 (C and D) or U2OS (G and H) cells, divided by the total SV40 DNA signal in respective lane. Bars in (B - D) and (F - H) represent the average of 3 to 4 independent experiments.

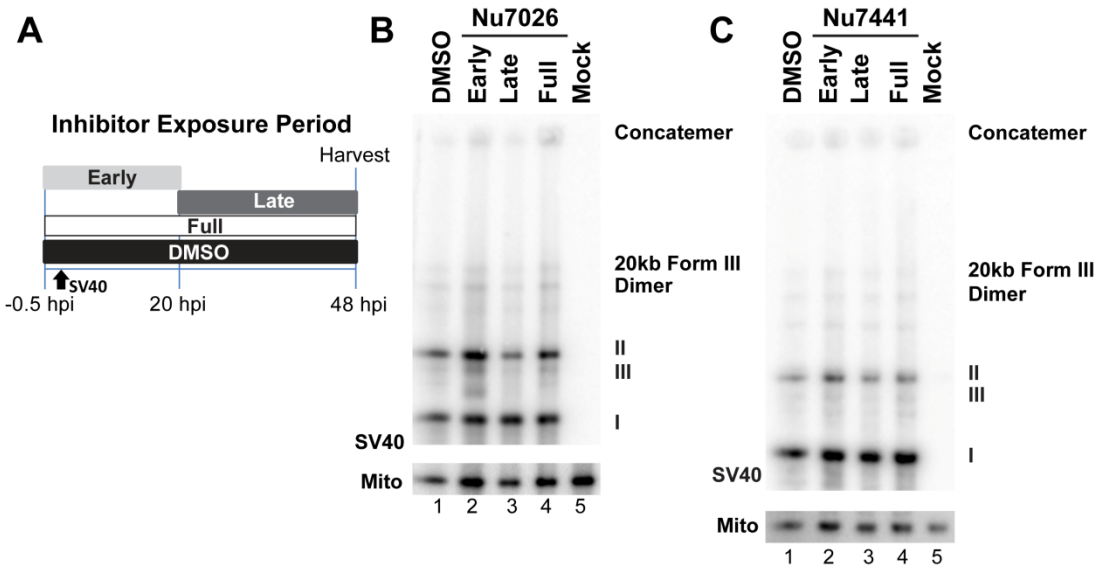

D

	Nu7026				Nu7441			
	DMSO	Early	Late	Full	DMSO	Early	Late	Full
Monomer (% of DMSO)	100%	91%	103%	86%	100%	99%	101%	122%
Total DNA (% of DMSO)	100%	98%	102%	89%	100%	98%	99%	120%
Concatemer (% of Total DNA)	0.8%	0.8%	0.6%	1.9%	1.1%	0.9%	0.8%	0.8%
Monomer (% of Total DNA)	81%	76%	83%	79%	89%	88%	90%	90%

Figure 19. DNA-PK$_{cs}$ activity is dispensable in unperturbed SV40 infection.
(A) Experimental scheme for treatment of BSC40 cells with DNA PK inhibitors during phases of a 48 h SV40 infection. (B, C) Southern blots of DNA extracted from BSC40 cells treated as in (A) with Nu7026 (B) or Nu7441 (C). (D) Quantification of SV40 replication products as in (B, C).

20A). As expected, ATRi caused a third of the cells to lose viability over 48 h, but SV40-infected and mock-infected cells were equally sensitive (Figure 20B). SV40 infection activated Chk1, as indicated by phosphorylation of Ser317 (Figure 20C, compare lane 1 with lane 5), and ATRi effectively suppressed ATR activation during each time window (Figure 20C, lanes 2-4). Additionally, the presence of ATRi during any phase of SV40 infection induced DNA-PK activation (Figure 20D, lanes 2-4).

Viral DNA replication strongly elicits ATR activation, which is required for SV40-induced S-phase arrest. To determine whether ATR has other roles in directly promoting viral DNA replication beyond the S phase checkpoint, the DNA replication products from the four cell populations and mock-infected cells were analyzed by southern blotting and quantified relative to mitochondrial DNA in the same samples. In the presence of ATRi, the level of total viral DNA replication products declined markedly relative to that in DMSO-treated control infections, amounting to only 10% of the control when ATRi was present for the full 48 h (Figure 21B, C). In cells exposed to ATRi during the late phase or throughout infection, the fraction of viral DNA products in monomers (forms I, II and III) dropped, whereas that in concatemers and other aberrant products rose (Figure 21B-E and Figure 22A). Analysis of viral replication products from SV40-infected U2OS cells exposed to ATRi demonstrated a similar requirement for ATR activity (Figure 22B-D). Taken together, these results indicate that infected cells require ATR activity before, as well as during viral chromatin replication, for normal accumulation of viral genomes.

Chk1 inhibition decreases viral DNA replication

ATR activation following DNA damage results in the activation of the downstream kinase Chk1. The kinase activity of Chk1 is essential for S phase arrest in response to replication stress, and Chk1-inhibited or -depleted cells demonstrate many of the same

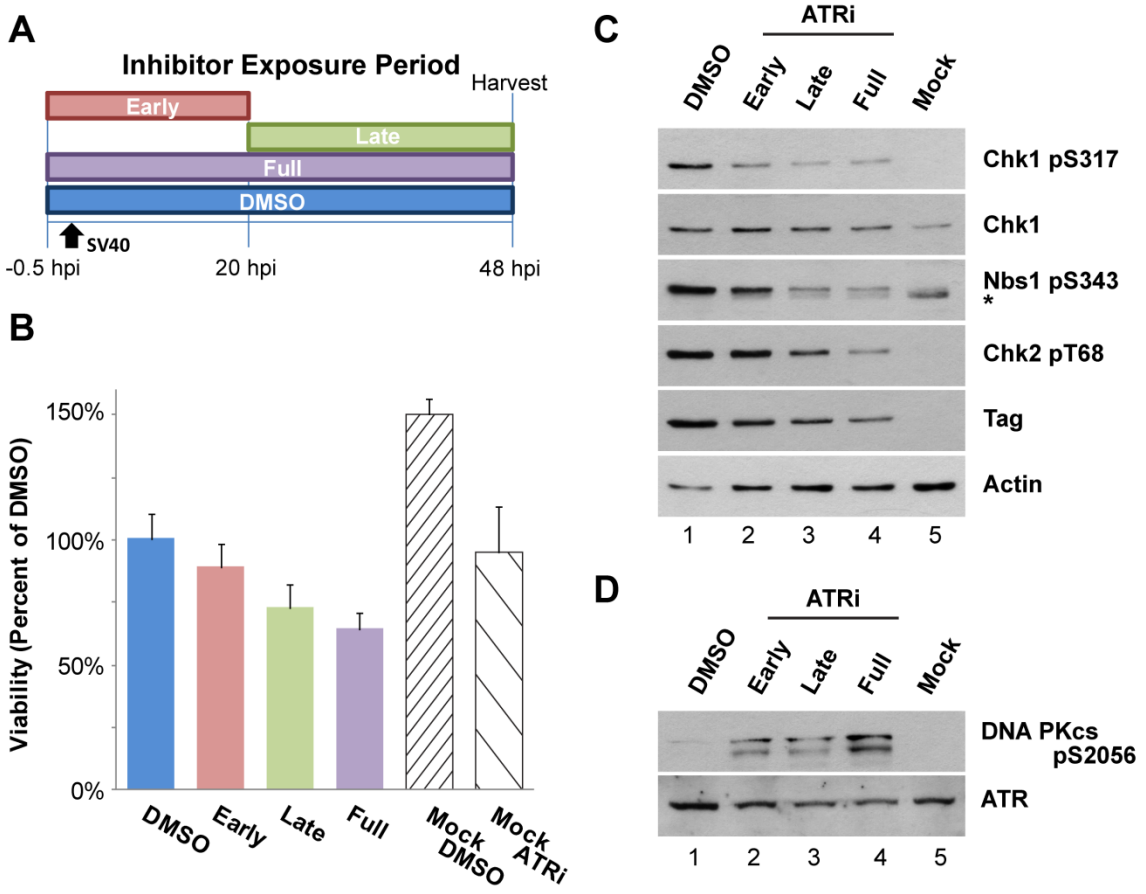

Figure 20. ATRi inhibits ATR activity in SV40-infected BSC40 cells.
(A) Exposure of SV40-infected BSC40 cells to ATRi during defined phases of a 48 h infection. (B) WST-1 viability assay of SV40-infected BSC40 cells treated with ATRi as described in (A). Values were normalized to SV40-infected cells in the presence of DMSO. Error bars represent four independent experiments. (C, D) Western blot of cell lysates from SV40-infected BSC40 cells exposed to ATRi as indicated.

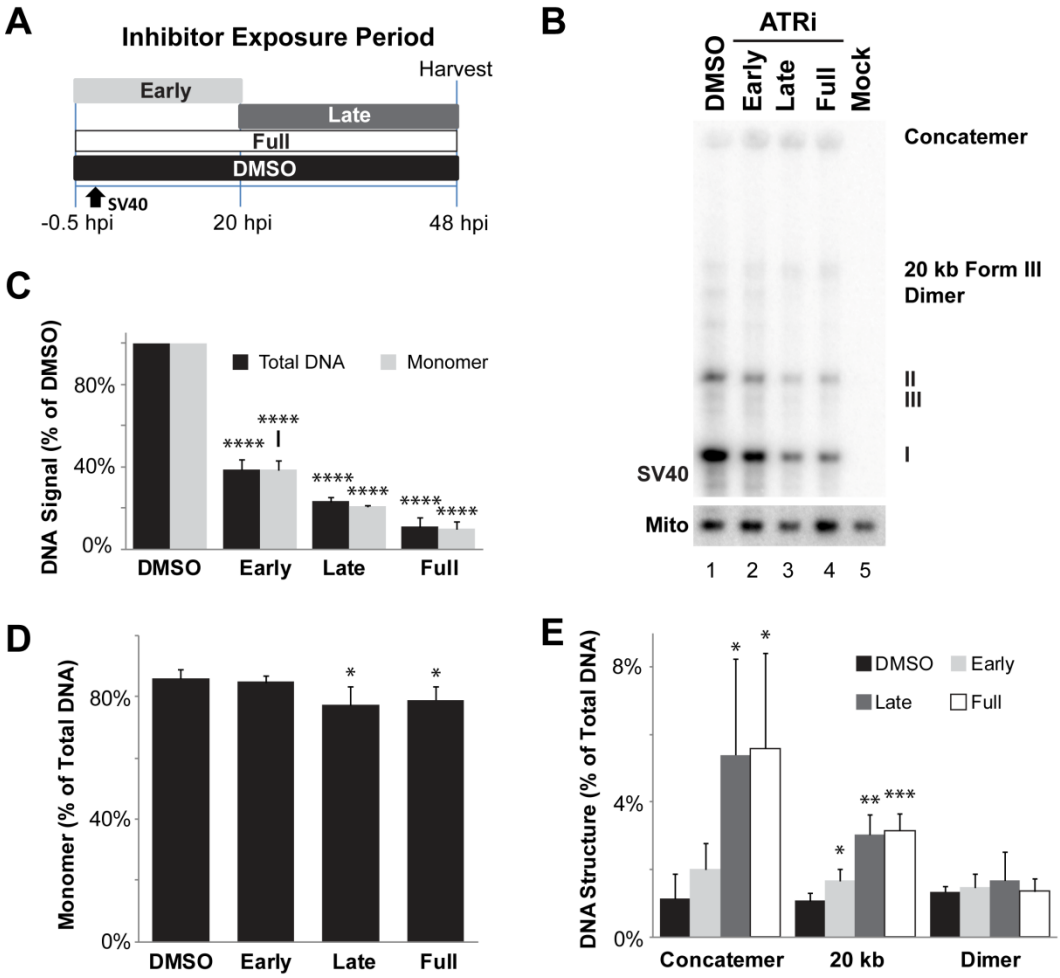

Figure 21. ATR is crucial for SV40 chromatin replication.
(A) Scheme for application of ATRi during phases of a 48 h SV40 infection. (B) Southern blot of DNA replicated in BSC40 cells when ATRi was present during phases of a 48 h SV40 infection described in (A). (C) Graph of total viral or SV40 monomer DNA signals normalized to SV40 DNA replicated in the presence of DMSO from southern blots as shown in (B). (D, E) Graph of monomer (D) or aberrant (E) structure(s) accumulated as a result of ATR inhibition from southern blots as shown in (B). Each bar in (C-E) shows the average from 3 to 4 independent experiments.

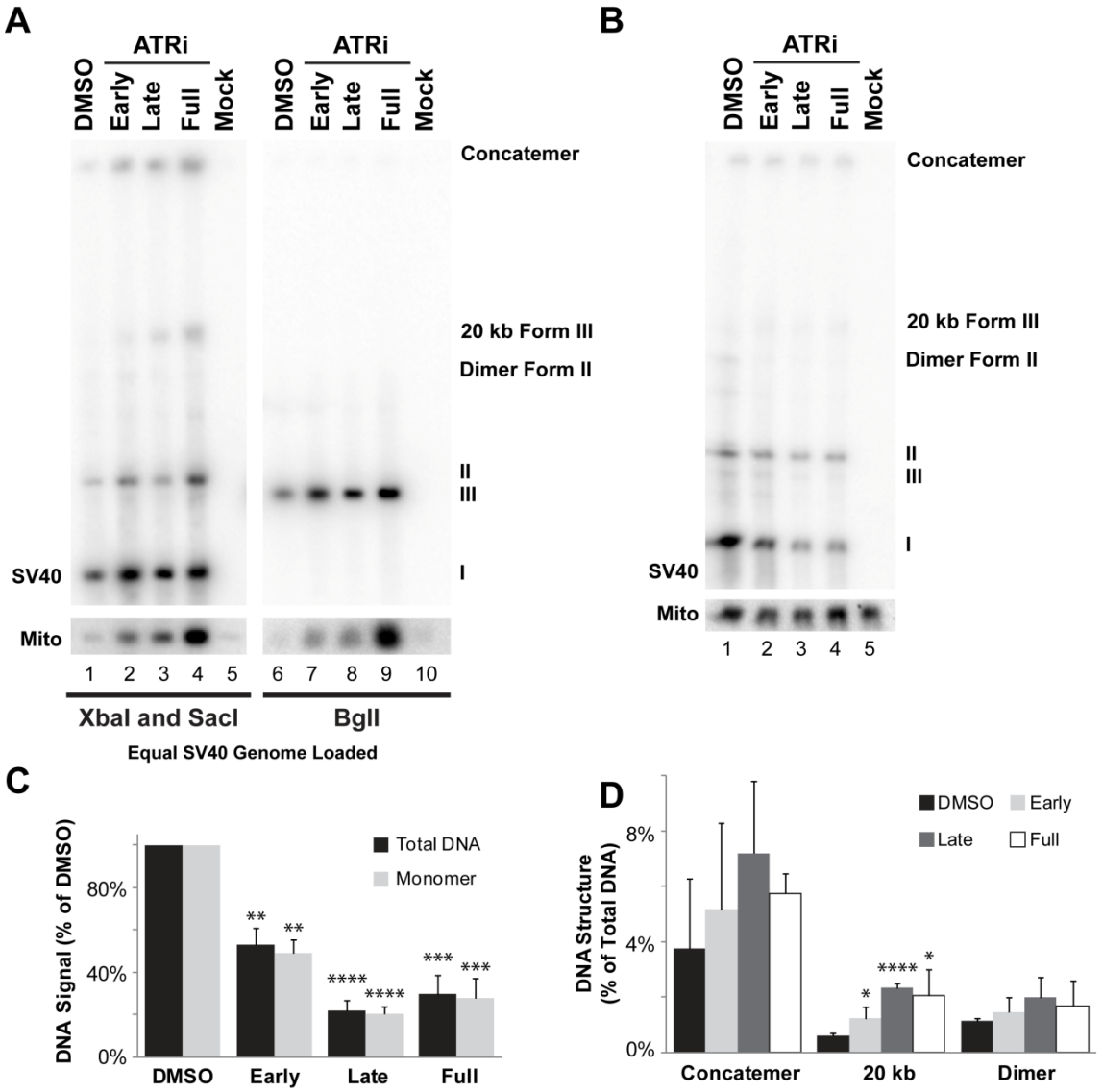

Figure 22. ATR is needed for efficient viral DNA replication in U2OS cells.
(A) Southern blot analysis of total DNA from BSC40 cells treated with ATRi during the indicated phases of infection as in figure 21A. Lanes 1-5: DNA digested with XbaI and SacI. Lanes 6-10: DNA digested with BglI. An equal amount of unit length SV40 DNA was loaded in each lane using the data in figure 21C. (B) Total DNA from SV40-infected U2OS cells treated with ATRi as in Figure 21A was analyzed by southern blotting. (C) Quantification of SV40 signal in total and monomeric SV40 DNA forms from infected U2OS cells treated with ATRi, normalized to the corresponding signals from infected cells treated with DMSO. (D) Fraction of total SV40 signal in the indicated DNA structures in infected U2OS cells exposed to ATRi. Bars in graphs in (C, D) represent the average of 3 to 4 independent experiments.

defects of ATR inhibition or knockdown (Toledo et al., 2011). The latter characteristic of ATR and Chk1 is not exhibited by ATM and its downstream kinase Chk2 (Bunz, 2011). Therefore, to test if the contribution of Chk1 to the S phase checkpoint was crucial for viral DNA replication, the Chk1 inhibitor UCN-01 (Busby, Leistritz et al., 2000) was exposed to SV40-infected BSC40 cells during phases of a 48 h SV40 infection (Figure 23A). At 48 hpi, viral and cellular DNA were extracted and subjected to southern blotting (Figure 23B). The presence of UCN-01 during any phase of infection resulted in a decrease in the amount of viral monomer (Form I, II, and III) and total viral DNA replication products (Figure 23B, C). SV40-infected cells exposed to UCN-01 during viral DNA replication or throughout infection decreased viral DNA replication products to 9% and 8% of DMSO, respectively (Figure 23C). Unlike ATR inhibition, Chk1 inhibition during viral DNA replication or throughout infection did not result in the accumulation of any aberrant product (Figure 23B, E). These data are consistent with a Chk1 kinase activity being essential for viral DNA replication.

Broken and/ or stalled forks accumulate in ATR inhibited SV40-infected cells

The structures of viral replication intermediates generated in the presence and absence of ATR kinase activity were characterized by using neutral 2d gel electrophoresis and southern blotting. As expected, BglI-digested SV40 replication intermediates from control infections displayed a strong double Y arc indicative of converging forks, X structures, and a weaker simple Y arc with both legs of similar intensity (Figure 24B). In contrast, BglI-digested replication intermediates from ATRi-treated cells yielded a novel pattern (Figure 24C). Although the double Y and X structure arcs closely resembled those in the DMSO control, the simple Y arc displayed much greater intensity in the leg closer to the 1n linear DNA (Figure 24B and C, enlarged box) than in the other leg closer to 2n linear DNA.

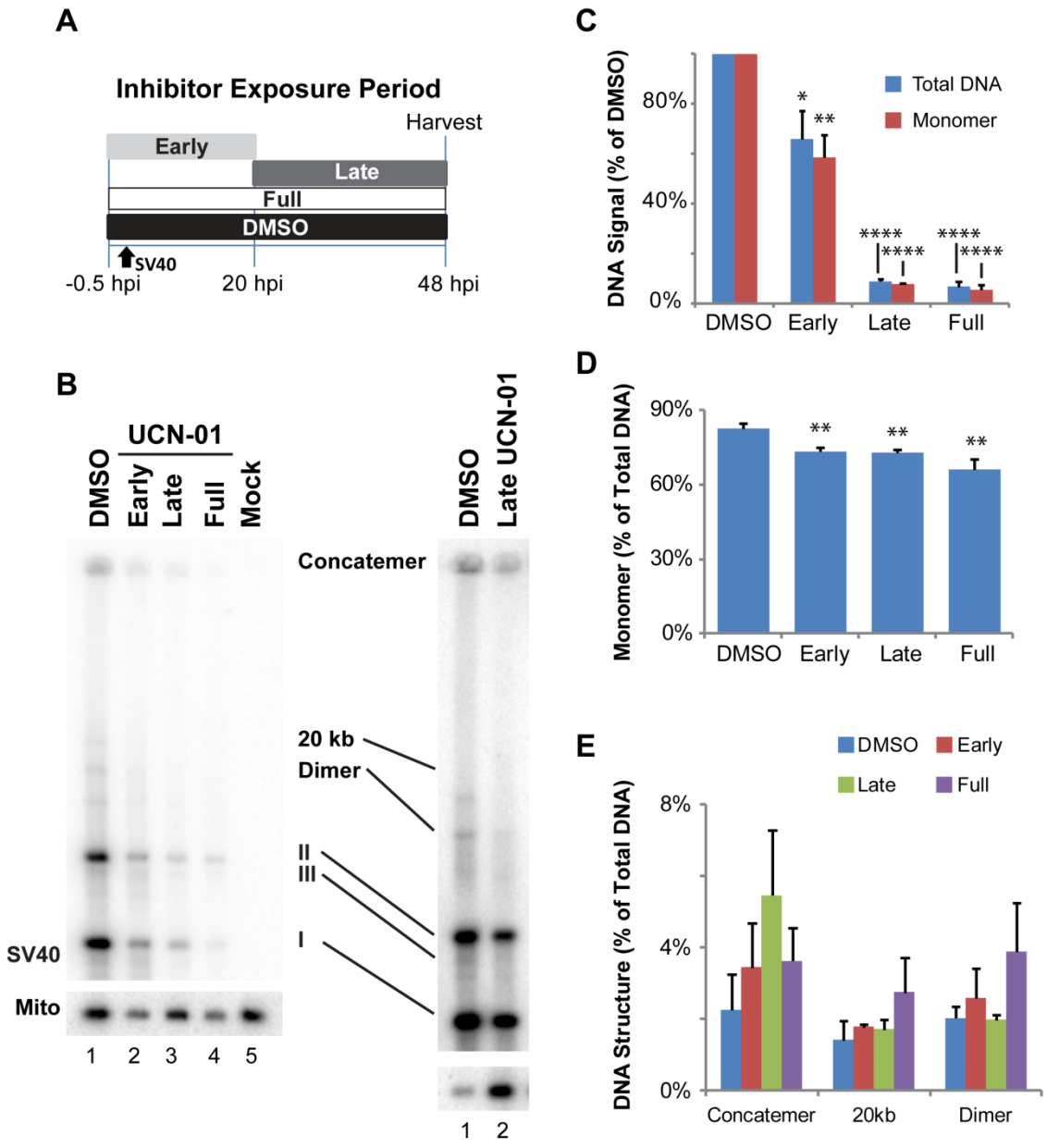

Figure 23. Chk1 is crucial for SV40 DNA replication *in cellulo*.
(A) Experimental scheme for treatment of BSC40 cells with UCN-01 during phases of a 48 h SV40 infection. (B) Southern blots of DNA extracted from BSC40 cells treated as in (A) with UCN-01. In the left panel, equal numbers of cells were loaded in each lane. In the right panel, equal quantities of monomer were loaded in each lane. (C) Graph of total viral or SV40 monomer DNA signals normalized to SV40 DNA replicated in the presence of DMSO from southern blots as shown in (B). (D, E) Graph of monomer (D) or aberrant (E) structure(s) accumulated as a result of Chk1 inhibition from southern blots as shown in (B). In (E), none of the bars are significantly different from the DMSO control. Each bar in (C-E) shows the average from 3 independent experiments.

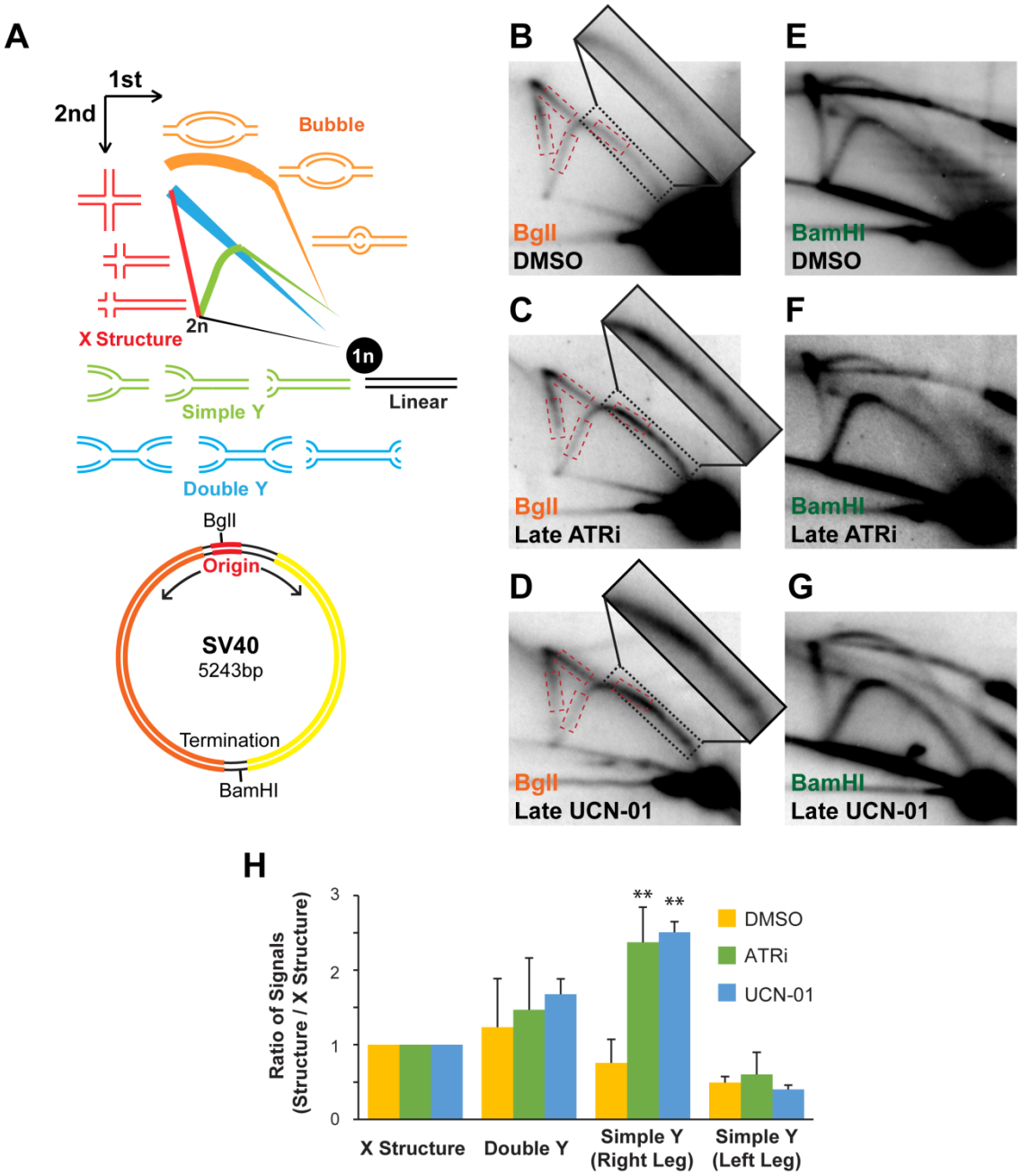

Figure 24. ATR or Chk1 inhibition results in fork stalling and breakage of converging forks.
(A) Top Panel: Schematic of replication intermediate migration patter on a neutral 2d gel generated from digested SV40 DNA. Bottom Panel: Map of the SV40 genome showing BglI and BamHI sites. (B, C, D, E, F, G) Southern blot of neutral 2d gel electrophoresis of BglI- (B, C, D) or BamHI-cut (E, F, G) DNA from SV40-infected BSC40 cells exposed to DMSO (B, E), ATRi (C, F), or UCN-01 (D, G) during the late phase of SV40 infection as described in figure 29A. Dashed boxes denote regions of each arc quantified in (H). (H) Graph of DNA signal from BglI digested DNA in X structure, double Y, right leg of the simple Y, or left leg of the simple Y arc divided by DNA signaling in the X structure arc. Each bar in (H) represents the average of 3 independent experiments.

This pattern is not consistent with rolling circle replication, which generates a uniformly intense simple Y arc (Figure 16) or with two stalled replication forks, of which one breaks, creating an asymmetric simple Y (Pohlhaus and Kreuzer, 2006). The observed pattern is also inconsistent with one normal replication fork and one slower moving fork, which would converge asymmetrically to generate a cone-shaped signal between the X structure arc and the Y arc (Lopes, Cotta-Ramusino et al., 2001). However, the new pattern observed could arise if one fork stalls prematurely (Figure 25, I, II), while the other fork progresses until it encounters the stalled fork and then breaks, generating a broken late Cairns intermediate (Figure 25, III, IV) (Friedman et al., 1995). Close inspection of the intense leg of the Y arc reveals that its intensity is uneven, suggesting that it may arise from a series of closely spaced break sites along the Y arc (Figure 24C). If the break sites reside 2.5 kb or less from the BglI cleavage site, the intensity of signals would be greater in the right leg of the simple Y arc, as observed (Figure 24C, box). This interpretation predicts that if replication products from the ATRi-treated infection were digested with BamHI, which cleaves 2.5 kb from the BglI site, the sites of breakage, and hence greater signal intensity, should shift to the left leg of the simple Y arc, closer to the 2n linear DNA (Figure 24A, F). Indeed, this shift was observed (compare Figure 24C with F), confirming that when the moving replication fork encountered a fork that had stalled in the presence of ATRi, the moving fork broke (Figure 25).

Chk1-inhibited cells amass broken and/ or stalled forks

The large decrease in viral DNA replication products observed when ATR or Chk1 is inhibited during viral DNA replication (Figures 21 - 23) suggests that decreased Chk1 activity in the presence of ATRi is responsible. To determine whether reduced Chk1 activation underlies the increase in broken, stalled replication forks when ATR is

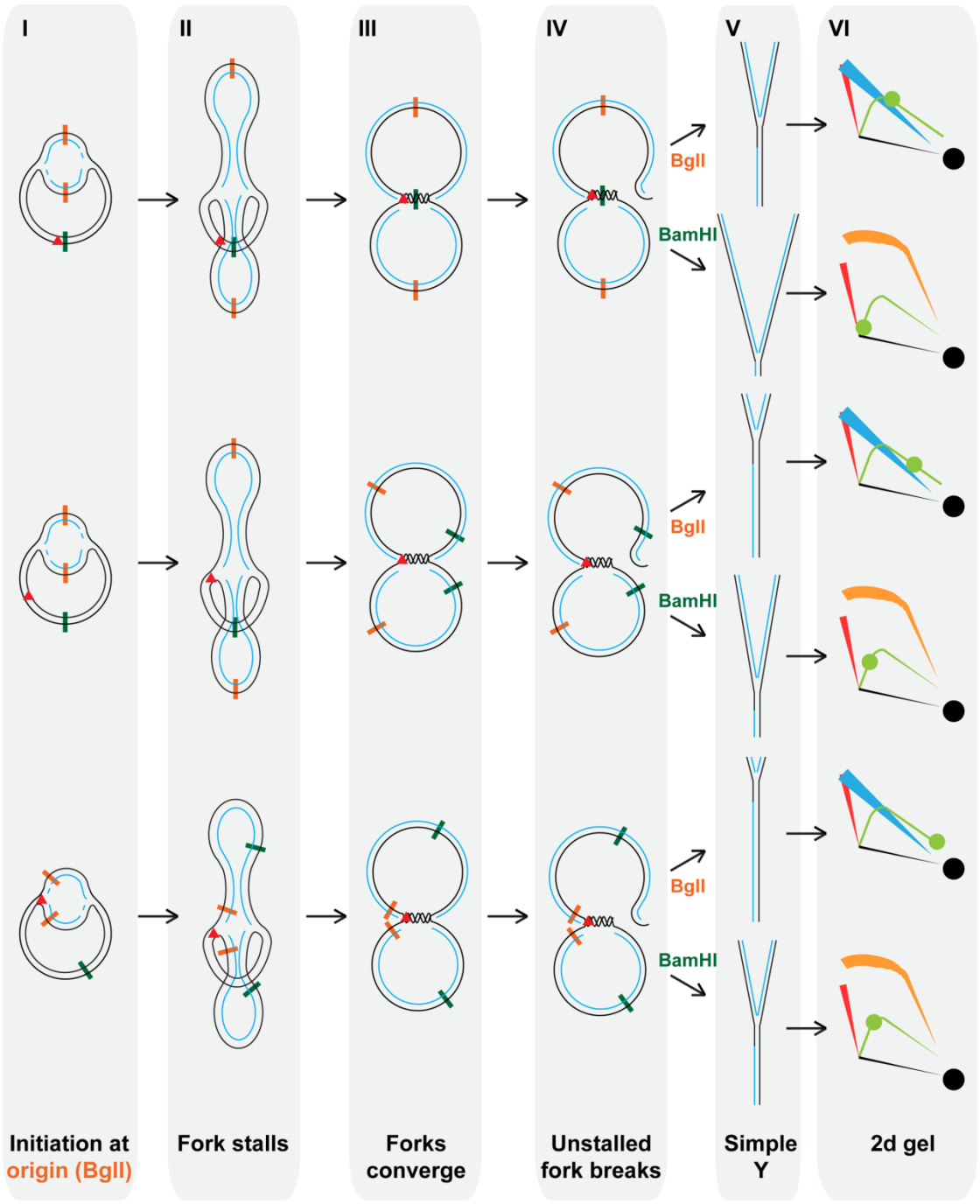
I
II
III
IV
V
VI
BglI
BamHI
BglI
BamHI
BglI
BamHI
Initiation at origin (BglI)
Fork stalls
Forks converge
Unstalled fork breaks
Simple Y
2d gel

Figure 25.

Figure 25. ATR inhibition results in replication fork stalling and breakage.
Diagrams of replication intermediates on a simple Y arc produced when ATR was inhibited. BamHI (green) and BglI (orange) sites are denoted by colored lines. I. Replication initiates at the origin and proceeds bidirectionally producing theta replication intermediates. II. Replisomes continue replication until one encounters a replication block (red triangle) causing one stalled fork. III. The stalled replication fork is closest to orange BglI site (viral origin of replication). The functional replisome continues replication and converges with the stalled replication fork. IV. One-sided DSB forms at the replicating fork of late Cairns intermediate shown in (III) as it translocates toward the stall site. V. Simple Y created by digestion of the broken late Cairns intermediate shown in (IV) with BglI or BamHI. VI. Diagram of the predicted outcome of the simple Y shown in panel (V) following neutral 2d gel electrophoresis and southern blotting. The stall point on the simple Y arc (light green circle) corresponds to the simple Y in panel (V).

inhibited, DNA replicated in the presence of UCN-01 for the final 28 h of a 48 h SV40 infection was examined by neutral 2d gel electrophoresis and southern blotting. BglI-cleaved DNA from Chk1-inhibited, SV40-infected cells migrated in a pattern akin to that observed after ATR inhibition, in a simple Y arc with a prominent right leg (Figure 24D). The uneven intensity in the right leg of the simple Y arc is indicative of stalling and breakage of replicative viral DNA when Chk1 is inhibited (Figure 25). BamHI-digested DNA replicated in the presence of UCN-01 displayed intensity on the opposite leg of the simple Y arc (Figure 24G). Quantification of the signal within defined regions of the double Y, two legs of the simple Y, and X structure arc (Figure 24B, C, D, red boxes) revealed that inhibition of ATR or Chk1 increased the intensity of the right leg of the simple Y arc 3.1 and 3.3 fold, respectively, relative to DMSO (Figure 24H). Thus, these results imply that the inhibition of downstream Chk1 kinase activity when ATR is inhibited is sufficient to account for the breakage of the unstalled fork when ATR is inhibited (Figure 25).

DNA-PK_{cs}, ATM, and ATR activities can partially compensate for each other in SV40 DNA replication

The similarity of the 2d gels when ATR or Chk1 are inhibited suggested to us that similar mechanisms might contribute to the generation of replication products when ATM, ATR, and DNA-PK_{cs} are inhibited. Furthermore, the degree of overlap between kinase substrates for ATM, ATR, and DNA-PK_{cs} opens the possibility that these kinases might substitute for each other when only one PIKK is inhibited (Tomimatsu, Mukherjee et al., 2009). The increased activation of DNA-PK_{cs} observed when either ATM or ATR are inhibited (Figures 13, 17, 20) suggests that NHEJ might contribute to aberrant product formation or repair the DNA as a last resort backup pathway when ATM or ATR directed pathways fail. Seldom used repair pathways can be difficult to observe when

the predominant repair pathway is active (e.g., MMEJ vs NHEJ (Goodarzi et al., 2013)). Thus, the combined inhibition a major DNA repair pathway along with a more seldom-used pathway can exacerbate the repair defect beyond the level observed when only the major pathway of repair is inactivated. This method can reveal the second, lesser used pathway of DNA repair. In the case of ATM, ATR, or DNA-PK_{cs} inhibition, inhibition of multiple kinase activities might allow further distinction among the roles of these kinases in directing repair of the broken replication forks observed in figures 16 and 24.

To this end, ATM, ATR, or DNA-PK_{cs} were inhibited alone or in combination during viral DNA replication (20-48 hpi) in BSC40 cells. As previously observed, either ATR or ATM inhibition alone decreased viral DNA replication and increased aberrant products (Figure 26A - D). On the other hand, DNA-PK_{cs} inhibition had no effect on viral DNA replication or aberrant product accumulation (Figure 26A - D). Combined ATM and ATR inhibition with Ku-55933 and ATRi did not further decrease total viral DNA replication beyond ATR inhibition alone (Figure 26A, B). However, the presence of Ku-55933 and ATRi during viral DNA replication resulted in a substantial increase in aberrant products, decreasing forms I, II, and III to just 37% of the total DNA signal (Figure 26B). Concatemers increased from 11-fold the level observed in DMSO when ATM was inhibited alone to 22 fold of DMSO when ATM and ATR were inhibited (Figure 26A, D). Additionally, the 20 kb product increased to roughly 8% of the total DNA products when ATM and ATR were inhibited together (Figure 26D).

The combined presence of Ku-55933 and Nu7026 during viral DNA replication had no additional effect on viral DNA replication beyond sole inhibition of ATM (Figure 26A, B), but decreased monomeric viral DNA products in favor of concatemers (Figure 26A, C, D). Concatemers increased to 29% when ATM and DNA-PK_{cs} were inhibited compared to 16% when only ATM was inhibited (Figure 26D). On the other hand, combined exposure of ATRi and Nu7026 to SV40 infected cells increased viral DNA

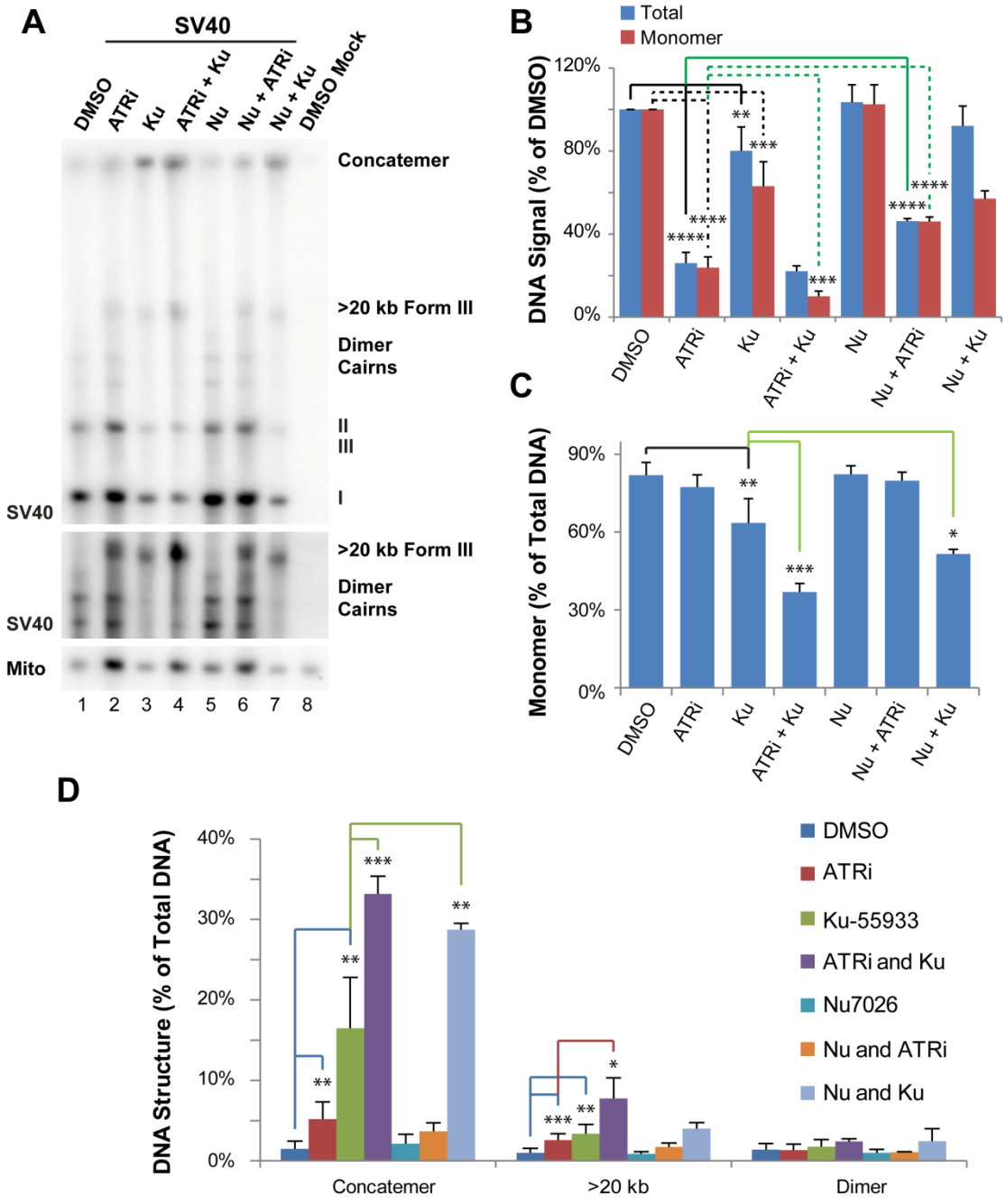

Figure 26. ATM, ATR, and DNA-PK$_{cs}$ have partially overlapping functions in SV40 DNA replication.

(A) Southern blot of DNA extracted from SV40-infected BSC40 cells treated with combinations of DMSO, ATRi, Ku-55933, and / or Nu7026 during the late phase of a 48 h infection as illustrated in figure 29A. The middle panel shows a longer exposure of a portion of the southern blot pictured in the top panel. (B). Graph of total viral or SV40 monomer DNA signals normalized to SV40 DNA replicated in the presence of DMSO from southern blots as shown in (A). (C, D) Graph of monomer (C) or aberrant (D) structure(s) accumulated as a result of multiple PIKK inhibition from southern blots as shown in (A). In (B - D), bars for DMSO, ATRi, and Ku-55933 show the average of 6 to 7 independent experiments. In the same panels, the bar for Nu-7026 shows the average of 4 independent experiments; Whereas, bars for combinations of inhibitors (Ku-55933 / ATRi, Nu7026 / ATRi, and Ku-55933 / Nu7026) show the average of 3 independent experiments.

replication by 1.8 fold of singular inhibition of ATR (Figure 26A, B). Despite the increase in viral DNA replication, no effect on aberrant product formation beyond that observed upon sole inhibition of ATR alone was found for the combined inhibition of ATR and DNA-PK_{cs} (Figure 26A, C, D). Collectively, these results indicate that some functional overlap exists between ATM and the related ATR and DNA-PK_{cs} kinases. Additionally, Figure 26 suggests that DNA-PK_{cs} and ATR do not have overlapping functions in the repair of replicating viral DNA.

Discussion

This study presents several lines of evidence that SV40 harnesses host DNA damage signaling for quality control of viral chromatin replication. We show that viral DNA replication in cultured cells is sufficient to induce DNA damage signaling at viral replication centers (Figures 10, 11, 12), suggesting that DNA lesions may arise in unperturbed replicating viral DNA. Importantly, damage signaling is vital to maintain viral replication centers (Figures 10, 13). Furthermore, suppression of ATM and/or ATR signaling increases the level of aberrant viral replication products at the expense of unit-length viral DNA (Figures 14 - 16, 18, 21 - 23, 26), implying that viral replication-associated damage in infected cells requires ATM and ATR signaling to promote repair of viral replication forks. Our results indicate that the defective replication intermediates resulting from inhibition of ATM (Figures 14, 15), ATR (Figures 21, 22), and Chk1 (Figures 23) are distinctive (Figure 27). Furthermore, our data suggest that ATM, ATR, and DNA-PK_{cs} are partially redundant in repairing one-ended DSBs (Figure 26). Taken together, our results support a model in which ATM, ATR, and Chk1 serve different but complementary roles in orchestrating repair at viral replication forks (Figure 27).

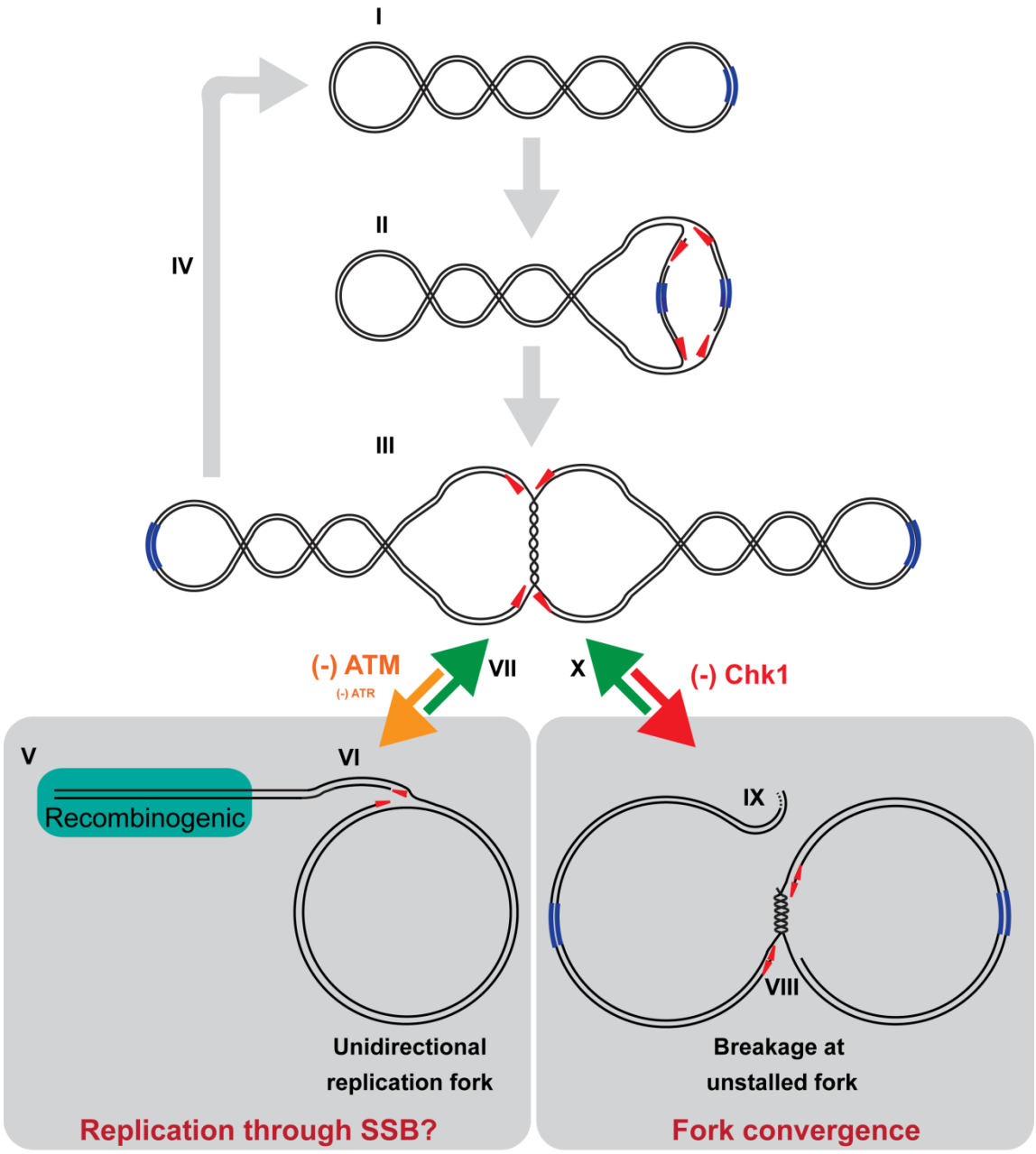

Figure 27. Model of ATM and ATR functions in SV40 DNA replication.
(I) Tag initiates viral DNA replication at the viral origin of replication (blue) and the two replication forks progress bidirectionally (red arrowheads). For simplicity, proteins are not shown. (II) Viral DNA replicates quickly until the forks converge to form a late Cairns intermediate (III), which slowly completes replication. (IV) Topoisomerase IIα decatenates fully replicated DNA molecules, yielding two form I daughter molecules. (V) When ATM is inhibited, a one-ended double strand break at a replication fork leads to loss of the replication machinery, while the other fork continues to replicate DNA, generating a rolling circle (VI). (VII) ATM and to a lesser extent ATR kinase activity facilitates the repair of one-ended double strand breaks. (VIII) When ATR or Chk1 is inhibited, a stalled replication fork remains stable until a functional replication fork approaches it, generating a broken replication intermediate (IX). (X) Chk1 kinase activity facilitates convergence of moving fork with the stalled fork. We suggest that in the presence of ATM, ATR, and Chk1, repair proteins act on the defective intermediates V and IX to reassemble an intermediate with two functional forks.

DNA damage signaling nucleates the assembly of SV40 replication centers

SV40 chromatin replication centers resemble over-sized host DNA damage response foci (for a comparison, see Figure 1 in ref (Zhao et al., 2008)), where diverse damage signaling and DNA repair proteins assemble on chromatin at a DNA lesion and dissociate when repair is completed (Ciccia et al., 2010; Lukas et al., 2011). Many of the same signaling and repair proteins are found at both viral replication centers and host damage response foci (Moody et al., 2009; Jiang et al., 2012; Shi et al., 2005; Zhao et al., 2008; Rohaly et al., 2010; Boichuk et al., 2010; Hein et al., 2009; Dahl et al., 2005). However, unlike the prominent viral replication centers, the punctate host damage response foci encompass megabase regions of chromatin, raising the question of how SV40 mini-chromosomes give rise to large subnuclear foci. The size of SV40 replication centers increases with the number of incoming viral genomes and with time post-infection in permissive primate cells (Zhao et al., 2008), suggesting that our ability to detect viral replication centers depends on the ability of each infected cell to generate 10^4 - 10^5 daughter genomes (Rigby et al., 1978). Moreover, unperturbed viral replication centers display nascent ssDNA (Sowd, unpublished) and DNA breaks (Sowd et al., 2013) that are likely responsible for activating checkpoint signaling, analogous to lesions that nucleate host damage response foci.

A major difference between SV40 replication centers and host damage response foci is that checkpoint signaling does not inhibit the viral replication machinery, whereas Chk2 phosphorylation of the purified host replicative helicase Cdc45/Mcm2-7/GINS inhibits its helicase activity *in vitro* (Ilves, Tamberg et al., 2012) and Chk1 inhibits Cdc45 recruitment to chromatin to initiate replication *in vivo* (Liu, Barkley et al., 2006). Based on these considerations, we suggest that SV40 replication centers serve as hubs where host replication and repair factors efficiently service many client viral genomes in close proximity. These hubs are nucleated and maintained by the assembly of the ATM and

ATR signaling complexes at sites of viral replication stress, followed by recruitment of downstream repair factors (Ciccia et al., 2010). Of note, all of the host proteins needed for SV40 DNA replication *in vitro* (Bullock, 1997; Borowiec et al., 1990; Waga et al., 1994) also function in host DNA repair (Bullock, 1997; Lydeard, Lipkin-Moore et al., 2010; Waga et al., 1994; Hashimoto et al., 2012). Thus, SV40, although it encodes only a single essential replication protein, has evolved a remarkable strategy to generate viral replication compartments.

ATM signaling orchestrates reassembly of viral replication forks, reducing unidirectional replication forks

Knockdown or inhibition of ATM in polyomavirus-infected cells reduced production of unit length viral genomes (Shi et al., 2005; Dahl et al., 2005; Zhao et al., 2008; Jiang et al., 2012). Since these studies evaluated only unit-length viral DNA, the aberrant viral replication products generated by unidirectional replication forks were overlooked (Figures 14, 15, 16). Interestingly, total intracellular DNA from unperturbed infected CV1P cells contains head-to-tail SV40 DNA repeats of 50 to 100 kb at very late times after infection (Rigby et al., 1978). These observations indicate that concatemers may be a normal product of viral replication, and suggests that inhibition of ATM activity might simply increase the frequency of unidirectional replication, advance its timing, or both.

Although replication-associated breaks may be a rare event during unperturbed viral DNA replication, the large number of replicating viral genomes would facilitate their detection, particularly when ATM activity is suppressed. Yet surprisingly, when undigested total intracellular DNA from an ATM-inhibited infection was analyzed by 2d gel electrophoresis, bidirectional replication arcs were still observed (see Appendix), and unit length monomeric viral DNA remained the predominant product when ATM was

inhibited (Figures 14, 15), supporting the notion that bidirectional DNA replication does not stop when ATM is inhibited. These observations can be most simply explained by a model in which theta-form SV40 replication intermediates (Figure 27, I-III) randomly break, giving rise to a few unidirectional forks that amplify the break by generating concatemers and branched concatemers (Preiser et al., 1996; Backert, 2002) (Figure 27, V, VI). Our data suggest that ATM kinase activity is required for repair of one-ended replication-associated DSBs to reassemble bidirectional replication intermediates (Figure 27, VII) (Petermann and Helleday, 2010; Hashimoto et al., 2012; Munoz-Galvan, Tous et al., 2012). Additionally, upon ATM inhibition, further concatemer formation is suppressed by ATR and DNA-PK_{cs} activation (Figure 26). These data suggest that ATR and to a lesser extent DNA-PK_{cs} kinase activities are able to facilitate the repair of one-ended DSBs (Figure 27, VII). Therefore, we propose that ATR directs the repair of a fraction of replication-associated breaks in cells with functional ATM (Figure 27, VII).

It is interesting to consider a possible role for unidirectional viral replication and its large concatemeric products in the tumorigenic activity of SV40, and more broadly of polyoma- and papillomaviruses. Concatemeric genomes of Merkel cell carcinoma virus and HPV are often integrated into human chromosomal DNA in tumors associated with these viruses (Chang and Moore, 2012; DeCaprio, 2009; DiMaio and Liao, 2006). The integration events and the consequences of long-term viral oncogene expression are primary risk factors for such cancers. It seems likely that in infected cells under conditions of insufficient ATM activity, the level of viral concatemers would rise. With inadequate ATM activity, breaks in host chromosomal DNA would also be less frequently repaired through accurate, homology-dependent repair. Thus, it is possible that viral DNA concatemers generated under conditions of insufficient DNA damage signaling might be inaccurately joined with broken host chromatin, contributing to viral tumorigenesis (Chia and Rigby, 1981).

How does ATR-Chk1 signaling orchestrate SV40 replication fork convergence?

SV40 chromatin replication is highly sensitive to inhibition of either ATR or Chk1 throughout a 48 h infection (Figures 21 - 23). One consequence of ATR inhibition is that infected cells continued to cycle throughout infection, rather than arresting in late S phase where viral DNA replication would be favored (Rohaly et al., 2010) (see Appendix). However, the most prominent SV40 replication defect induced by ATRi and UCN-01 was the tendency of converging replication forks to stall and break (Figure 24). Since Chk1 is activated directly by ATR kinase activity (Liu et al., 2000), we think that the failure of Chk1 to phosphorylate one or more of its substrates results in the increased fork stalling and breakage observed in our studies (Figure 24). Our data imply that after initiating replication at the viral origin, one replisome encounters an unknown replication block at variable positions in the viral genome (Figure 25, I and II, red triangle). Since the two sister Tag helicases need not remain coupled after initiation, they can proceed asynchronously as they replicate the viral genome bidirectionally (Sowd et al., 2012; Moarefi et al., 1993; Schneider, Weisshart et al., 1994; Weisshart et al., 1999; Yardimci, Wang et al.). Thus, the functional, unstalled replisome continues replication until it approaches the stalled fork (Figure 25, III). We suggest that without ATR or Chk1 activity, the unstalled fork cannot converge with the stalled fork and breaks, yielding the pattern observed on the simple Y arc (Figure 24C, D, F, G, 25, IV-VI). Consistent with this interpretation, fork convergence represents a slow step during unperturbed SV40 DNA replication in infected cells and occurs in a ~1 kb region around the BamHI site (Tapper, Anderson et al., 1982; Tapper and DePamphilis, 1980; Tapper et al., 1979), suggesting that specialized host proteins and Chk1-dependent modifications may be needed to complete replication.

Our observation that ATRi and UCN-01 renders SV40 fork convergence prone to DNA breakage is reminiscent of common fragile sites in the human genome, which suffer gaps and breaks in Seckel Syndrome cells that express defective ATR alleles and upon Chk1 knockdown (Casper et al., 2004; Durkin, Arlt et al., 2006). Thus, SV40 and other small DNA tumor virus genomes may harbor a potential fragile site in the DNA region where the two viral replication forks converge. Consistent with this speculation, C-terminal truncation of the polyomaviral T antigen encoded in the "fragile site" could render an integrated viral genome replication-defective and perhaps more tumorigenic (Shuda, Feng et al., 2008; Chang et al., 2012; Gjoerup et al., 2010; An, Saenz Robles et al., 2012). Similarly, the viral "fragile site" where replication forks converge would correspond to common viral genome breakpoints in integrated high risk papillomaviral genomes in cervical cancer (Schwarz, Freese et al., 1985; Kadaja, Isok-Paas et al., 2009; Woodman, Collins et al., 2007).

ATM, ATR, and DNA-PK$_{cs}$: Collaborating for genome maintenance

Recent studies have suggested that ATR and DNA-PK$_{cs}$ kinase activities may become crucial when ATM activity is lost or inhibited in cancer cells (Toledo, Murga et al., 2011; Riabinska, Daheim et al., 2013). The examination of viral DNA replication when ATM and ATR or DNA-PK$_{cs}$ were inhibited together indicates a portion of replication-associated DNA breaks can be dealt with utilizing pathways that are promoted by ATR or DNA-PK$_{cs}$ (Figure 26). Since ATR or DNA-PK$_{cs}$ inhibition alone lead to a minor increase and no increase in concatemers, respectively, our data suggest that the pathways facilitated by these PIKKs are not as prevalent in cells with fully functional ATM (Figure 27, VII). The activation of DNA-PK$_{cs}$ that coincides with ATM inhibition raises the possibility that DNA-PK$_{cs}$ and NHEJ might be able to repair a subset of broken viral DNA replication forks. This mode of NHEJ repair has been associated

with the aberrant metaphase spreads observed in FancD2 deficient cell lines (Adamo, Collis et al., 2010). Even with some capacity to repair broken DNA replication forks, the repair catalyzed by DNA-PK_{cs} and NHEJ is likely highly error-prone.

On the other hand, differences underlying repair of replication-associated DSBs by ATM and ATR facilitated pathways are not well understood. ATM activation elicits the recruitment of numerous proteins that serve as hubs for the recruitment of repair factors (Lukas et al., 2011) and relaxation of chromatin structure (Ziv et al., 2006). Viral DNA is heavily transcribed and is likely enriched in histone modifications associated with euchromatin. Thus, it is difficult to understand how relaxation of chromatin structure would contribute to viral DNA replication fidelity. ATR also is able to perform many of the same recruitment functions, including γH2AX spreading at damaged DNA through TopBP1 binding to MDC1 (Wang, Gong et al., 2011) and RNF8 recruitment to MDC1 (Marteijn, Bekker-Jensen et al., 2009). Thus, both ATR and ATM can promote the recruitment of Brca1 and 53BP1 to damaged DNA.

A key difference between ATM and ATR is the DNA substrates that activate the kinases. In the context of SV40 DNA replication, a plausible initiating event to generate a one-ended break is replication through a SSB (Figure 27, V). A DSB on the leading or lagging strand can dramatically change the efficiency of ATR activation. Breakage of the lagging strand would more efficiently activate ATR due to the larger amount of ssDNA contained on the lagging strand (Hashimoto et al., 2012). Yet, the leading strand likely contains little to no ssDNA (Hashimoto et al., 2012), and replication through a SSB on the leading strand would therefore be more likely to less efficiently activate ATR. On the other hand, ATM would be robustly activated by breakage of either the leading or lagging strand because both would recruit MRN with similar efficiencies to the DSB. For that reason, ATM activation by a replication-associated break, like a DSB induced by ionizing radiation, would likely be immediate, whereas ATR activation would have a time

delay (Ciccia et al., 2010). In keeping with previous observations (Derheimer et al., 2010), we suggest a model wherein the lack of ATM kinase activity at broken replication forks might slow the repair of the DSB. Slowed repair kinetics would give enough time for the functional viral fork to generate repeats of DNA that are difficult to repair correctly using homology-directed repair promoted by ATR (Figure 27, V). Further experimentation will be required to determine the mechanisms that underlie the defects in DNA replication observed when ATR or ATM are inhibited.

CHAPTER III

ATM AND ATR KINASES PROMOTE S PHASE ARREST DURING SV40 INFECTION

Introduction

Small DNA tumor viruses include several important human pathogens that cause either fatal illnesses or are associated with cancer (DeCaprio et al., 2013; Psyrri et al., 2008). The two primary families of this group are *Polyomaviridae* and *Papillomaviridae*. These families share several characteristics in that they each have small (5-8 kb) circular, supercoiled dsDNA genomes that encode multifunctional viral proteins required for viral replication. In spite of the multitude of activities that are mediated by the polyomavirus Tag (Gjoerup et al., 2010) and papillomavirus E1, E2, E6, and E7 (DiMaio et al., 2006) proteins, these viruses require cellular S phase to replicate their genomic content (Sowd et al., 2012; Moody and Laimins, 2010).

To accomplish S phase arrest, both virus families activate the DNA damage response kinases ATM and ATR (Sowd et al., 2012; McFadden and Luftig, 2013). ATR and ATM phosphorylate and activate the cellular checkpoint kinases Chk1 and Chk2, respectively (Ciccia et al., 2010). In turn, Chk1 and Chk2 phosphorylate p53 and the Cdc25 family of phosphatases to promote cell cycle arrest (Deckbar, Jeggo et al., 2011). However, in cells infected with polyomaviruses or papillomaviruses, p53 is inactivated (Levine, 2009). A mechanistic understanding of how the infected cells arrest is poorly elucidated.

Polyomavirus SV40 is a useful model for examining the cellular mechanisms exploited by small DNA tumor viruses (DeCaprio et al., 2013; Rozenblatt-Rosen, Deo et al., 2012) and the functions of cellular DNA replication machinery (Waga et al., 1998).

SV40 activation of the DNA damage response (Sowd et al., 2013) and S phase arrest (Rohaly et al., 2010) has been particularly well characterized. DNA damage signaling emanates from viral DNA replication (Sowd et al., 2013), and ATR kinase activation is crucial for SV40-induced S phase arrest (Rohaly et al., 2010). Even with this progress, the individual contributions of the ATM-Chk2 and ATR-Chk1 pathways to S phase checkpoint function in SV40 infection are not well understood.

In this study, we used specific inhibitors of ATM (Ku-55933 (Hickson et al., 2004)) and ATR (VE-821 (ATRi) (Reaper et al., 2011)) to define the contribution of ATM and ATR kinases to S phase checkpoint function during discrete phases of SV40 infection. We found that the ATM-Chk2-mediated checkpoint is needed only during a portion of SV40 infection, whereas the ATR-Chk1 S phase checkpoint is needed throughout viral infection. These results shed further light on how small DNA tumor viruses use DNA damage signaling during their lytic life cycles.

Results

ATM kinase activity contributes to S phase arrest in the early phase of infection

ATM kinase activity contributes to the cell cycle checkpoints that follow DNA damaging agents such as ionizing radiation (McKinnon, 2012). As such, we hypothesized that the ATM-Chk2 pathway during SV40 infection might contribute to virus-induced S phase arrest. Thus, the state of the cell cycle was examined in SV40-infected cells treated for different periods of times with the ATM inhibitor Ku-55933 (Sowd et al., 2013). BSC40 cells were infected and exposed to Ku-55933 during an early (-0.5 - 20 hpi: viral entry, early gene transcription, G1 to S transition) or late (20 - 48 hpi: viral DNA replication and egress) phase or throughout the 48 h infection (full) (Figure 28A). SV40-infected cells exposed to the inhibitor solvent, DMSO, served as the

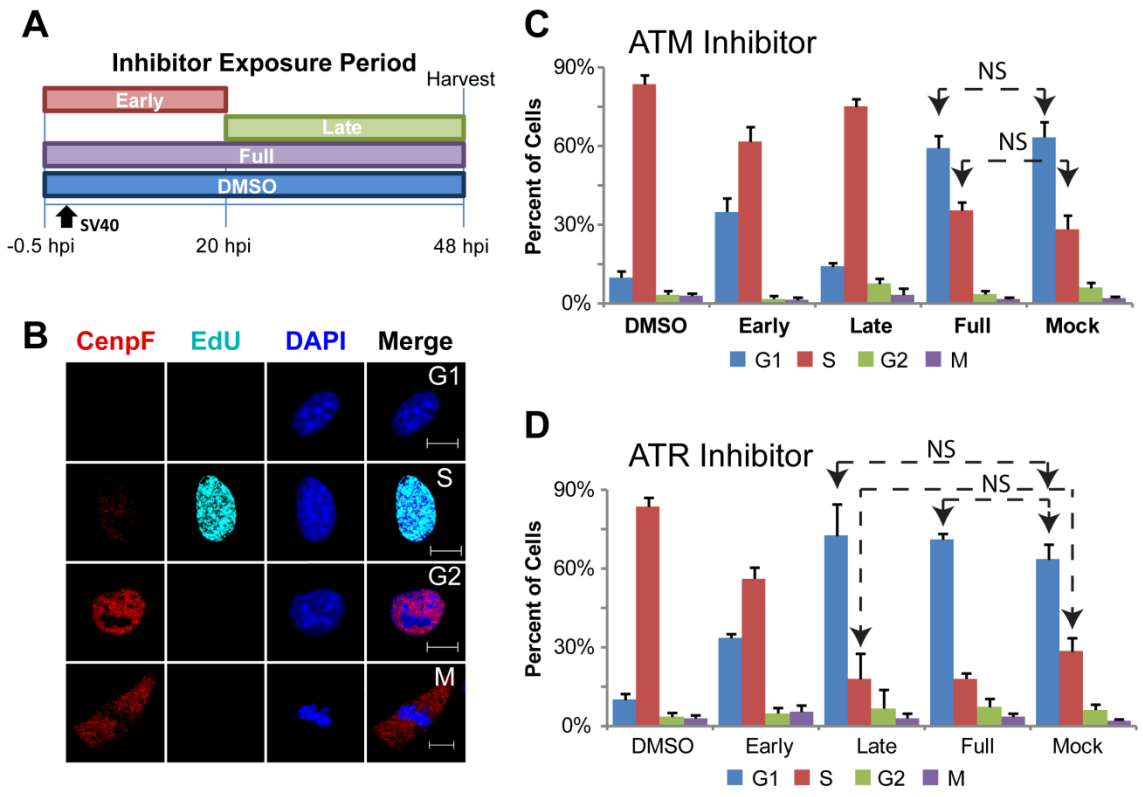

Figure 28. ATM and ATR contribute to S phase arrest during SV40 infection in BSC40 cells. (A) Experimental scheme for treatment of cells with inhibitor during phases of a 48 h SV40 infection. Early: inhibitor present from -0.5 to 20 hpi. Late: inhibitor present from 20 to 48hpi. DMSO and Full: solvent or inhibitor, respectively, present from -0.5 to 48 hpi. (B) Representative images of fixed and then permeablized BSC40 cells. Prior to fixation cells were incubated for 5 minutes with 10 μM EdU. Scale bar represents 10μm. Note: Cells in G1 do not stain for CenpF or contain EdU pulse label. S phase cells have EdU pulse label whereas G2 cells lack EdU pulse label, but contain nuclear CenpF. Mitotic cells have cytoplasmic CenpF and condensed chromatin. (C, D) Graphs of the stage of the cell cycle of cells exposed to Ku-55933 (C) or ATRi (D) as in (A). Cell cycle stage was determined as described in (B). In (C) and (D), all G1 and S bars are significantly different ($p<0.05$ two tailed student's t test) than DMSO or Mock controls except those denoted NS (not significant). Graphs in (C) and (D) show the average of 3 independent experiments.

positive control for S phase arrest, and uninfected cells were used determine the state of the cell cycle in an asynchronous population of cells (Figure 28A). To determine the state of the cell cycle at 48 hpi, each population of cells was exposed to a 5 minute EdU pulse-labeling followed by fixation and immunostaining for CenpF and a Click reaction for detection of EdU incorporation. On the basis of the fluorescent signal intensities for CenpF and EdU, the stage of the cell cycle could be determined (Figure 28B) (Lobrich et al., 2010; Liao, Winkfein et al., 1995; Zhu, Mancini et al., 1995). As expected, a substantial percentage of mock-infected cells were in G1 and S phase (Figure 28C). Upon SV40 infection in the presence of DMSO, ~90% of SV40-infected BSC40 cells arrested in S phase, consistent with checkpoint activation (Figure 28C). The presence of Ku-55933 during the early phase of infection resulted in an approximately 25% increase in the number of cells in G1 with a corresponding decrease in S phase cells relative to DMSO-treated SV40-infected cells (Figure 28C). Inhibition of ATM during the late phase of infection had only a minor effect on SV40-induced S phase arrest (Figure 28C), whereas ATM inhibition throughout infection increased the G1 cell population to 59% of cells, a percentage similar to asynchronous mock-infected BSC40 cells (Figure 28C). Taken together, the results suggest that the ATM-Chk2 pathway of checkpoint induction is required during the early phase of infection for efficient S phase arrest.

ATR enforces S phase arrest during all phases of SV40 infection

Since ATM function in viral induction of S phase arrest is required only during a particular phase of viral infection, we thought that the same might be true for ATR. To determine if ATR kinase activity was necessary to promote S phase arrest, BSC40 cells were infected with SV40 in the presence or absence of ATRi during three time windows (Figure 28A). These ATRi- or DMSO-treated populations of cells were labeled with EdU and fixed for immunostaining with CenpF. Again, SV40 infection in the presence of

DMSO induced a strong S phase arrest, whereas mock-infected cells demonstrated an asynchronous cell cycle (Figure 28D). Similar to early ATM inhibition, ATR inhibition early during infection increased the percentage of G1 cells by ~24% (Figure 28D). However, inhibition of ATR during viral DNA replication or throughout infection substantially increased the fraction of cells in G1 to levels similar to those found in asynchronous mock-infected cells (Figure 28D). We conclude that ATR is essential during all phases of infection for the induction of the S phase arrest by SV40.

Discussion

The SV40 pseudo-S phase: an ATM/ATR collaboration

ATM and ATR kinases phosphorylate and activate Chk2 and Chk1, respectively, resulting in S phase arrest (Bunz, 2011). Our results imply that ATM and ATR kinases contribute differently to the S phase arrest occurring during SV40 infection. Whereas ATM activity is only needed during the early phase of SV40 infection (Figure 28C), ATR kinase is needed throughout infection to activate Chk1 and enforce the S phase checkpoint (Figure 28D). It is possible that the number of replicating viral genomes early during viral infection (0-20 hpi) does not provide sufficient replication stress to elicit the ATR-Chk1 kinase activity required to arrest cells in S phase. Yet during timepoints with robust viral DNA replication, the amount of ATR-Chk1 activation is sufficient to induce cell cycle arrest in S phase.

Our data suggest that the ATM-Chk2 and ATR-Chk1 pathways lead to S phase arrest early in infection, and the ATR-Chk1 pathway alone arrests cells in S phase later during SV40 infection (after 20 hpi). A model has been proposed wherein ATR-dependent p21 accumulation inhibits S phase CDK activity during SV40 infection (Rohaly et al., 2010). However, we have not been able to observe p21 accumulation at

any timepoint during SV40 infection (see Appendix). Therefore, it appears that the virus-induced S phase arrest may be due to the degradation or sequestration of Cdc25 family members by Chk1- and/ or Chk2- dependent phosphorylation (Boutros, Lobjois et al., 2007). Thus, it will be interesting to determine how S phase arrest occurs during SV40 infection.

CHAPTER IV

ATM ACTIVITY INHIBITS DNA-PK$_{cs}$ ACTIVATION AND LOCALIZATION TO VIRAL REPLICATION CENTERS DURING SV40 INFECTION

Introduction

A diverse set of protein functions is required to ensure the timely, accurate duplication of the genome. Amongst the well-known polymerase, helicase, ligase, and topoisomerase activities (Waga et al., 1998; Masai et al., 2010) of the replisome is the S phase checkpoint kinase, ATR. ATR along with related kinases ATM and DNA-PK$_{cs}$, which are members of the PIKK family, regulate DNA damage signaling in response to various endogenous and exogenous stresses (Ciccia et al., 2010). ATR kinase function is primarily activated by DNA replication stress through the capacity of the ATR/ATRIP complex to sense stretches of RPA-bound ssDNA (Zou et al., 2003). In conjunction with ATR, ATM and DNA-PK$_{cs}$ function to promote DNA repair and are primarily activated in response to DSBs (Ciccia et al., 2010). To identify DSBs, ATM and DNA-PK$_{cs}$ rely on MRN and Ku, respectively (Goodarzi et al., 2013). DNA-PK$_{cs}$ kinase activation solely influences the pathway used to repair the DSB and promotes NHEJ (Neal et al., 2011). On the other hand, activation of either ATM or ATR is accompanied by activation and recruitment of numerous factors that influence DNA repair and arrest of both the cell cycle and DNA replication (Ciccia et al., 2010).

Several DNA repair proteins are also used as part of the cellular DNA replication process. Amongst these factors is an abundance of activities from the HR pathway. Depletion of factors from this pathway is associated with various DNA replication defects, including slowed DNA synthesis (Davies, North et al., 2007), instability of

nascent DNA strands (Schlacher et al., 2011), anaphase bridges owing to un-replicated DNA entering mitosis (Chan, North et al., 2007; Chan, Palmai-Pallag et al., 2009; Laulier, Cheng et al., 2011), and increased genome breakage in both the presence and absence of replication stress (Franchitto and Pichierri, 2011; Hashimoto et al., 2012; Wechsler et al., 2011). Several of these characteristics are reminiscent of the defects observed in Seckel syndrome cells, which harbor hypomorphic mutations in the ATR gene providing a possible link between HR and DNA damage signaling (Alderton et al., 2004; Casper et al., 2004; O'Driscoll et al., 2003). HR function has been primarily demonstrated to repair DSBs that are formed during S phase, with NHEJ repairing the majority of DSBs during other phases of the cell cycle (Goodarzi et al., 2013).

Classic models of DNA replication do not hypothesize DSBs to form as an consequence of metazoan genome replication. However, recent evidence examining expression of common fragile sites in the human genome, which are prone to gaps and breakage upon replication stress, suggests that replisome convergence may be a source of DNA breakage during chromatin replication (Debatisse, Le Tallec et al., 2012). Similar to studies of cellular DNA replication, recent evidence suggests that polyomaviruses and papillomaviruses might utilize a more complex milieu of DNA replication factors than previously anticipated (Zhao et al., 2008; Boichuk et al., 2010; Moody et al., 2009; Gillespie, Mehta et al., 2012; Sowd et al., 2013). Yet unlike cellular DNA replication, infection of cells by polyomaviruses and papillomaviruses is accompanied by intense ATM and ATR activation (Zhao et al., 2008; Orba, Suzuki et al., 2010; Jiang et al., 2012; Moody et al., 2009; Sakakibara et al., 2011). Additionally, viral DNA replication is resistant to DNA damage checkpoint signaling (Sowd et al., 2012).

ATM and ATR kinase activities are required to facilitate the repair of replication-associated breaks on viral chromatin during SV40 DNA replication (Sowd et al., 2013). SV40 also has been used to identify and characterize numerous cellular DNA replication

factors (Waga et al., 1998; Sowd et al., 2012). Thus, DNA damage signaling and repair proteins used by SV40 DNA replication might represent a set of factors employed during normal cellular DNA replication to prevent replication-associated DSBs.

To further clarify the role of DNA damage signaling and repair during SV40 infection, we determined the subnuclear localization of several factors involved in DSB repair in SV40 infected cells. Small molecule inhibitors of ATM and ATR were used to examine the localization of NHEJ and HR proteins during SV40 infection in the presence and absence of DNA damage signaling. We show that viral replication centers selectively recruit homology-directed repair and exclude NHEJ factors. Our results indicate that ATM kinase but not ATR kinase activity is required for the proper localization of several HR factors and suppression of DNA-PK_{cs} kinase activation at viral DNA replication centers. Our results lend further insight into mechanisms influencing the decision to repair DSBs by HR or NHEJ during S phase.

Results

Viral replication centers colocalize with homology-directed repair

Previous studies have examined the localization of several DNA repair factors with ill-defined functions in SV40 infected cells (Zhao et al., 2008; Boichuk et al., 2010). Several of these factors, including MRN, Rad51, FancD2, and Brca1 function in homology-directed repair (Ciccia et al., 2010) and might act to repair broken DNA resulting from viral DNA replication (Sowd et al., 2013). To further define what activities of DSB repair are recruited to or localized near viral DNA replication centers, the nuclear localization of chromatin-bound homology-directed repair proteins, which includes SSA and HR factors, was examined in SV40-infected BSC40 and U2OS cells using fluorescence microscopy.

CtIP, whose activities are required for homology-directed repair, formed intense foci that colocalized with Tag in SV40-infected BSC40 and U2OS cells (Figure 29A). Furthermore, the Rad51 loader Brca2, the single-strand annealing protein Rad52, and the dHJ dissolvase BTR (BLM, RMI1/2, and Topoisomerase IIIα) colocalized on chromatin with viral DNA replication centers in infected BSC40 and U2OS cells (Figure 29B-G). Examination of the localization of the BTR component BLM during a 60 h time course of SV40 infection in BSC40 cells revealed that BLM colocalization with viral DNA replication centers was greatest at times >24 hpi (Figure 30) when viral DNA is actively being replicated (see Figure 14A, DMSO). This timeframe of BLM colocalization correlated well with EdU incorporation at Tag foci (Figure 30) and is reminiscent of that found for MRN and Tag colocalization in SV40 infected cells (Zhao et al., 2008). Similar timing of colocalization was displayed for RMI1/RMI2, topoisomerase IIIα, Brca2, and CtIP (data not shown) suggesting that localization of homology-directed repair to viral replication centers is a characteristic of HR repair factors in SV40-infected cells.

NHEJ proteins do not localize to Tag foci in SV40-infected cells

Similar to HR protein recruitment to viral replication centers, SV40 infection induces ATM and ATR DNA damage signaling in a time frame that closely mirrors viral DNA replication. Thus, a related PIKK, DNA-PK$_{cs}$, might be activated with similar kinetics during SV40 infection. To assess the level of DNA-PK and DNA-PK$_{cs}$ kinase activation during viral infection, steady-state levels of DNA-PK factors and signaling in extracts of SV40-infected BSC40 cells were determined by immunoblotting over a 60 h time course (Figure 31). These blots revealed that ATR and ATM began to phosphorylate substrates Chk1 and Chk2, respectively, at 24 hpi (Figure 31A). ATM and ATR kinase activities were greatest from 36 through 48 hpi, after which they began to decline (Figure 31A, compare lanes 4, 5 to lane 6). On the other hand, DNA-PK$_{cs}$

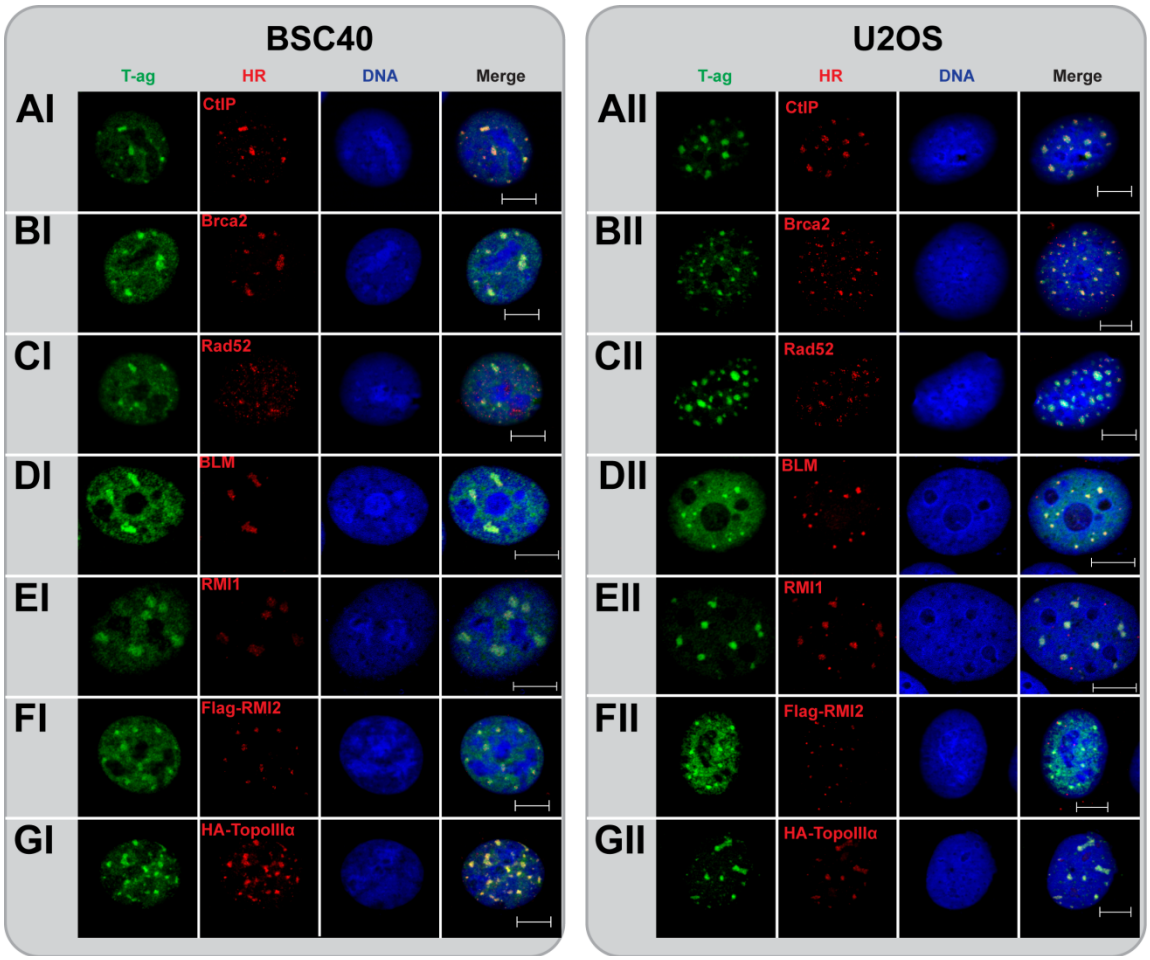

Figure 29. SV40 DNA replication centers colocalize with HR proteins.
(A - G) Images of chromatin bound Tag and the indicated HR factors from SV40-infected BSC40 (I) or U2OS (II) cells at 48 hours post infection. Vectors for expression of HA-topoisomerase IIIα or Flag-RMI2 were transfected 24 h prior to infection. Scale bars represent 10 μm.

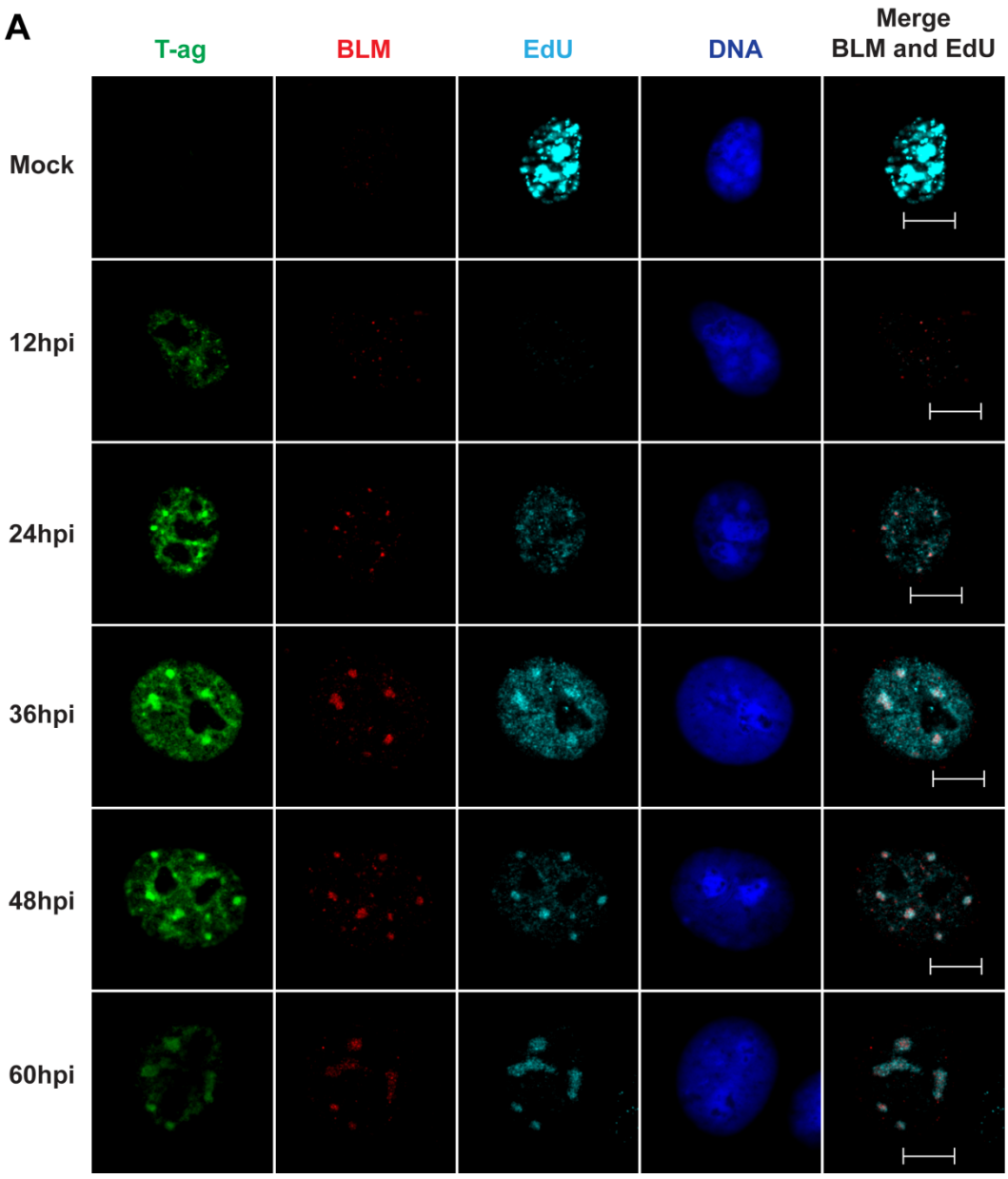

Figure 30. BLM colocalization with Tag correlates with SV40 DNA replication.
(A) Representative micrographs of chromatin-bound BLM, Tag, and Alexa Fluor 647 conjugated EdU from SV40-or mock-infected BSC40 cells at the indicated timepoints. Merge shows EdU and BLM only. Scale bars represent 10 μm.

kinase activation was observed most strongly at 48 hpi and more weakly at 36 and 60 hpi, as assessed by DNA-PK_{cs} autophosphorylation at S2056 (Figure 31B, compare lane 1 to lanes 4-6). The phosphorylation state of T2609 on DNA-PK_{cs}, a residue phosphorylated by ATM, ATR and DNA-PK_{cs} following DNA damage (Chen et al., 2005; Chen et al., 2007; Uematsu et al., 2007; Yajima et al., 2006; Meek et al., 2007), did not change during viral infection (data not shown, see Figure 34E). The total protein levels of Ku70, Ku80, and DNA-PK_{cs} were stable throughout 60 h of SV40 infection (Figure 31A, B, compare lanes 1-6). Thus, these results show that the timing of DNA-PK_{cs} kinase activation during SV40 infection does not correlate well with viral DNA replication.

To determine whether the limited DNA-PK_{cs} kinase activation observed at 48 hpi was associated with localization of the DNA-PK holoenzyme to viral DNA replication centers, chromatin-bound NHEJ proteins Ku70, Ku80, and DNA-PK_{cs} were examined by fluorescence microscopy at 48 hpi in SV40-infected BSC40 and U2OS cells. DNA-PK_{cs}, Ku70, and Ku80 showed little preference for binding at or near viral DNA replication centers in both BSC40 and U2OS cells (Figures 32 and 33). Auto-phosphorylated DNA-PK_{cs} on S2056 was not abundant in SV40-infected cells at 48 hpi and did not associate with viral DNA replication centers (Figures 32B and 33B). Close inspection of viral replication centers revealed that DNA-PK_{cs} and Ku70/80 appeared to be excluded from Tag foci (Figures 32 and 33, arrows, enlarged boxes). Lines tracing through viral replication centers confirmed that intense Ku70/80 and DNA-PK_{cs} foci did not colocalize with Tag (Figures 32 and 33). These results are consistent with previous findings demonstrating that DNA-PK_{cs} kinase activity is not required for SV40 DNA replication (Sowd et al., 2013). Instead, viral DNA replication appears to be resistant to DNA-PK_{cs} activation and NHEJ function, but not ATM, ATR, or homology-directed repair.

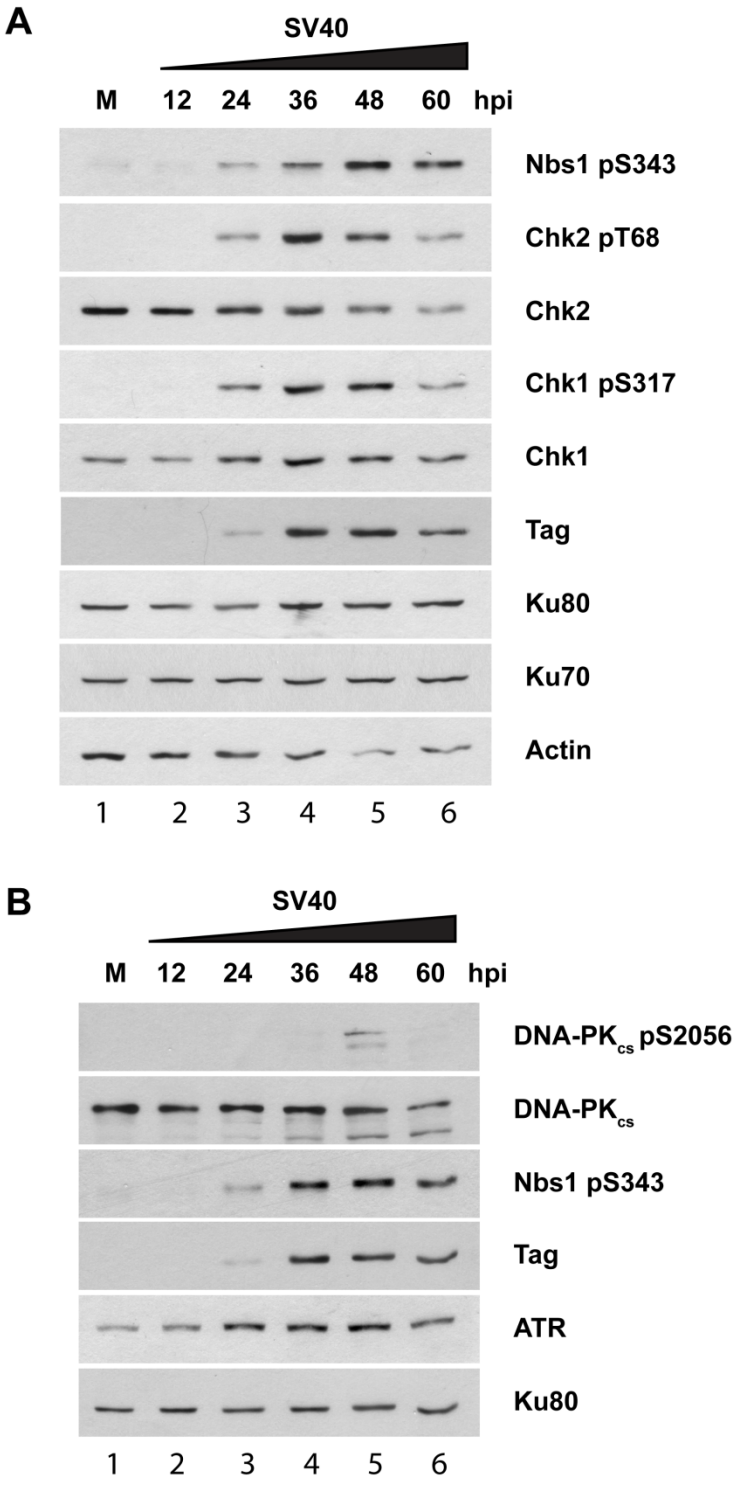

Figure 31. DNA-PK components are stable throughout SV40 infection.
(A - B) Western blots of cell lysates from SV40- or mock-infected BSC40 cells at the indicated timepoints.

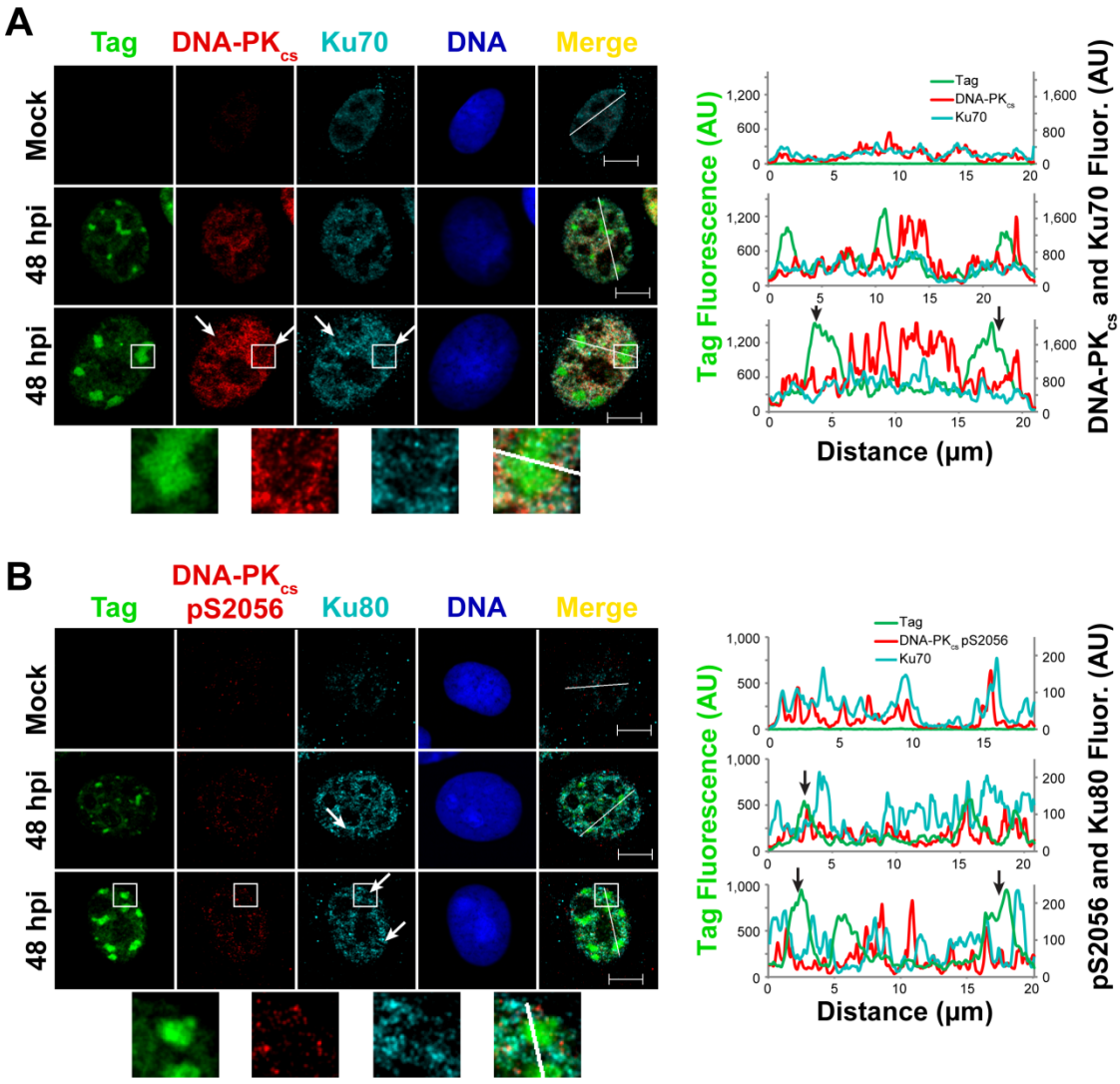

Figure 32. Factors that promote NHEJ do not co-localize with Tag in SV40-infected BSC40 cells. (A, B) Representative pictures of chromatin-bound Tag or DNA-PK from SV40- or mock-infected BSC40 cells at 48 hpi. Merged images shows DNA-PK$_{cs}$, Ku, and Tag. Bottom panel of (A) and (B) shows an enlargement of the region of the boxed area. Arrows in point to area on line in which DNA-PK exclusion is more easily observed. The fluorescence intensity in arbitrary units (AU) along the line shown in the merged image is graphed in the right panel. Scale bars represent 10 μm.

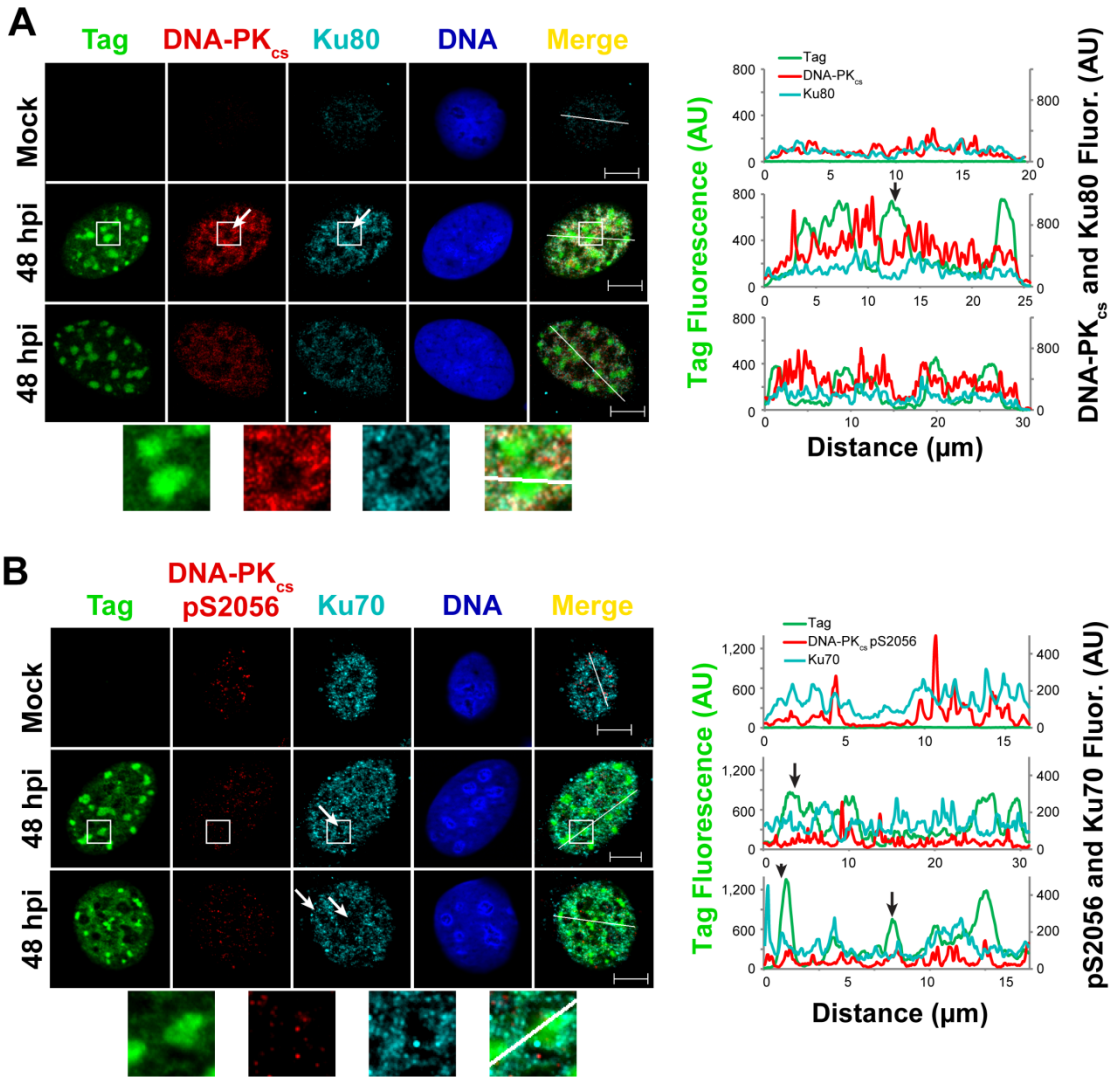

Figure 33. NHEJ proteins are not localized to viral replication centers in SV40-infected U2OS cells.

(A, B) Representative images of chromatin-bound Tag or DNA-PK from SV40- or mock-infected U2OS cells at 48 hpi. Merged images shows DNA-PK$_{cs}$, Ku, and Tag. Bottom panel of (A) and (B) shows an enlargement of the region of the boxed area. Arrows in point to area on line in which DNA-PK exclusion is more easily observed. The fluorescence intensity in arbitrary units (AU) along the line shown in the merged image is graphed in the right panel. Scale bars represent 10 μm.

ATR inhibition does not disrupt viral DNA replication centers

ATM and ATR phosphorylate a plethora of targets at damaged DNA including factors that influence HR and NHEJ (Matsuoka et al., 2007; Chapman et al., 2012). The vigorous activation of ATM and ATR that accompanies viral DNA replication (Figure 31) suggests that the kinase activities of these enzymes might influence the factors or activities of the factors localized to viral DNA replication centers. As such, ATM and ATR kinases might indirectly compromise NHEJ function at viral replication centers. Yet prior to testing this hypothesis, a more thorough understanding of effects of ATR inhibition on viral replication centers was required. ATM inhibition disrupts viral DNA replication centers and results in aberrant Tag staining pattern (Zhao et al., 2008; Sowd et al., 2013). Furthermore, expression of a dominant-negative kinase-ablated ATR or inhibition of ATR at any point during SV40 infection precluded the S phase arrest normally observed in SV40-infected cells (Rohaly et al., 2010) (Figure 28). Therefore, I reasoned that a more limited exposure to ATRi might be more appropriate to compare the effects of ATM or ATR inhibition on viral DNA replication centers.

To determine the timing of aberrant replication center formation upon exposure of SV40-infected cells to the specific ATM inhibitor Ku-55933 (Hickson et al., 2004), the chromatin-bound Tag staining pattern was monitored by immunofluorescence microscopy from infected cells when Ku-55933 was added to the medium during the final 4, 8, 16, and 24 h of a 48 h infection. Cells stained with DMSO demonstrated intense Tag foci that accompany infection, with a smaller percentage of cells showing a weak, aberrant Tag staining pattern (Figure 34A, B). However, the presence of Ku-55933 for 4 h prior to the 48 hpi timepoint increased aberrant, dispersed Tag staining to on average 23% of cells (Figure 34A). Inhibition of ATM during the final 8 h of a 48 h infection resulted in 49% of cells displaying a dispersed Tag staining pattern that lacked viral replication centers (Figure 34A, B). Further exposure to Ku-55933 beyond 8 h caused

no further increase in the dispersed Tag staining pattern (Figure 34A). The percentage of cells displaying a weak Tag staining remained stable for Ku-55933 exposures of less than 16 h (Figure 34A). At exposures of 24 h or greater, the weak Tag staining began to increase (Figure 34A and data not shown). These data suggest that the presence of Ku-55933 for as little as 8 h is sufficient to produce aberrant Tag replication center patterns. Therefore, an 8 h exposure to ATRi was utilized to limit cell cycling of SV40-infected cells in the presence of ATRi.

To determine whether ATR contributes to viral replication center stability, cells were infected with SV40, and ATM or ATR were inhibited during the final 8 h of a 48 h infection using Ku-55933 and VE821 (ATRi) (Reaper et al., 2011), respectively. At 48 hpi, the cells were processed for immunostaining of chromatin-associated proteins. Again, infection in the presence of DMSO had no effect on viral DNA replication centers, and Ku-55933 induced replication center dispersion (Figure 34B). The presence of ATRi for as little as 8 h increased the percentage of cells lacking noticeable Tag foci (weak) to 58% on average, but no effect on Tag staining patterns was observed (Figure 34B and 35). We conclude that ATR inhibition does not affect Tag replication centers in the same manner as ATM inhibition.

Inhibition of ATM or ATR kinase activity increases DNA-PK activation

Inhibition of ATM or ATR for extended periods during SV40 infection accompany robust DNA-PK_{cs} activation during SV40 infection (Sowd et al., 2013). To test whether the presence of Ku-55933 or ATRi during a shorter period of infection inhibited ATM/ATR and corresponded with increased DNA-PK activation, protein lysates from SV40- or mock-infected BSC40 cells treated with DMSO, ATRi, or Ku-55933 during the final 8 h of a 48 h SV40 infection were subjected to immunoblotting. Again, ATR and ATM phosphorylation of Chk1 and Chk2, respectively, increased in DMSO-treated,

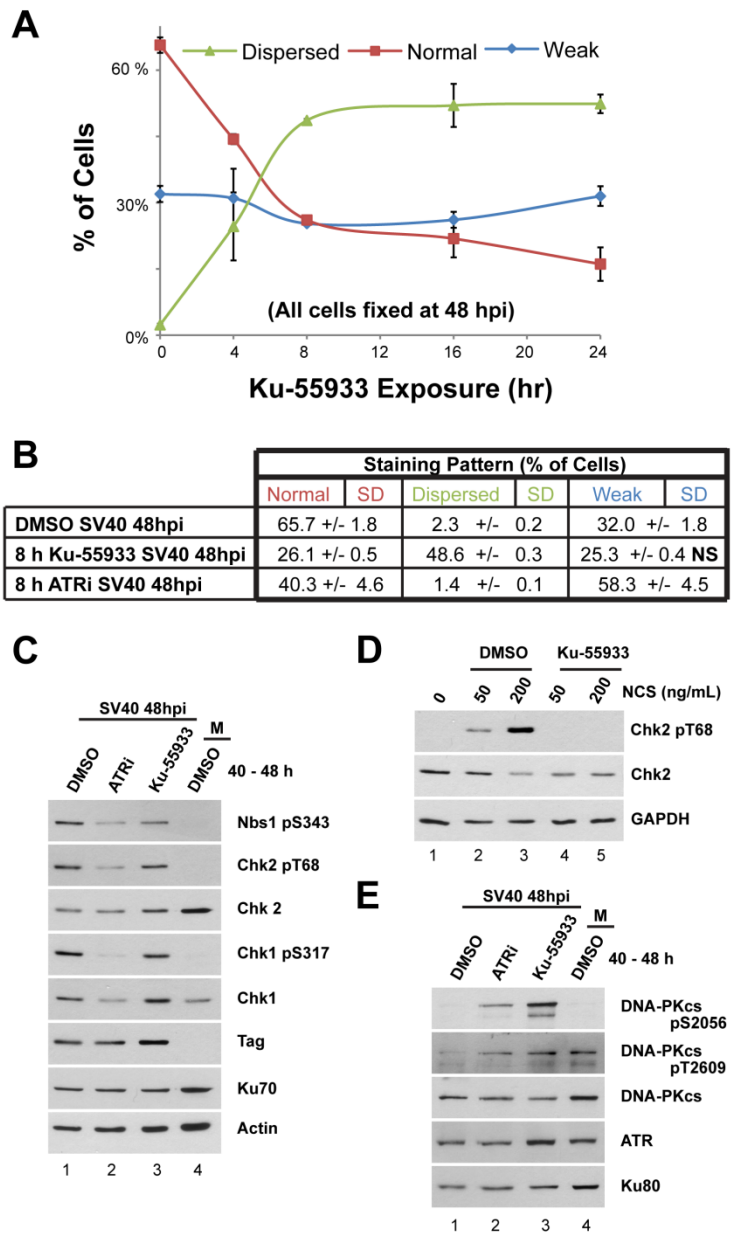

	Staining Pattern (% of Cells)					
	Normal	SD	Dispersed	SD	Weak	SD
DMSO SV40 48hpi	65.7 +/- 1.8		2.3 +/- 0.2		32.0 +/- 1.8	
8 h Ku-55933 SV40 48hpi	26.1 +/- 0.5		48.6 +/- 0.3		25.3 +/- 0.4	**NS**
8 h ATRi SV40 48hpi	40.3 +/- 4.6		1.4 +/- 0.1		58.3 +/- 4.5	

Figure 34. Unlike Ku-55933, the presence of ATRi does not affect viral DNA replication centers. (A) Graph of Tag staining patterns of SV40-infected BSC40 cells treated with Ku-55933 for the last 0, 4, 8, 16, 24 h of a 48 h SV40 infection. No points on weak line are statistically significant from SV40 infected cells treated with DMSO during the final 24 h of a 48 h infection (0 h Ku-55933). All data points on the dispersed and normal staining pattern lines are significantly different than the 0 h Ku-55933 control ($p < 0.05$). Each data point on the graph represents the average of 3 independent experiments. (B) Tabulated Tag staining patterns of SV40-infected cells exposed to DMSO, Ku-55933, or ATRi during the final 8 h of a 48 h infection. Table shows the average of 3 independent experiments. (C - E) Western blots of cell lysates extracted from SV40-infected BSC40 cells exposed to DMSO, ATRi, or Ku-55933 from 40 - 48 hpi (C, E) or cells treated with the indicated amounts of NCS for 30 minutes (D).

SV40-infected cells relative to mock-infected cells (Figure 34C, compare lane 1 to 4). The presence of ATRi during the final 8 h of infection inhibited Chk1 phosphorylation (Figure 34C, compare lane 1 to 2). However, Ku-55933 treatment from 40 - 48 hpi resulted in only a minor decrease in Chk2 phosphorylation relative to SV40-infected cells in the presence of DMSO (Figure 34C, compare lane 1 to 3). Notably, the phosphorylation of ATM substrate Nbs1 was decreased in the presence of Ku-55933 (Figure 34C, compare lane 1 to 3). Importantly, Ku-55933 effectively inhibited the phosphorylation of Chk2 following exposure to the radiomimetic drug neocarzinostatin (NCS) (Figure 34D, compare lanes 1 - 3 to 4 - 5). This latter result confirms that Ku-55933 effectively inhibits ATM and suggests that the residual Chk2 phosphorylation is a result of ATM phosphorylating Chk2 prior to Ku-55933 exposure (Chk2 half-life > 6 h (Antoni et al., 2007)). As determined by S2056 phosphorylation, DNA-PK_{cs} was weakly activated by SV40 infection (Figure 34E, compare lane 1 to 5), yet inhibition of either ATR or ATM during the final 8 h of a 48 h SV40 infection elicited robust DNA-PK_{cs} auto-phosphorylation on S2056 (Figure 34E, compare lane 1 to 2, 3). SV40 infection or inhibition of ATM or ATR during SV40 infection had only minor effects on the phosphorylation of DNA-PK_{cs} residue T2609, a reported ATM, ATR, and DNA-PK_{cs} target (Figure 34E) (Chen et al., 2007; Uematsu et al., 2007; Yajima et al., 2006). These data imply that ATM and ATR kinases might prevent DNA-PK_{cs} activation during SV40 DNA replication.

ATM kinase activity prevents DNA-PK activation at the viral replication center

The increased DNA-PK_{cs} activation observed as a consequence of ATM or ATR inhibition might correspond to a change in the distribution of DSB repair factors to SV40 DNA replication centers. To examine whether DNA damage signaling during SV40 infection influences the association of DNA repair factors with viral DNA replication

centers, the subcellular localization of several HR and NHEJ proteins was assessed by immunofluorescence microscopy of SV40-infected BSC40 cells. As observed previously, an EdU pulse and chromatin-bound Rad51, CtIP, and BLM but not DNA-PK co-localized with Tag at 48 hpi in DMSO-treated BSC40 cells (Figure 35A, B, C). Again in cells with Tag staining, viral DNA replication centers were unaffected by ATR inhibition (Figure 35 A, B, C). The EdU signal was more intense in ATRi-treated cells than in DMSO-treated cells (Figure 35A, compare DMSO to ATRi fluorescence signal intensity). Furthermore, the HR proteins Rad51, CtIP, and BLM colocalized with Tag and EdU pulse labeling when ATR was inhibited (Figure 35A, B). In spite of increased Ku70 focus intensity following ATRi treatment (Figure 35C graph), activated DNA-PK_{cs} and Ku70 still did colocalize with Tag (Figure 35C). Examination of DNA-PK_{cs} and Ku80 localization yielded identical results to those observed for Ku70 (data not shown).

The presence of Ku-55933 during the final 8 h of a 48 h SV40 infection revealed weaker Rad51 staining that still co-localized with the dispersed Tag immunostaining (Figure 35A). Similar to ATR inhibition, the EdU signal remained co-localized with Tag when ATM was inhibited (Figure 35A). Also, the EdU fluorescent signal was increased by ATM inhibition (Figure 35A). However, unlike Rad51, HR proteins CtIP and BLM no longer colocalized with the dispersed Tag signal when ATM was inhibited (Figure 35B). Consistent with the immunoblotting results, DNA-PK was strongly activated upon ATM inhibition during the final 8 hr of a 48 h SV40 infection (Figure 35C, DNA-PK_{cs} pS2056). Furthermore, the fluorescent signals from immunostains of DNA-PK_{cs} pS2056, Ku70, DNA-PK_{cs}, and Ku80 co-localized with Tag in the presence of Ku-55933 (Figure 35C, see enlargement and data not shown). Taken together, these results indicated that ATM kinase activity has a major role in preventing DNA-PK activation at replicating viral DNA at Tag foci.

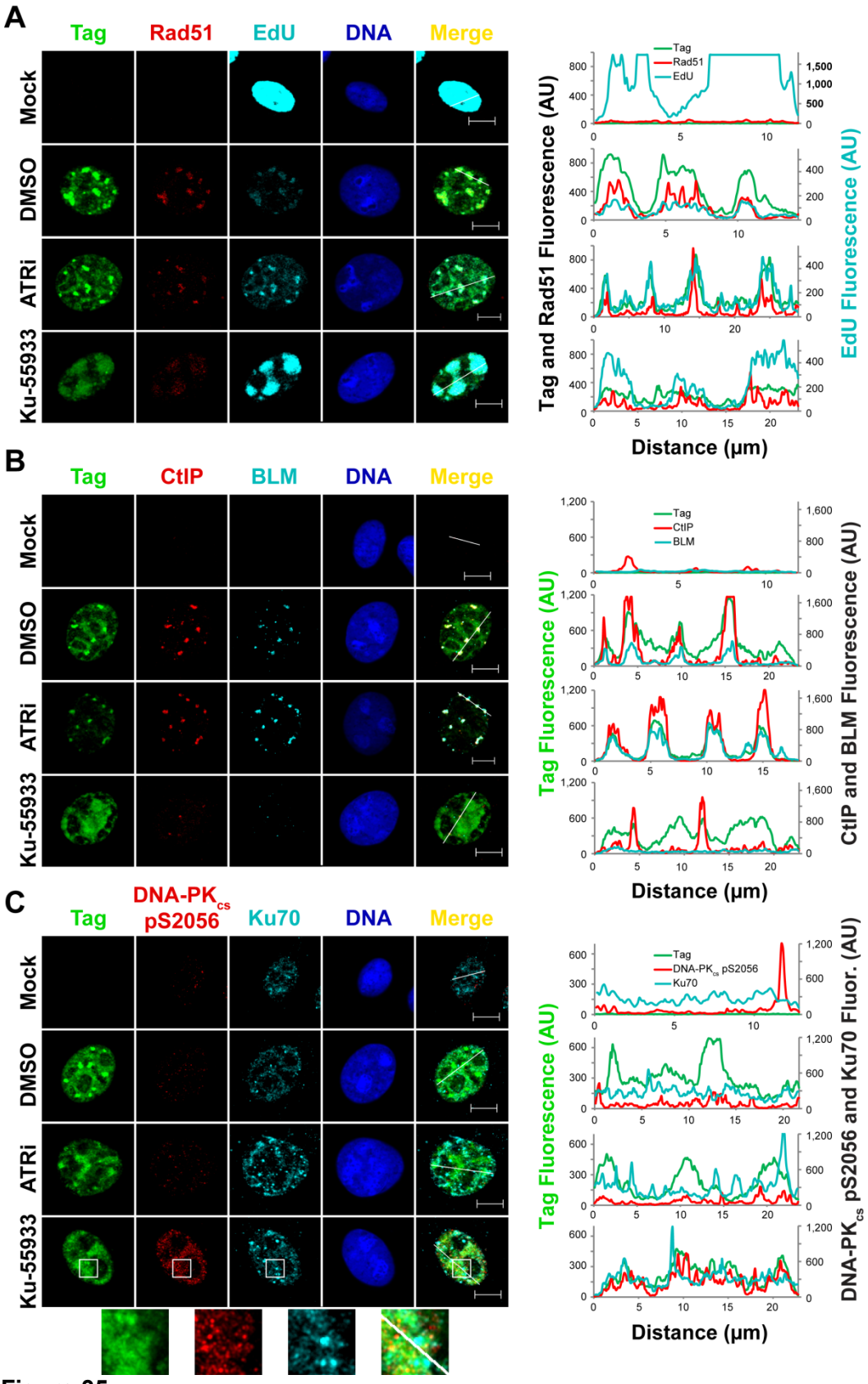
A
Tag
Rad51
EdU
DNA
Merge
Mock
DMSO
ATRi
Ku-55933
Tag
Rad51
EdU
Tag and Rad51 Fluorescence (AU)
EdU Fluorescence (AU)
Distance (μm)
B
Tag
CtIP
BLM
DNA
Merge
Mock
DMSO
ATRi
Ku-55933
Tag
CtIP
BLM
Tag Fluorescence (AU)
CtIP and BLM Fluorescence (AU)
Distance (μm)
C
Tag
DNA-PKcs pS2056
Ku70
DNA
Merge
Mock
DMSO
ATRi
Ku-55933
Tag
DNA-PKcs pS2056
Ku70
Tag Fluorescence (AU)
DNA-PKcs pS2056 and Ku70 Fluor. (AU)
Distance (μm)

Figure 35.

Figure 35. ATM inhibition affects the localization of DNA repair proteins during SV40 chromatin replication.

(A) Immunofluorescence microscopy of the indicated factors from SV40- or mock-infected BSC40 cells treated with DMSO, ATRi, or Ku-55933 during the final 8 h of a 48 h SV40 infection. Prior to fixation at 48 hpi, non-chromatin bound proteins were extracted from cells. The fluorescence intensity in arbitrary units (AU) along the line shown in the merged image is graphed in the right panel. Scale bars represent 10 μm.

Discussion

Our data demonstrate that through the action of ATM and ATR kinases, SV40 recruits a complex set of DNA repair activities to viral DNA replication centers. This study presents several lines of evidence suggesting that ATM kinase activity during viral DNA replication modulates the preference for homology-directed repair over NHEJ. We show that viral DNA replication centers selectively colocalize with HR factors but not NHEJ proteins (Figures 29, 30, 32, and 33). Additionally, DNA-PK_{cs}, whose kinase activities are required for NHEJ, is not robustly activated by SV40 infection (Figure 31), supporting the idea that proteins or DNA structures present at replicating chromatin might obstruct the NHEJ pathway. Importantly, DNA damage signaling is vital to maintain viral replication centers (Figures 34). Aberrant viral DNA replication centers only formed following ATM kinase inhibition during viral DNA replication, suggesting that ATM promotes the stable recruitment of repair factors to the replication center. Furthermore, we present data that ATM kinase activity, but not ATR kinase activity is required for the colocalization of CtIP and BLM, but not Rad51 with Tag (Figure 35). Additionally, inhibition of ATM kinase activity alone prevented NEHJ association and activation at the viral DNA replication center (Figure 35), indicating that ATM and not ATR activity prevents NHEJ at the replicating DNA. Collectively, our results lend support to the hypothesis that ATM and ATR activities promote different aspects of repair during viral DNA replication.

ATM activation blocks DNA-PK_{cs} function at viral DNA replication centers

The prevention of DNA-PK recruitment to viral DNA replication centers and kinase activation during SV40 DNA replication is reminiscent of the effect of the cell cycle on NHEJ function. DNA-PK_{cs} kinase function is markedly decreased during S

phase in response to several DNA-damaging agents (Chen et al., 2005). Perhaps this decrease in DNA-PK function results from the activation of homology-directed repair during S phase (Sartori et al., 2007; Huertas et al., 2009; Yun et al., 2009), thereby resulting in an increased competition between MRN/CtIP and Ku for binding to and processing of exposed ends of the DSB. As both MRN/CtIP and Ku possess activities that promote repair of DSBs by either HR or NHEJ, respectively (Chapman et al., 2012), binding one protein (e.g., Ku) prior to the other (e.g., MRN/CtIP) might channel repair in one direction or another. However, such a model does not explain how ATM kinase activity influences the observed lack of recruitment of DNA-PK or CtIP/BLM to viral DNA replication centers (Figure 35).

ATM is not required for homologous recombination (Rass et al., 2013), but its activity influences the repair kinetics of DSBs (Berkovich et al., 2007). Therefore, a more plausible model for how ATM activity mediates DNA repair at viral DNA replication centers may be that ATM kinase activity activates or promotes stable association of factors that function in homology-directed repair (Matsuoka et al., 2007; Derheimer et al., 2010). Such a mechanism might be able to prevent DNA-PK activation. ATM directely phosphorylates several candidates, including both CtIP (Li, Ting et al., 2000) and BLM (Ababou, Dutertre et al., 2000). However, the number of substrates phosphorylated following DNA damage by either ATM and ATR is enormous (Matsuoka et al., 2007).

A second possibility is that ATM kinase activation results in the recruitment of a protein to viral DNA replication centers that blocks DNA-PK activation. Brca1 is to be recruited to DSBs in an ATM-dependent manner (Derheimer et al., 2010) and localizes to viral DNA replication centers (Boichuk et al., 2010). Thus, Brca1 binding adjacent to the DSB may promote MRN/CtIP binding and subsequent DSB end resection preventing DNA-PK activation (Chapman et al., 2012). Further effort will be required to distinguish

the intricacies of ATM signaling that promote homology-directed repair at the viral replication center and prevent DNA-PK activation and subsequent NHEJ.

CHAPTER V

PERSPECTIVES AND FUTURE DIRECTIONS

Introduction

Our studies of SV40 DNA replication have resulted in three discoveries that have helped shed light on both the mechanisms of viral and cellular DNA replication. First, we identify that viral DNA replication is associated with increased DNA damage signaling and repair factor accumulation at the viral DNA replication center, marked by Tag (Figures 10-12, 29-31). This primary result implies that unperturbed viral and likely cellular DNA replication requires DNA repair to efficiently replicate viral and cellular genomes, respectively. The type of damage (e.g., base modifications, inter-strand crosslinks, intra-strand crosslinks, or DSBs) that requires ATM- and ATR-directed DNA repair is debatable.

Second, we expand on this preliminary finding by demonstrating that ATM kinase prevents accumulation of DSBs during viral DNA replication, likely by promoting 5' to 3' end resection at the DSB termini (Figures 14-16, 26, 35). If and how ATM contributes to cellular DNA replication has been the subject of debate (Gamper et al., 2012). Furthermore, what aspect of ATM signaling might channel DNA repair toward one pathway or another has remained elusive (Rass et al., 2013; Berkovich et al., 2007). Thus, the identification of a defect in 5' to 3' end resection recruitment, a key step in homology-directed repair, with a subsequent activation of NHEJ at the DSB (Figures 34, 35) implies that ATM is able to directly influence DSB repair at unmodified replication-associated DSBs.

Third, the insights gained from viral DNA replication pertaining to the ATR-Chk1 pathway are the first molecular verification of DNA replication fork-associated breakage upon inhibition of the ATR-Chk1 pathway in the setting of metazoan cells (Figures 21-25). The results pertaining to ATR and Chk1 kinase activities indicate that the ATR-Chk1 pathway is not required for the repair of one-ended DSBs (Figure 26), delineating the ATM and ATR mediated pathways from one another. Yet, our data, consistent with previous data obtained in *Saccharomyces cerevisiae* (Lopes et al., 2001), demonstrate that viral replication fork convergence is a source of replication fork stalling and breakage that necessitates ATR-Chk1 phosphorylation to orchestrate this pathway.

The three aforementioned discoveries will be further discussed along with implications on how cellular DNA is repaired by ATM and ATR signaling. Additionally, the use of ATM and ATR kinase inhibitors as anti-virals against human small DNA tumor virus infections or chemotherapeutic agents for cancer treatment will be examined. Overall, we suggest that our observations are the result of the failure to repair DNA lesions by MMR, NER, or BER causing increased numbers of modified bases or SSBs in the viral genome that might necessitate ATM and ATR mediated DNA repair pathways.

DNA damage signaling induction by viral DNA replication

The timing of SV40 DNA replication and DNA damage signaling inside infected cells is closely correlated (Zhao et al., 2008). I have elaborated upon this finding by further expanding the list of cellular components found at or near the SV40 DNA replication center (Figures 10 -13, 29). Contrary to initial insights (Boichuk et al., 2010; Hein et al., 2009), large, irregular Tag foci and DNA damage signaling at the Tag foci were not observed in the absence of a functional viral origin of replication or viral helicase (Figure 10 B - D). Differentiating our studies from previous work (Boichuk et al.,

2010; Hein et al., 2009) was the use of the SV40 origin, SV40 early promoter, and times after transfection that correlate well with actual viral infection (Figure 10). Our experiments suggest that the Tag foci are the viral DNA replication centers. Furthermore, we conclude that viral DNA replication is a prerequisite for DNA damage signaling in the context of transfection and likely permissive infection.

These data are inconsistent with Tag expression in the absence of viral DNA replication being able to activate DNA damage signaling to form intense γH2AX foci during the timeframe of permissive infection. However, in the absence of the viral origin, it is difficult to rule out the possibility that prolonged Tag expression has adverse effects, due to a failure to perform its normal functions. This might explain how deregulated expression of polyomaviral Tag (Boichuk et al., 2010; Hein et al., 2009) and HPV E1 and E2 (Sakakibara et al., 2011; Fradet-Turcotte, Bergeron-Labrecque et al., 2011) proteins might contribute to increased tumorigenesis in abortive infection. However, in the context of permissive infection, our experimental data raise questions about the relevance of the Bub1-Tag interaction as a cause of genomic instability.

The DNA damage checkpoint and SV40

In SV40-infected cells, the activation of ATM or ATR should arrest cells in S or at the G2/M transition. Cell cycle arrest during SV40 infection depends on ATR signaling (Okubo, Lehman et al., 2003; Rohaly et al., 2010). Therefore, we suggest that upon the G1 to S transition in SV40 infected cells, the combined contributions of premature S phase entry and broken DNA, produced during viral DNA replication, should provide enough replication stress that ATR kinase activity does not decrease during viral DNA replication. This concept is implied by the increasing ATR activity that occurs between

24 and 48 hpi (Figure 31) and the complete reliance of SV40 DNA replication on ATR signaling during the late phase of SV40 infection (Figure 28).

However, why both ATM and ATR kinase activities are required for proper S phase arrest prior to 20 hpi is not well elucidated from our studies (Figure 28). The decrease in total SV40 DNA replication when ATR or ATR were inhibited early during SV40 infection is consistent with both ATM and ATR kinase function being crucial to virally-induced S phase arrest (Figures 14, 21, 22). A plausible explanation for the different contributions of ATM and ATR to S phase arrest during SV40 infection might be that the type of DNA damage elicited prior to 20 hpi differs from that which accumulates during robust viral DNA replication. For instance, early during infection (0 - 20 hpi), premature entry into S phase is likely to have a larger contribution to ATR and ATM activation than would be observed at later time points (greater than 20 hpi). Another possibility is that the amount of activation needed to reach the threshold to activate a cell cycle checkpoint requires signaling of both ATM and ATR prior to 20 hpi during SV40 infection. After 20 hpi, the viral DNA is actively being replicated, and the amount of replication stress from viral fork convergence (Figures 24, 25) emanating from viral DNA replication centers might sufficiently activate ATR to facilitate the S phase checkpoint. Importantly, these models are not mutually exclusive.

One might address how DNA damage signaling affects the early phase of infection by arresting cells in G1, S, or G2/M followed by SV40 infection. The arrested cell populations could be infected in the presence or absence of ATM or ATR inhibitors from 30 minutes prior to infection through 20 hpi. Such experiments would allow the differentiation of replication stress via forced G1 to S transition and maybe even premature mitosis. However, the circumstances that activate ATM and ATR as a result of SV40 DNA replication (20 hpi and beyond) cannot be determined by this line of experimentation. The mechanisms that contribute to DNA damage signaling inside

SV40-infected cells after 20 hpi are likely elicited by cellular DNA replication. Thus, the DNA replication-dependent activation of ATM and ATR that occurs after 20 hpi may be more important to understanding the types of DNA replication-associated damage contributing to the control of cellular genome stability than DNA damage signaling produced in the early phase of infection (during Tag accumulation and Tag mediated G1 to S transition).

ATR and ATM function: insights from a virus

Due to the ability to activate a cell cycle checkpoint, ATM and ATR kinase activities are implied to have an indirect role in viral DNA replication. The finding that aberrant structures and intermediates (Figures 14, 15, 16, 18, 21, 22, 24, 26) amass when either kinase is inhibited during viral DNA replication demonstrates the crucial role of each kinase in orchestrating viral DNA replication. Our direct examination of the DNA replication intermediates by 2d gel electrophoresis from SV40-infected cells when ATM, ATR, or Chk1 kinase is inhibited (Figures 16, 24) lends new insights into the DNA replication defects of viral and cellular replication. Although we observe pronounced defects in viral DNA replication, our studies do not determine what aspect of viral DNA replication actually initiates the kinase activities of ATM and ATR.

Based on the differences in aberrant product accumulation and DNA breakage products (Figures 14-16, 21, 22, 24, 26), the type of DNA damage that requires ATM or ATR signaling during unperturbed viral (and likely cellular) DNA replication is likely distinct. Our data indicate that replicating SV40 DNA breaks upon replication fork convergence in ATR-inhibited cells (Figure 25), but due to the nature of rolling-circle replication, the site of breakage could not be assessed in ATM-inhibited cells. Analysis of genome replication by 2d gel electrophoresis from *Saccharomyces cerevisiae*

harboring mutations that abrogate the functions of ATR or Chk1 orthologs suggests that ATR and Chk1 are needed to prevent fork stalling and breakage upon DNA replication stress (Lopes et al., 2001). Knockdown of ATR or Chk1, but not ATM, in human cells results in expression of common fragile sites in the human genome with and without replication stress (Casper et al., 2002; Durkin et al., 2006). Common fragile sites are late replicating regions of the genome (Le Tallec, Dutrillaux et al., 2011; Letessier, Millot et al., 2011) associated with ultrafine anaphase bridges during mitosis (Chan et al., 2009). Collectively, we suggest that the ATR-Chk1 pathway is required for some aspect of fork convergence (Figure 27, step X), perhaps as a result of fork slowing and stalling upon viral fork convergence (Tapper et al., 1982; Tapper et al., 1980; Tapper and DePamphilis, 1978). I hypothesize that the defect in fork convergence may be separate from the S phase checkpoint defect that occurs when the ATR-Chk1 pathway is inhibited. Therefore, I propose that the Chk1 phosphorylation targets that promote replication fork convergence are likely DNA repair and DNA replication proteins rather than factors that promote cell cycle progression.

Models for ATR and ATM prevention of replication-associated breaks

Substrates of the ATR-Chk1 pathway that mediate fork convergence are not the only component that requires a more thorough understanding. Mechanisms defining how DNA breaks upon fork convergences are lacking in the metazoan system. However, models suggest that upon replication stress, unidirectional replication forks stall and regress to form Holliday junctions (Petermann et al., 2010; Ray Chaudhuri, Hashimoto et al., 2012). Regressed forks (Holliday junctions) accumulate in both yeast harboring mutations in either ATR and Chk1 orthologs after exposure to hydroxyurea, implying a link between the ATR-Chk1 pathway and fork regression (Lopes et al., 2001;

Sogo, Lopes et al., 2002; Raveendranathan, Chattopadhyay et al., 2006). At the stalled replication fork, the regressed fork is then hypothesized to be cleaved by Holliday junction resolvases resulting in an one-ended DSB (Petermann et al., 2010; Petermann, Orta et al., 2010).

Although an attractive model which explains fork breakage upon replication fork convergence when ATR or Chk1 activity is decreased (Figure 27), we do not support a model whereby aberrant cleavage of regressed replication forks occurs. Stalled DNA replication forks remain stable during viral fork convergence and the unstalled fork breaks when the ATR-Chk1 pathway is inhibited (Figures 24, 25), which is inconsistent with the model put forth by Petermann and Helleday. Perhaps more importantly, data pertaining to Holliday junction resolvases is not consistent with any sort of promiscuous replication fork cleavage during S phase in the absence of ATR-Chk1 kinase signaling. This statement is supported by the mechanisms that regulate cellular Holliday junction resolvase function. First, Mus81/Eme1, the endonuclease proposed to cleave stalled replication forks in yeast and humans, is activated by a DNA damage induced Chk1-dependent phosphorylation in *Schizosaccharomyces pombe* (Dehe, Coulon et al., 2013). Second, Holliday junction resolvases are not active during S phase in yeast or human systems. CDK-dependent phosphorylations that occur during G2 and M phases are required for the Holliday junction resolvase activity of Gen1 and Mus81/Eme1/Slx1/Slx4 (Matos, Blanco et al., 2011; Matos, Blanco et al., 2013; Dehe et al., 2013). Lastly, the activation of Mus81 endonuclease activity that follows DNA damage is required for efficient repair of replication-associated DSB and loss of this function results in cell death (Hanada, Budzowska et al., 2007), implying that Chk1 activation of Holliday junction resolvases, like Mus81/Eme1, may be crucial for efficient replication fork recovery after replication stress.

A second pathway that could function in viral (and cellular) DNA replication fork convergence is catalyzed by the Fanconi anemia pathway of inter-strand DNA crosslink repair (Moldovan and D'Andrea, 2009). The viral DNA replication center colocalizes with several factors that are known to function in inter-strand crosslink repair and HR, a sub-pathway of inter-strand crosslink repair. Similar to ATR and Chk1 inhibition or knockdown, defects in either pathway result in increased expression of common fragile sites (Franchitto et al., 2011; Debatisse et al., 2012), ultrafine anaphase bridge formation (Chan et al., 2009; Chan et al., 2007; Laulier et al., 2011), and genome breakage during unperturbed DNA replication (Hashimoto et al., 2012; Chu et al., 2009; Moldovan et al., 2009; Wechsler et al., 2011). These data suggest that HR and Fanconi anemia pathways are used during every cell cycle to promote genome integrity. Thus, these pathways might represent viable substrates of ATR and Chk1 in fork convergence.

The Fanconi anemia pathway is activated at stalled forks (Moldovan et al., 2009). Furthermore, the Fanconi anemia pathway is activated by ATR dependent phosphorylations (Andreassen, D'Andrea et al., 2004) indicating that inter-strand crosslink repair is a key substrate of ATR-Chk1 kinase signaling. Therefore to implicate the Fanconi anemia pathway in SV40 replication fork convergence, FancM or Faap24, proteins which initiate inter-strand crosslink repair (Moldovan et al., 2009), could be knocked down in SV40 infected cells. SV40 genomic DNA could then be extracted from FancM, Faap24, and control knock down cells and subjected to 2d gel electrophoresis and southern blotting. If FancM knockdown phenocopies ATR inhibition, then we can conclude that the Fanconi anemia pathway is used to facilitate fork convergence and maybe even remove of the replisome.

To more broadly address what DNA repair factors influence fork breakage of the unstalled fork upon replication fork convergence when ATR-Chk1 signaling is decreased, we suggest the use of neutral sucrose gradients to isolate replicating viral

chromatin (Su and DePamphilis, 1976; Otto and Fanning, 1978). This technique can be combined with mass spectrometry technologies to identify differences the proteins associated with replicating viral chromatin in the presence or absence of robust ATR/Chk1 kinase signaling. We support the notion that replicating viral chromatin will contain different repair factors when Chk1 is inhibited. Importantly, neutral sucrose gradients and mass spectrometry might enable the identification of the crucial Chk1 kinase substrate needed to prevent fork stalling and breakage of the unstalled fork. Chk1 exhibits a weak consensus phosphorylation sequence (Blasius, Forment et al., 2011), thus the aforementioned technique circumvents problems associated with identification of Chk1 phosphorylation sites based on consensus amino acid sequence. I believe that SV40 may reveal the secrets of the mechanisms that promote cellular replication fork convergence.

The repair of DSBs induced by ionizing radiation (IR) is slowed in AT cells compared to normal cells, implying that some portion of DSB repair necessitates ATM kinase activity (Berkovich et al., 2007). With that in mind, it may be possible that the type of break sustained by the viral replication fork, whether it be on the leading or lagging strand, determines whether ATM or ATR is required to repair the broken DNA. Additionally, ATM and ATR signaling might activate or recruit a different set of factors to replicating chromatin. Even with the differences observed in the amount of DNA undergoing rolling circle DNA replication when ATM or ATR were inhibited, how the DNA initially forms a rolling circle is unclear. A probable explanation is that replication through a SSB forms a DSB (Petermann et al., 2010). Examination of viral genome replication when SSB repair is inhibited using PARP inhibitors such as Olaparib (Menear, Adcock et al., 2008) would allow this question to be definitively answered. Importantly, ATM-null cells are particularly sensitive to PARP inhibition (Radhakrishnan, Bebb et al., 2013). Thus, examination of SV40 DNA replication when both ATM and SSB repair are

inhibited might enhance an understanding of the defects that accompany viral concatemer formation and help address the molecular aspects of the synthetic lethality that occurs upon ATM and PARP inhibition in p53 null cell lines.

Viral replication centers: hubs of homology-directed DNA repair

SV40 DNA replication centers recruit a diverse set of proteins and functions (Rohaly et al., 2010; Sowd et al., 2012; Zhao et al., 2008; Boichuk et al., 2010). Prior to my studies, the contribution of these proteins, particularly ATM and ATR, to viral DNA replication was not well elucidated. My results indicate that ATM activity at the viral replication center correlates with reduced DNA-PK_{cs} activation at Tag foci (Figures 13, 35). Mechanisms promoting this phenomenon are not well understood inside the infected cell. Additionally, the aspects of DNA damage signaling during cellular DNA replication that prevent DNA-PK_{cs} activation at replicating DNA are poorly elucidated. Notably, mutation of PIKK phosphorylation sites on Ku70/80 has no effect on NHEJ or HR (Neal et al., 2011), implying that ATM and ATR kinase activities do not directly control Ku70/80 binding to DNA. Although ATM and ATR phosphorylate DNA-PK_{cs} at residue T2609 (Chen et al., 2007; Uematsu et al., 2007; Yajima et al., 2006), phosphorylation of T2609 is not robust during unperturbed SV40 infection (Figure 34), which is consistent with decreased phosphorylation of this residue during cellular S phase (Chen et al., 2005). The phosphorylation of T2609 on DNA-PK_{cs} occurs somewhat more prominently when ATR or ATM is inhibited (Figure 34), supporting the model proposed by Meek et al. whereby phosphorylation of this residue is a step during NHEJ (Meek et al., 2007). Perhaps phosphorylation of other residues on DNA-PK_{cs} by ATM or ATR controls NHEJ at areas of robust DNA replication, but the model pertaining

to the ABCDE patch of DNA-PK_{cs} regulating NHEJ is not consistent with recent data and current models of the regulation of DSB repair (Neal et al., 2011).

Another possibility that might prevent DNA-PK activation and subsequent NHEJ at replicating viral and perhaps cellular DNA is the large amounts of ssDNA at the site of breakage that can occur during S phase. This ssDNA could be attributable to the tracts of ssDNA on the lagging strand of the replication fork (Hashimoto et al., 2012), leading strand polymerase stalling and subsequent fork breakage, or even increased 5' to 3' end resection during S phase (Goodarzi et al., 2013). Large tracts of ssDNA at the DSB were found to be more weakly bound *in vitro* by Ku70/80 (Foster, Balestrini et al., 2011). Weakened Ku binding might prevent NHEJ at replication forks. However, this mechanism does not explain why ATM and not ATR kinase signaling affected Ku and DNA-PK_{cs} recruitment to viral DNA replication centers (Figure 35). The effect of Ku-55933 on the localization of Ku and DNA-PK_{cs} in SV40-infected cells makes it more probable that 5' end resection mediated by CtIP/MRN and BLM/Exo1/Dna2 plays a major role in the prevention of NHEJ during viral genome amplification (Figure 35). Since the proteins that promote 5' end resection are recruited to viral DNA replication centers in an ATM-dependent manner (Figure 35), 5' end resection of broken viral DNA represents a plausible explanation for the lack of DNA-PK at Tag foci. ATM and ATR signaling is associated with more stable recruitment of repair enzymes to damaged DNA (Ciccia et al., 2010). Thus, the stabilization and/or activation of DNA repair enzymes might be primarily mediated by ATM during viral DNA replication. CtIP is a substrate of ATM signaling (Li et al., 2000), but several other ATM substrates likely influence end resection (Matsuoka et al., 2007). Additionally, FancD2, a DNA interstrand crosslink repair protein that colocalizes with Tag in SV40-infected cells (Boichuk et al., 2010), affects DNA-PK activation at cellular replication forks (Adamo et al., 2010). Thus, several mechanisms are possible that might affect Ku70/80 binding in an ATM-dependent

manner. A greater understanding of the difference in substrate preferences of ATM and ATR might aid in determining how NHEJ is prevented during viral and cellular DNA replication.

Despite the observed defects in DSB repair localization upon ATM inhibition (Figure 35) and DNA replication when ATM or ATR are inhibited (Figures 14, 15, 16 18, 21, 22, 24, 26), it is not known what DNA repair pathways contribute functionally to preventing aberrant viral DNA structures or general viral DNA replication (Figure 27, I-IV, VII). Colocalization at replicating viral DNA does not imply function, therefore functional studies using SV40-infected cells in which homology-directed repair is decreased need to be performed. Such experiments will allow us to determine if homology-directed repair, HR and SSA, actually affects concatemer formation and gross viral DNA replication in SV40-infected cells in a manner similar to ATM inhibition. To address this aspect, abrogation of homology-directed repair by CtIP knockdown in SV40-infected cells could be employed. Additionally, it may be prudent to verify that the decreased localization of homology-directed repair proteins to viral replication centers upon ATM inhibition (Figure 35) corresponds reduced binding to the viral genome as measured by chromatin immunoprecipitation. Such experiments will aid in elucidating the roles of the repair pathways utilized by the virus and cellular DNA replication.

Are ATM and ATR good drug targets for anti-virals and chemotherapeutics?

Specific inhibitors of crucial steps in DNA replication and repair, similar to those used in these studies, have paved the path for science to investigate essential pathways contributing to genome maintenance. More importantly, insights gained from experiments with inhibitors of DNA replication and repair have allowed clinicians to use DNA replication or repair inhibitors as chemotherapeutic agents in a clinical setting. We

observed distinct SV40 DNA replication defects associated with ATM or ATR-Chk1 inhibition (Figure 27) providing further evidence of the possible effectiveness of inhibition of DNA damage signaling during DNA replication. Both ATRi (VE-821) and Ku-55933 possess great possibilities for use as chemotherapeutic agents when combined with more potent inducers of DNA damage (e.g., topoisomerase inhibitors or ionizing radiation) (Hickson et al., 2004; Reaper et al., 2011). Like many other common chemotherapeutics, ATRi and UCN-01 target actively proliferating cells, due to the heavy reliance of S phase cells on ATR-Chk1 signaling and the S phase checkpoint (Toledo et al., 2011). Similarly, when combined with DNA damaging agents, ATM inhibition further exacerbates chromosomal aberrations that accumulate as a consequence of DSB formation (Choi, Gamper et al., 2010).

In theory, ATM and ATR may represent useful targets for chemotherapeutics and anti-virals against persistent infections of BK virus or JC virus in immunocompromised patients. In spite of this, inhibition of DNA damage signaling has some major drawbacks. ATM kinase inhibition results in more severe phenotypes than loss of the ATM gene itself implying that we do not understand the pathways that ATM controls as well as was first expected (Choi et al., 2010). Prolonged ATR inhibition is severely toxic to cells, leading to chromosomal aberrations and decreased colony forming ability (Toledo et al., 2011; Reaper et al., 2011; Couch, Bansbach et al., 2013). Furthermore, neither ATM, ATR, or Chk1 inhibition completely stops the production of unit length viral products (Figures 14, 15, 21, 22, 23), implying that infectious virus is still produced from infected cells albeit at lower levels. Although treatment of immunocompromised BK virus or JC virus patients with Ku-55933 or ATRi might work to lower the viral load inside the patient, these drugs would need to be administered either persistently or in pulses (e.g., 2 - 8 h with drug, 1 week off drug) throughout the rest of the patient's life.

Based on cellular phenotypes of ATR-inhibited or ATR-null cells (Wright, Keegan et al., 1998; Brown et al., 2000), persistent ATRi treatment would likely kill the patient. Although persistent Ku-55933 might be possible, the accumulation of recombinogenic viral concatemers (Figures 14, 15) and chromosomal aberrations (Choi et al., 2010) would likely make the patient prone to carcinogenesis. Therefore, I suggest that pulses of ATRi and/or Ku-55933 be administered to immunocompromised JC virus or BK virus infected patients to decrease viral DNA replication (Figure 26) and possibly viral load. Importantly, these two drugs could likely be administered in a similar manner for use as chemotherapeutics. However, the aforementioned limitations for the use of ATRi and Ku-55933 as anti-virals still apply to their use as chemotherapeutic agents.

Further studies of the downstream pathways promoted by ATM and ATR during SV40 DNA replication will aid in the discovery of new druggable targets for use as anti-virals and chemotherapeutic agents. Notably, the ATM and ATR pathways are essential for both viral genome and host genome stability, therefore knowledge gained from my research is readily applicable to DNA repair mechanisms and both polyomavirus and cellular DNA replication. I suggest that it will be highly beneficial to continue to study SV40 as both a model for small DNA tumor virus DNA replication and cellular genome replication. The insights gained from the study of SV40 regarding DNA replication, cell cycle regulation, and transcription are likely only the tip of the iceberg. Thus, I firmly believe that future work using viral systems in conjunction with multi-cellular and yeast eukaryotic systems will continue to define the mechanisms exploited by viruses and in cancer.

CHAPTER VI

MATERIALS AND METHODS

Cells and SV40 infection

BSC40 and U2OS cells were cultured in complete Dulbecco's modified Eagle's medium (DMEM supplemented with 10% fetal bovine serum) at 37°C with 5% CO_2. For indirect immunofluorescence, cells were grown on an 18 x 18 mm glass cover slip (Fisher) in 35 mm dishes. Prior to SV40 infection, equal numbers of cells were plated into dishes. A duplicate dish was counted to determine total cell number, and cells were infected with DMEM containing SV40 at a multiplicity of infection of 10 (BSC40) or 115 (U2OS) focus forming units/cell. Mock infections were performed in parallel, by using, an equal volume of DMEM lacking virus.

WST-1 viability assay

BSC40 cells were plated into wells of a 96 well plate and treated with ATRi as described in materials and methods under the inhibitors and treatments subheading. At 48 hpi, WST-1 assay was performed according to manufacturer protocol (Roche). To obtain the viability of ATRi treated SV40-infected or mock infected cells compared to SV40-infected cells in the presence of DMSO (Viability (% of DMSO), the OD of mock or SV40-infected cells in the presence/ absence of ATRi was divided by the OD generated from SV40 infected cells in the presence of DMSO.

Plasmids and transfection

pMini SV40-wt and pMini SV40-D474N were as previously described (Zhou et al., 2012). The In-1 mutation (Cohen et al., 1984; Virshup et al., 1992) was introduced by

standard site-directed mutagenesis into pMini SV40 wt and verified by DNA sequencing. pMini SV40-In-1 contains a single G-C base pair insertion at position 1 of the SV40 genome, abrogating the BglI site.

For transfection, 2 ug of supercoiled pMini SV40-wt or mutant plasmid was transfected into a semi-confluent 35 mm plate of BSC40 cells using Fugene HD (Roche) as per manufacturer protocol. For ectopic expression of HA-topoisomerase IIIα or Flag-RMI2, 2ug of supercoiled pCMV-HA-Topoisomerase IIIα or pIRES-neo-Flag-RMI2 were transfected 24 h prior to SV40 infection as previously described.

Low molecular weight DNA extraction

Equal numbers of cells transfected with pMini-SV40 plasmid were resuspended in 383 µL T10E (20 mM Tris pH 7.5 and 10 mM EDTA). SDS and RNAse A were added to a final concentration of 0.6% and 0.1 mg/mL, respectively. To ensure equal cell lysis, tubes were inverted ten times prior to addition of NaCl to a final concentration of 1M to bring the final volume to 500 µL. High molecular weight DNA was allowed to precipitate overnight at 4°C. DNA was spun at 17000xg for 30 min to pellet host genomic DNA. Equal volumes of supernatant were kept and twice extracted with saturated phenol (pH 7.9) followed by one extraction with 24:1 chloroform: isoamyl alcohol. The resulting supernatants were precipitated with sodium acetate and ethanol. DNA pellets were dissolved in T0.1E overnight and then digested with 20 U of DpnI overnight to digest unreplicated DNA. Following re-precipitation of DNA with sodium acetate and ethanol, DNA was dissolved in 25 µL of T0.1E per $5x10^5$ cells. Equal volumes of DNA were loaded on gels for southern blots.

DNA Isolation

Total intracellular DNA was prepared from infected and mock-infected cells. For each experiment, all samples were prepared from an equal number of cells. Cell pellets were resuspended in 0.4 ml of TE (10 mM Tris pH 8.0, 1 mM EDTA). SDS, RNase A, proteinase K, and Tris pH 7.5 were added to a final concentration of 0.4%, 0.2 mg/ml, 50 ug/ml and 100 mM, respectively, in a total volume of 0.5 ml. Following overnight digestion at 37°C, each sample was extracted twice with Tris-saturated phenol (pH 7.9) and once with 24:1 chloroform: isoamyl alcohol. DNA was precipitated with sodium acetate and ethanol. DNA was allowed to dissolve in T0.1E (10 mM Tris pH 8.0, 0.1 mM EDTA) for 2 days, and then digested overnight at 37°C with 40 U of SacI-HF and XbaI (both from New England Biolabs). Digested DNA was re-precipitated and then dissolved in 50 µL of T0.1E per 2.5 x 10^5 cells. Equal volumes of DNA were loaded on gels for southern blots unless otherwise indicated.

Immunoblots

Whole cell lysates were prepared as previously described [1], except that 1 mM $NaVO_4$ and 5 mM NaF were added during lysis to inhibit phosphatases. Samples containing 10 µg of protein were analyzed by SDS-PAGE and western blotting. The following antibodies were used: anti-Tag (Pab101, [4]), anti-actin (I-19, Santa Cruz), anti-Chk1 (G-4, Santa Cruz), anti-Chk1 pS317 (Cell Signaling), anti-Chk2 pT68 (Y171, Epitomics), anti-Chk2 (EPR4325, Epitomics), anti-Nbs1 pS343 (EP178, Epitomics), anti-ATR (N-19, Santa Cruz), anti-DNA-PK_{cs} (G-4, Santa Cruz), anti-Ku80 (C-20, Santa Cruz), anti-Ku70 (M-19, Santa Cruz), anti-DNA PK_{cs} pS2056 (EPR5670, Epitomics), anti-GAPDH (0411, Santa Cruz), and anti-DNA PK_{cs} pT2609 (abcam).

Immunofluorescence microscopy

To visualize chromatin-associated proteins, soluble proteins were pre-extracted from cells, followed by fixation and immunostaining as described (Zhao et al., 2008). For EdU labeling of DNA, 10 μM EdU nucleoside in complete DMEM was added to cells for 5 min. At 48 hpi, cover slips were processed for immunostaining and click reaction according to the manufacturer's protocol (Invitrogen). All micrographs were taken using an AxioObserver Z1 (Zeiss) equipped with a 63x Plan Apochromat (NA 1.4) oil objective (Zeiss) and an apotome (0.6 μm z slice) (Zeiss). To quantify Tag staining patterns in SV40-infected BSC40 cells treated with Ku-55933 as in Figure 13D, aberrant and normal Tag staining patterns from 3 independent experiments, each with at least 50 cells, were counted and the average values were graphed. To determine what phases of the cell cycle SV40-infected cells exposed to Ku-55933 or ATRi were in (Figure 28), the staining pattern of CenpF, EdU, and DAPI (Lobrich et al., 2010) in each cell was counted from at least 300 cells. The average values were graphed in figure 28C and D.

Primary antibodies used for immunostaining were anti-Tag (Pab101), rabbit anti-Tag (in house), anti-γH2AX (JBW301, Millipore), anti-Cdc45 (Bauerschmidt, Pollok et al., 2007), anti-PCNA (PC10, Santa Cruz), anti-polymerase δ p125 (C-2, Santa Cruz), DNA anti-polymerase ε (3C5.1, Santa Cruz), anti-RFC1 (H-300, Santa Cruz), anti-CtIP (H-300, Santa Cruz), anti-Brca2 (ab-1, Calbiochem), anti-Rad52 (H-300, Santa Cruz), anti-BLM (C-18, Santa Cruz), anti-RMI1 (Novus), anti-Flag (M-2, Sigma), anti-HA (abcam), anti-CenpF (abcam), anti-DNA-PK_{cs} (G-4, Santa Cruz), anti-Ku80 (C-20, Santa Cruz), anti-Ku70 (M-19, Santa Cruz), and anti-DNA-PK_{cs} pS2056 (EPR5670, Epitomics). Secondary antibodies used for immunostaining were anti-mouse conjugated to Alexa Fluor 488 (Invitrogen), anti-rabbit conjugated to Alexa Fluor 555 (Invitrogen), anti-goat conjugated to Alexa Fluor 555 (Invitrogen), anti-goat conjugated to Alexa Fluor 647

(Jackson ImmunoResearch), and anti-rat conjugated to Dylight 649 (Jackson ImmunoResearch).

Use of PIKK Inhibitors

Ku-55933, kindly provided by Astra-Zeneca, was used as described (Zhao et al., 2008; Hickson et al., 2004). Importantly, Ku-55933 did not inhibit sixty off-target kinases. It specifically inhibits purified ATM with an IC50 of 12.9 nM, whereas it inhibits the related kinases mTOR and DNA-PK with IC_{50} values of 2500 nM and 9300 nM, respectively, *in vitro* (Hickson et al., 2004). Caffeine (Sigma) was dissolved to 24 mM in DMEM and used at a final concentration of 8 mM to inhibit ATM and ATR (Sarkaria et al., 1999). ATRi and Nu7441 were generous gifts from Dr. David Cortez. ATRi dissolved in DMSO at 5 mM was used at a final concentration of 5 μM (Reaper et al., 2011). ATRi selectively inhibits ATR with a K_i of 13 nM, whereas at least a 100-fold higher concentration is required *in vitro* to inhibit the related kinases ATM (K_i = 16000 nM), DNA-PK (K_i = 2200 nM), mTOR (K_i = 1000 nM), and PI3Kgamma (K_i = 3900 nM) (Reaper et al., 2011). Nu7441 was dissolved in DMSO to 2 mM and applied to cells at 1 μM (Hardcastle, Cockcroft et al., 2005; Leahy, Golding et al., 2004). Nu7026 (EMD) was dissolved to 5 mM in DMSO and used at a final concentration of 10 μM (Veuger, Curtin et al., 2003). UCN-01 was dissolved in DMSO to 300 μM and applied to cells at a final concentration of 300nM (Busby et al., 2000).

DMEM containing inhibitor or solvent was added to cells 30 min prior to infection. At time zero, DMEM with inhibitor or solvent was removed, and fresh warm DMEM containing inhibitor or solvent and SV40 was added to cells. Cells were gently rocked every 15 min during the first 2 hpi. At 2 hpi, complete DMEM containing inhibitor or solvent was added to each dish of cells. At 20 hpi, medium was aspirated and cells were washed once with PBS to remove residual inhibitor or solvent. Fresh medium containing

inhibitor or solvent was then added to cells and infections were allowed to proceed until the chosen endpoint. Solvent control treatments utilized the solvent concentration present in the inhibitor-treated medium. To treat cells with inhibitors during the final 8 h of a 48 h SV40 infection, the same procedure was used except the media was removed from the cells at 40 hpi and replaced with fresh media containing either inhibitor or DMSO.

Agarose gel electrophoresis

One-dimensional 0.6 - 0.7 % agarose gels in 1x TAE were electrophoresed at 10 V/cm for 1.5 h. Neutral 2d gel electrophoresis was performed as previously described (Friedman et al., 1995) with the following modifications. The first dimension of the gel was electrophoresed at 1 V/cm through a 0.4% 1x TAE for 22 h. 1x TAE was found to enhance separation of D-loop arc (data not shown). The second dimension was electrophoresed at 5.5 V/cm through a 1.1% 1x TBE gel containing 0.5 ng/ml ethidium bromide for 5.5 h with circulation.

Southern blotting analysis

Southern blotting was performed using radiolabeled probes for SV40 and BSC40 mitochondrial DNA as described (Zhou et al., 2012). A probe for human mitochondrial DNA was generated by PCR amplification (primers: U2OS Mito-F ACG CGA TAG CAT TGC GAG AC; U2OS Mito-R CTT TGG GGT TTG GTT GGT TCG), followed by random priming. Hybridized blots were visualized using a Typhoon Trio laser scanning imager (GE Healthcare) and quantified using ImageQuant 5.2 (GE Healthcare).

Bands or arcs corresponding to each DNA structure of interest were quantified and the value from a region of the blot without signal, e.g. Mock for SV40 probe, was subtracted as background. To compare the level of a DNA structure after a given

treatment (e.g. DNA structure (% of Total DNA)), the total signals for the DNA were summed, and the signal of a discrete DNA structure (e.g. form I monomer) were divided by the total signal in the lane (e.g. [form I monomer signal] / [total signal in the lane]). To quantify variations in replication between treatments, all SV40 DNA signals were normalized using the respective mitochondrial DNA signal. Normalized signals were then divided by the normalized signal present in the infected solvent control to yield the DNA signal (% of DMSO).

The southern blot signals from an equal area of each arc in neutral 2d gels were quantified (boxed areas in Figures 16C, D, E, F and 24 B - D). Background signal in an area of equal size was subtracted, and the values for each arc were normalized to the value for the double Y (Figure 16H), bubble arc (Figure 16I), or X structure (Figure 24H).

Statistics

Statistics were performed in Microsoft Excel using the data analysis package. Prior to t-test, single factor ANOVA analysis was performed. If ANOVA resulted in $p < 0.5$, a two sample t-test assuming unequal variances was performed. One-tailed p values from student's t test are denoted by the number of asterisk(s): * $p < 0.05$ ** $p < 0.01$ *** $p < 0.001$ **** $p < 0.0001$. Unless otherwise noted on the graph, all one tailed p values were generated by comparing data from SV40 infection in the presence of inhibitor to that from SV40 infection in the presence of DMSO. Unless otherwise indicated, bar graphs present the average of 3 to 4 independent experiments and error bars represent standard deviation.

APPENDIX A

ATM AND ATR KINASE ACTIVITIES IMPEDE LINEAR PRODUCT FORMATION DURING SV40 DNA REPLICATION

Introduction and Research Summary

The products of ATR and ATM DNA damage signaling were previously examined by 1d gel electrophoresis to identify aberrant DNA replication products that accumulated upon the inhibition of either ATM or ATR in SV40-infected cells (Sowd et al., 2013). Concatemers, head to tail repeats of the viral genome, were identified to be the primary aberrant replication product generated in either ATM or ATR inhibited SV40-infected cells (Sowd et al., 2013). In this study no decrease in other more transient DNA replication structures (i.e. catenated DNA) was observed. In spite of these observations, 1d electrophoresis has one major problem: electrophoresis of a complex milieu of DNA intermediates cannot differentiate DNAs with different structures that migrate the same distance from the well (ie. Linear monomeric DNA (form III) from catenated supercoiled (form I) dimer (Cat I)) (Pohlhaus et al., 2006). To combat this problem, previous studies of plasmid DNA replication in *Xenopus laevis* extracts have employed neutral 2d gel electrophoresis of undigested circular DNA to characterize DNA replication in the extracts and examine the effects topoisomerase inhibitors on the replication products (Lucas, Germe et al., 2001; Martin-Parras, Lucas et al., 1998).

In this technique, the first dimension of electrophoresis separates DNA on the basis of molecular weight, and the second dimension separates primarily by differences in DNA structure (Figure 36A). We have utilized this technique to further characterize the defects that accompany viral DNA replication upon the inhibition of ATM, ATR, or

both kinases. Our results reveal that compared to DNA replication in the presence of inhibitor solvent (DMSO), inhibition of ATM, ATR or both kinases increases the amount of large broken DNAs migrating greater than one linear genome length. Several canonical and non-canonical DNA replication intermediates decreased in the presence of ATRi, Ku-55933, or both inhibitors including catenated forms (Cat I, Cat I/II, and Cat II/II). Our results are consistent with ATM and ATR kinase activities having roles in promoting viral genome stability.

To further clarify the defects associated with ATM or ATR inhibition, BSC40 cells were infected with SV40 virus and exposed to specific small molecule inhibitors of ATM (Ku-55933 (Hickson et al., 2004)), ATR (ATRi (Reaper et al., 2011)), or combined inhibition (ATRi and Ku-55933) during the final 20 h of a 48 h SV40 infection. Undigested DNA from DMSO or inhibitor exposed SV40-infected cells was then subjected to 2d gel electrophoresis and southern blotting (Figure 36 B - E). Viral DNA replicated in the presence of DMSO demonstrated the expected topological forms of circular DNA (Figure 36 A, B). These forms included the prominent forms I and II monomer that can be easily visualized by 1d gel electrophoresis (Figure 36A, top panel) and several lesser forms (θ replication intermediates (bidirectional), nicked dimer (two unit length linear monomers fused together into a circle), and catenated forms) (Figure 36B). Several of these minor intermediates of viral DNA replication were either indistinguishable from each other or migrated very closely to another by 1d electrophoresis (Figure 36B, top panel). Importantly, the prominent θ replication intermediate arcs were both visualized (Figure 36B, bottom panel).

DNA extracted from ATR inhibited SV40-infected cells showed a smooth linear arc that extended beyond 15 kb form III (Figure 36C). These large linear molecules were absent from DMSO treated SV40 infected cells and are indicative of the products of rolling circle replication (Figure 36A). Additionally, southern blots from ATRi treated

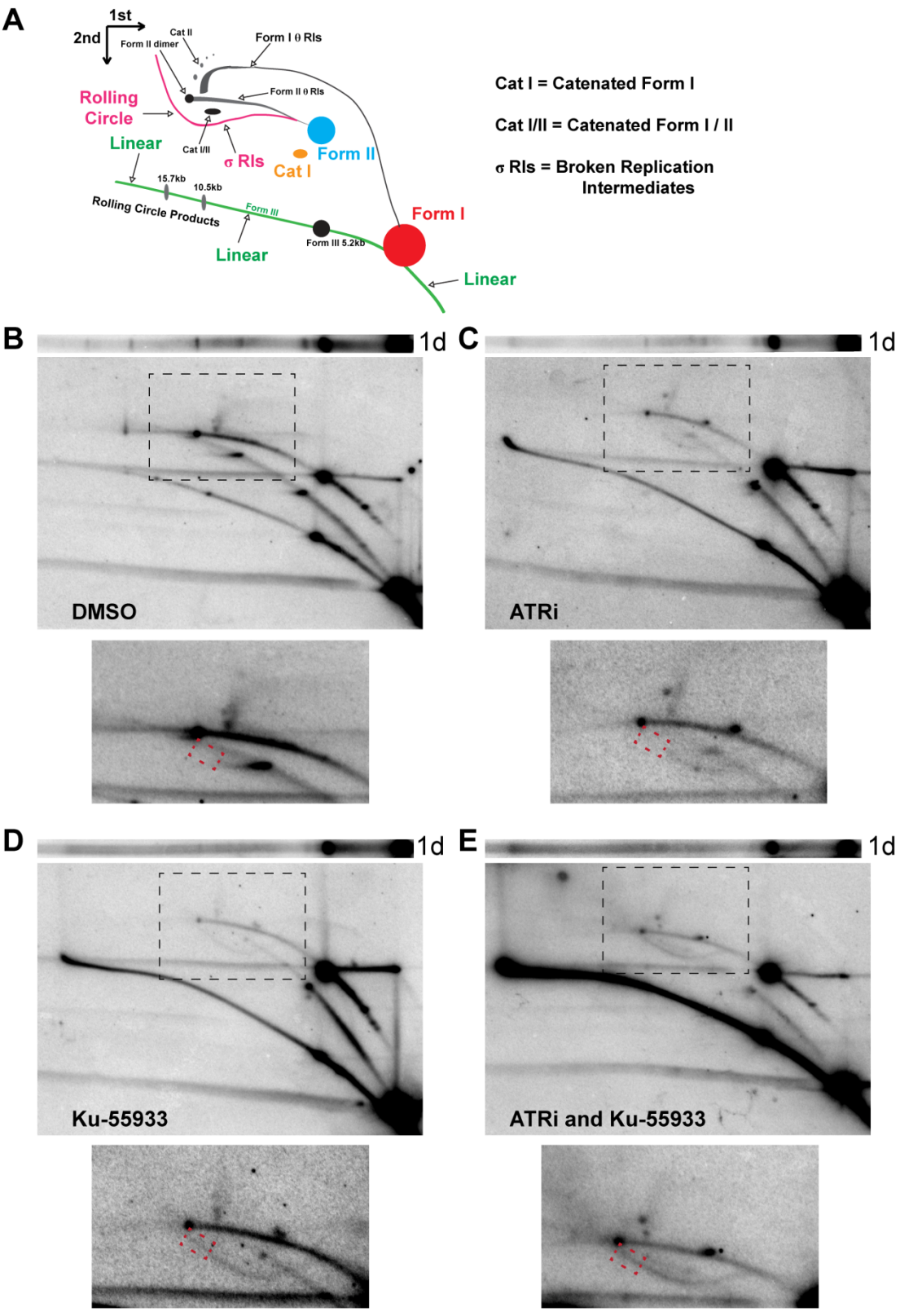
A
1st
2nd
Cat II
Form II dimer
Form I θ RIs
Form II θ RIs
Rolling Circle
Linear
Cat I/II
σ RIs
Cat I
Form II
15.7kb
10.5kb
Rolling Circle Products
Form III
Linear
Form III 5.2kb
Form I
Linear
Cat I = Catenated Form I
Cat I/II = Catenated Form I / II
σ RIs = Broken Replication Intermediates
B
1d
DMSO
C
1d
ATRi
D
1d
Ku-55933
E
1d
ATRi and Ku-55933

Figure 36.

Figure 36. ATM or ATR inhibition increases unidirectional replication forks and large linear viral replication products.

(A) Diagram of undigested 2d gel electrophoresis of circular dsDNA (Lucas et al., 2001). (B, C, D, E) Southern blots of the first dimension of a neutral 2d gel (top panel) or 2d gel (middle panel) from SV40-infected BSC40 cells exposed to DMSO (B), ATRi (C), Ku-55933(D), or ATRi and Ku-55933 (E) during the last 28 h of a 48 h SV40 infection. Bottom panel: Enlargement of the picture within the boxed area in middle panel. Exposure of the bottom panel was increased to enhance visualization of θ and σ replication intermediates shown in (A).

cells demonstrated an arcs corresponding to both bidirectional (θ) and unidirectional (σ) replication (Figure 36C, enlarged box). Head to tail dimers, cat I/II, and cat II/II were all substantially decreased when ATR was inhibited compared to DMSO (Figure 36, compare bottom panel in C to B). Similarly, inhibition of ATM resulted in a strong arc of large linear products (> 15 kb) resulting from rolling circle DNA replication (Figure 36D, middle panel). Close examination of the replication intermediates from SV40 infected cells treated with Ku-55933 revealed that both a θ and σ replication intermediates were present in the replicating DNA consistent with ongoing bidirectional and unidirectional DNA replication (Figure 36D, bottom panel). Again, DNA from ATM inhibited cells had substantially decreased amounts of dimer and nicked catenated forms (Figure 36, compare D to B).

DNA from cells treated with both Ku-55933 and ATRi had a robust arc of linear intermediates greater than 5.23 kb (Figure 36E, middle panel). Similar to DNA from ATM inhibited cells, this DNA had a prominent σ arc that continued to a rolling circle (Figure 36E, bottom panel, red box). However, both forms II and I θ replication intermediate arcs were much weaker in DNA from ATR and ATM inhibited cells than from cells in which DNA was replicated presence of DMSO (Figure 36 bottom panel, compare red box in E to B). The number of rolling circles also corresponded with a decrease in catenated products and dimer (Figure 36E, middle panel).

Consistent with previous results, comparison of the σ arcs generated from replication associated DSBs (Pohlhaus et al., 2006) from ATR and ATM inhibited cells demonstrated that the σ arc from sole ATR inhibition did not continue beyond 2n (Figure 36C, D red box). The absence of larger rolling circles is consistent with the tendency of viral DNA to stall and break upon ATR inhibition (Sowd et al., 2013). Collectively, we conclude that ATM and ATR kinase function is crucial for the prevention of accumulation of broken linear DNA during viral DNA replication.

Materials and Methods

Cell culture, SV40 infection, DNA isolation, and inhibitor treatments were all as described in chapter VI. 2d gel electrophoresis was as described in the chapter VI with the following modification. The second dimension of the 2d gel run for 7 h through a 0.95% 1xTBE agarose gel.

APPENDIX B

ELICITATION OF SV40 PSEUDO-S PHASE IS NOT MEDIATED BY P21 DEGRADATION

Introduction and Research Summary

To replicate the viral genome, small DNA tumor viruses, including the polyomaviridae and papillomaviridae families, require machinery present in cellular S phase. The S phase arrest elicited by these viruses has been particularly well studied for members of polyomaviridae which contains human pathogens BKV, JCV, MCV, and the primate virus SV40. In particular, primate polyomaviridae family members activate the cellular S phase arrest using DNA damage signaling through the two related DNA damage signaling kinases ATM and ATR (Orba et al., 2010; Okubo et al., 2003; Jiang et al., 2012; Sowd et al., 2013). ATR was previously observed to play an essential role in the S phase arrest of SV40-infected cells through its ability to phosphorylate and stabilize a p53 splice variant (Rohaly et al., 2010). This splice variant was found to activate transcription of the CDK inhibitor p21 thereby arresting cells in S phase (Rohaly et al., 2010).

In spite of this result, S phase arrest in response to high levels of ATR-Chk1 kinase activities that follow DNA damage has been well established to rely upon the degradation or nuclear exclusion of Cdc25 family phosphatases (Boutros et al., 2007). In primates, Cdc25 family phosphatases contain three major members that dephosphorylate inhibitory phosphorylation sites on CDKs (Boutros et al., 2007). Thus, these phosphatases promote cell cycle progression. In response to DNA damage, Cdc25A and Cdc25B are degraded, whereas Cdc25C is excluded from the nucleus.

The results which follow are an initial attempt to verify the findings of Roholy et al., and determine the mechanism(s) which promote S phase arrest in SV40-infected cells.

To elucidate the effects of ATM and ATR signaling on p21 accumulation during SV40 infection, SV40-infected BSC40 cells were exposed to specific inhibitors of ATM (Ku-55933 (Hickson et al., 2004)) or ATR (VE-821 (ATRi) (Reaper et al., 2011)) during phases of a 48 h SV40 infection (Figure 37A). These cellular populations were subjected to western blotting for proteins that fluctuate in cycling cells (Cyclin A, Cyclin B, Cdt1, and Geminin) or accumulate in cells arrested in S-G2 (Geminin and p21). Relative to mock-infected cells, SV40-infected cells in the presence of inhibitor solvent DMSO had high levels of Cyclin A, Cyclin B, and Geminin (Figure 37B, compare lane 1 to lane 5). The high cyclin A levels in SV40-infected cells compared to Mock-infected cells is consistent with S phase arrest, whereas the high geminin levels are indicative of cellular origin firing inhibition and cell cycle checkpoint (Masai et al., 2010). The amount of p21 in these SV40-infected cells was substantially less than uninfected cells (Figure 37B, compare lane 1 to lane 5). Importantly, inhibition of ATM had no affect on p21 levels in SV40-infected cells (Figure 37B, compare lane 1 to lanes 2-4). Consistent with the failure to arrest in S phase observed Figure 28C, cyclin A levels were decreased by the presence of Ku-55933 during the early phase and throughout infection (Figure 37B, compare lane 1 to lanes 2, 4). Notably, geminin levels were decreased by ATM inhibition at any point during SV40 infection (Figure 37B).

As ATR was found to have a large affect on the ability of SV40 infected cells to arrest (Figure 28D), p21 accumulation was examined in the populations of ATRi inhibited cells described in figure 37A by western blotting (Figure 37C). Similar to ATM inhibition, inhibition of ATR had no effect on p21, with p21 still not accumulating during SV40 infection (Figure 37C, compare lane 1 to lanes 2 - 4). Again, populations of SV40-infected cells that cycled upon ATR inhibition had lower levels of cyclin A (Figure 37C,

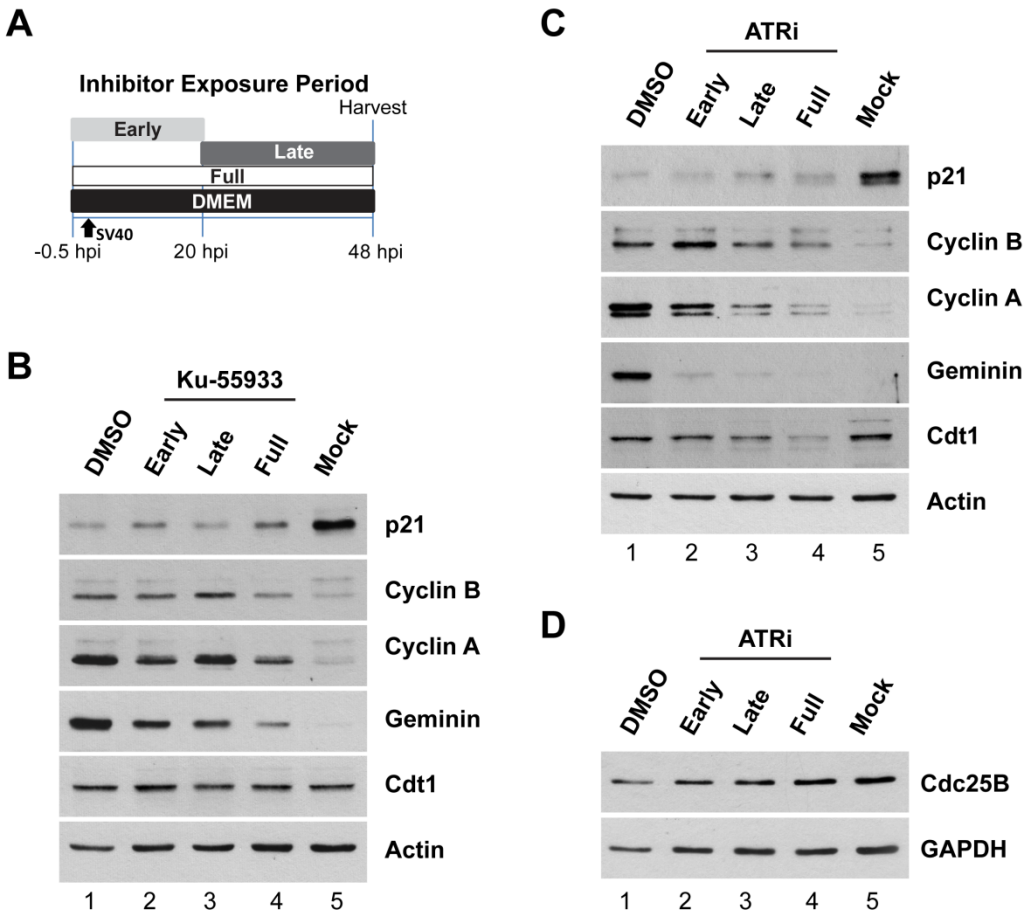

Figure 37. p21 is not induced by SV40 infection.
(A) Experimental scheme for exposure of cells to ATR or ATM inhibitor during phases of a 48 h SV40 infection. Early: inhibitor present from -0.5 to 20 hpi. Late: inhibitor present from 20 to 48hpi. DMSO and Full: solvent or inhibitor, respectively, present from -0.5 to 48 hpi. (B, C, D) Western blots of cell extracts from SV40- or mock-infected BSC40 cells exposed to Ku-55933 (B) or ATRi (C, D) and blotted for the indicated proteins.

compare lane 1 to lanes 2 - 4). Geminin levels in SV40-infected cells exposed to ATRi were greatly decreased to levels similar to mock-infected cells implying that ATR depended phosphorylations might affect the accumulation of Geminin in SV40 infected cells (Figure 37C, compare lane 1 to lanes 2 - 4). Examination of DMSO treated SV40-cells for Cdc25B revealed that Cdc25B was not affected by SV40 infection (Figure 37D, compare lane 1 to lane 5). Consistent with the well established abrogation of p53 function in SV40 infected cells, our data indicates that p21 is not the mechanism that modulates S phase arrest in SV40-infected cells. Additionally, my data suggests that Cdc25B degradation is unlikely the mechanism promoting S phase arrest in SV40 infected cells.

Materials and Methods

Cell culture, SV40 infection, western blots, and inhibitor treatments were all as described in chapter VI.

APPENDIX C

SV40 LARGE T ANTIGEN IS PHOSPHORYLATED BY ATM AND ATR

Introduction and Research Summary

DNA damage signaling through ATM and ATR dependent pathways has been demonstrated to phosphorylate numerous substrates (Matsuoka et al., 2007) collectively resulting in S phase arrest and facilitation of DNA repair (Ciccia et al., 2010). The infection of cells with the polyomavirus SV40 was demonstrated to activate ATM and ATR, but not DNA-PK_{cs} (Rohaly et al., 2010; Sowd et al., 2013; Shi et al., 2005). Notably, SV40 Tag was identified to be directly phosphorylated by ATM (Shi et al., 2005) and DNA-PK_{cs} *in vitro* (Chen, Lees-Miller et al., 1991; Wang et al., 1999). S120 of Tag is a consensus ATM, ATR, and DNA-PK_{cs} known to modulate SV40 DNA replication (Fanning, 1994; Sowd et al., 2012). The phosphorylation of this residue of Tag was previously demonstrated to fluctuate upon ATM knockdown in SV40 infected cells (Shi et al., 2005). As a result of this, ATM function during SV40 infection was proposed be necessary to phosphorylate S120 of Tag, enhancing viral DNA replication (Shi et al., 2005). However, this phosphorylation event on Tag is known inhibit viral replication *in vitro* (Fanning, 1994) and several kinases are likely able to phosphorylate this site.

To investigate ATM and ATR phosphorylation of Tag, ATM or ATR were inhibited with Ku-55933 (Hickson et al., 2004) or VE-821 (ATRi) (Reaper et al., 2011) during phases of a 48 h SV40 infection (Figure 38A). Infection in the presence of DMSO increased the level of S120 phosphorylation (Figure 38B). Inhibition of ATM during early or throughout infection, decreased S120 phosphorylation greatly (Figure 38B, compare lane 1 to lanes 2, 4), whereas inhibition late more mildly decreased

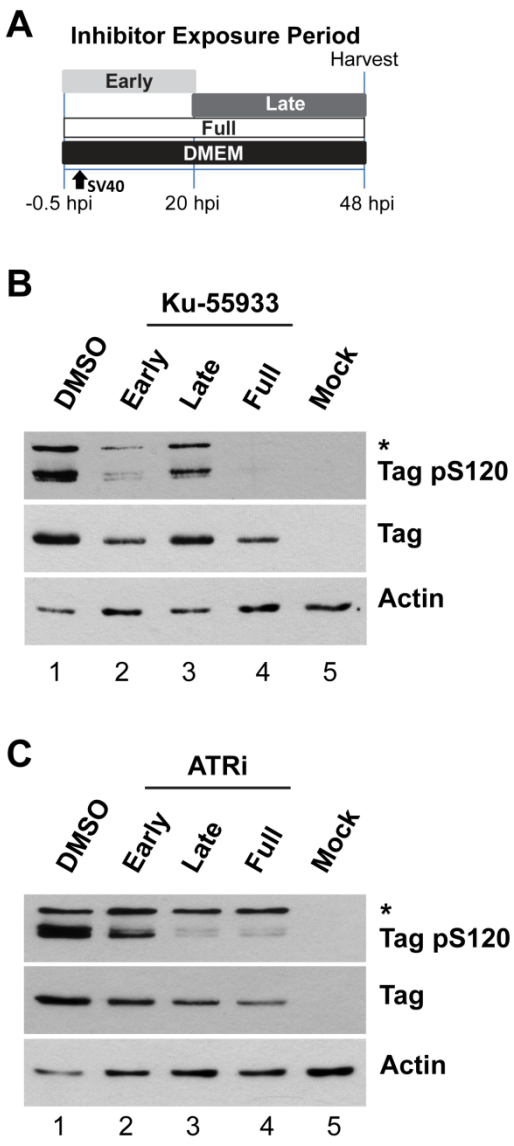

Figure 38. ATM and ATR phosphorylate residue S120 of SV40 Tag
(A) Scheme for treatment of cells with inhibitor during phases of a 48 h SV40 infection. Early: inhibitor present from -0.5 to 20 hpi. Late: inhibitor present from 20 to 48hpi. DMSO and Full: solvent or inhibitor, respectively, present from -0.5 to 48 hpi. (B, C) Western blots of cell extracts from SV40- or mock-infected BSC40 cells exposed to Ku-55933 (B) or ATRi (C) and probed for the indicated proteins. In (B) and (C), * denotes nonspecific band.

phosphorylation S120 on Tag (Figure 38B, compare lane 1 to lane 3). On the other hand, compared to SV40-infected cells exposed to DMSO throughout infection, ATR inhibition at any point during SV40 infection greatly decreased Tag phosphorylation on S120 (Figure 38C, compare lane 1 to lane). These results imply that ATR is the main kinase that phosphorylates serine residue 120 of Tag.

However, caution should be taken when concluding this from Figure 38C. Every ATRi treatment used in Figure 38C greatly decreases SV40 DNA replication (Figures 21, 22) and decreases virally induced S phase arrest (Figure 28D) which would decrease ATM activation. This decrease in ATM activation was observed upon ATRi treatment (Figure 20C), further substantiating this notion. Compared to ATR inhibition, the presence of Ku-55933 early and throughout infection decreases SV40 DNA replication (Figure 14E, F) and decreases S phase arrest (Figure 28C). Thus, these treatments cannot be interpreted for their effects on Tag phosphorylation as ATR signaling is affected by the decrease in viral DNA replication (Figure 13B).

However unlike other Ku-55933 treatments and all ATRi treatments, the inhibition of ATM late during SV40 infection does not affect viral DNA replication, S phase arrest, or ATR activity (Figures 13, 14). Since inhibition of ATM during the late phase of infection partially decreases the phosphorylation of Tag on S120 (Figure 38B), our results indicate that other kinases, likely ATR or DNA-PK_{cs}, phosphorylate Tag on S120. Based on this, we conclude that ATR and ATM phosphorylate Tag on S120 during unperturbed SV40 infection.

Materials and Methods

Cell culture, SV40 infection, western blots, and inhibitor treatments were all as described in chapter VI.

REFERENCES

Ababou, M., Dutertre, S., Lecluse, Y., Onclercq, R., Chatton, B. and Amor-Gueret, M. (2000). "ATM-dependent phosphorylation and accumulation of endogenous BLM protein in response to ionizing radiation." Oncogene. 19(52): 5955-63.

Adamczewski, J. P., Gannon, J. V. and Hunt, T. (1993). "Simian virus 40 large T antigen associates with cyclin A and p33cdk2." J Virol. 67(11): 6551-7.

Adamo, A., Collis, S. J., Adelman, C. A., Silva, N., Horejsi, Z., Ward, J. D., Martinez-Perez, E., Boulton, S. J. and La Volpe, A. (2010). "Preventing nonhomologous end joining suppresses DNA repair defects of Fanconi anemia." Mol Cell. 39(1): 25-35.

Alderton, G. K., Joenje, H., Varon, R., Borglum, A. D., Jeggo, P. A. and O'Driscoll, M. (2004). "Seckel syndrome exhibits cellular features demonstrating defects in the ATR-signalling pathway." Hum Mol Genet. 13(24): 3127-38.

An, P., Saenz Robles, M. T. and Pipas, J. M. (2012). "Large T antigens of polyomaviruses: amazing molecular machines." Annu Rev Microbiol. 66: 213-36.

Andreassen, P. R., D'Andrea, A. D. and Taniguchi, T. (2004). "ATR couples FANCD2 monoubiquitination to the DNA-damage response." Genes Dev. 18(16): 1958-63.

Antoni, L., Sodha, N., Collins, I. and Garrett, M. D. (2007). "CHK2 kinase: cancer susceptibility and cancer therapy - two sides of the same coin?" Nat Rev Cancer. 7(12): 925-36.

Bachrati, C. Z., Borts, R. H. and Hickson, I. D. (2006). "Mobile D-loops are a preferred substrate for the Bloom's syndrome helicase." Nucleic Acids Res. 34(8): 2269-79.

Backert, S. (2002). "R-loop-dependent rolling-circle replication and a new model for DNA concatemer resolution by mitochondrial plasmid mp1." EMBO J. 21(12): 3128-36.

Bakkenist, C. J. and Kastan, M. B. (2003). "DNA damage activates ATM through intermolecular autophosphorylation and dimer dissociation." Nature. 421(6922): 499-506.

Balakrishnan, L. and Bambara, R. A. (2011). "Eukaryotic lagging strand DNA replication employs a multi-pathway mechanism that protects genome integrity." J Biol Chem. 286(9): 6865-70.

Ball, H. L., Myers, J. S. and Cortez, D. (2005). "ATRIP binding to replication protein A-single-stranded DNA promotes ATR-ATRIP localization but is dispensable for Chk1 phosphorylation." Mol Biol Cell. 16(5): 2372-81.

Bauerschmidt, C., Pollok, S., Kremmer, E., Nasheuer, H. P. and Grosse, F. (2007). "Interactions of human Cdc45 with the Mcm2-7 complex, the GINS complex, and DNA polymerases delta and epsilon during S phase." Genes Cells. 12(6): 745-58.

Bell, S. P. and Dutta, A. (2002). "DNA replication in eukaryotic cells." Annu Rev Biochem. 71: 333-74.

Berkovich, E., Monnat, R. J., Jr. and Kastan, M. B. (2007). "Roles of ATM and NBS1 in chromatin structure modulation and DNA double-strand break repair." Nat Cell Biol. 9(6): 683-90.

Blasius, M., Forment, J. V., Thakkar, N., Wagner, S. A., Choudhary, C. and Jackson, S. P. (2011). "A phospho-proteomic screen identifies substrates of the checkpoint kinase Chk1." Genome Biol. 12(8): R78.

Boichuk, S., Hu, L., Hein, J. and Gjoerup, O. V. (2010). "Multiple DNA damage signaling and repair pathways deregulated by simian virus 40 large T antigen." J Virol. 84(16): 8007-20.

Borowiec, J. A., Dean, F. B., Bullock, P. A. and Hurwitz, J. (1990). "Binding and unwinding--how T antigen engages the SV40 origin of DNA replication." Cell. 60(2): 181-4.

Boutros, R., Lobjois, V. and Ducommun, B. (2007). "CDC25 phosphatases in cancer cells: key players? Good targets?" Nat Rev Cancer. 7(7): 495-507.

Brown, E. J. and Baltimore, D. (2000). "ATR disruption leads to chromosomal fragmentation and early embryonic lethality." Genes Dev. 14(4): 397-402.

Bugreev, D. V., Hanaoka, F. and Mazin, A. V. (2007). "Rad54 dissociates homologous recombination intermediates by branch migration." Nat Struct Mol Biol. 14(8): 746-53.

Bullock, P. A. (1997). "The initiation of simian virus 40 DNA replication in vitro." Crit Rev Biochem Mol Biol. 32(6): 503-68.

Bunz, F. (2011). DNA Damage Signaling Downstream of ATM. Molecular Determinants of Radiation Response. T. L. DeWeese and M. Laiho. New York, Springer 35-52.

Busby, E. C., Leistritz, D. F., Abraham, R. T., Karnitz, L. M. and Sarkaria, J. N. (2000). "The radiosensitizing agent 7-hydroxystaurosporine (UCN-01) inhibits the DNA damage checkpoint kinase hChk1." Cancer Res. 60(8): 2108-12.

Cam, H. and Dynlacht, B. D. (2003). "Emerging roles for E2F: beyond the G1/S transition and DNA replication." Cancer Cell. 3(4): 311-6.

Campbell, K. S., Mullane, K. P., Aksoy, I. A., Stubdal, H., Zalvide, J., Pipas, J. M., Silver, P. A., Roberts, T. M., Schaffhausen, B. S. and DeCaprio, J. A. (1997). "DnaJ/hsp40 chaperone domain of SV40 large T antigen promotes efficient viral DNA replication." Genes Dev. 11(9): 1098-110.

Casper, A. M., Durkin, S. G., Arlt, M. F. and Glover, T. W. (2004). "Chromosomal instability at common fragile sites in Seckel syndrome." Am J Hum Genet. 75(4): 654-60.

Casper, A. M., Nghiem, P., Arlt, M. F. and Glover, T. W. (2002). "ATR regulates fragile site stability." Cell. 111(6): 779-89.

Cegielska, A., Moarefi, I., Fanning, E. and Virshup, D. M. (1994). "T-antigen kinase inhibits simian virus 40 DNA replication by phosphorylation of intact T antigen on serines 120 and 123." J Virol. 68(1): 269-75.

Chan, K. L., North, P. S. and Hickson, I. D. (2007). "BLM is required for faithful chromosome segregation and its localization defines a class of ultrafine anaphase bridges." EMBO J. 26(14): 3397-409.

Chan, K. L., Palmai-Pallag, T., Ying, S. and Hickson, I. D. (2009). "Replication stress induces sister-chromatid bridging at fragile site loci in mitosis." Nat Cell Biol. 11(6): 753-60.

Chang, Y. and Moore, P. S. (2012). "Merkel cell carcinoma: a virus-induced human cancer." Annu Rev Pathol. 7: 123-44.

Chang, Y. P., Xu, M., Machado, A. C., Yu, X. J., Rohs, R. and Chen, X. S. (2013). "Mechanism of origin DNA recognition and assembly of an initiator-helicase complex by SV40 large tumor antigen." Cell Rep. 3(4): 1117-27.

Chapman, J. R., Taylor, M. R. and Boulton, S. J. (2012). "Playing the end game: DNA double-strand break repair pathway choice." Mol Cell. 47(4): 497-510.

Chen, B. P., Chan, D. W., Kobayashi, J., Burma, S., Asaithamby, A., Morotomi-Yano, K., Botvinick, E., Qin, J. and Chen, D. J. (2005). "Cell cycle dependence of DNA-dependent protein kinase phosphorylation in response to DNA double strand breaks." J Biol Chem. 280(15): 14709-15.

Chen, B. P., Uematsu, N., Kobayashi, J., Lerenthal, Y., Krempler, A., Yajima, H., Lobrich, M., Shiloh, Y. and Chen, D. J. (2007). "Ataxia telangiectasia mutated (ATM) is essential for DNA-PKcs phosphorylations at the Thr-2609 cluster upon DNA double strand break." J Biol Chem. 282(9): 6582-7.

Chen, Y. R., Lees-Miller, S. P., Tegtmeyer, P. and Anderson, C. W. (1991). "The human DNA-activated protein kinase phosphorylates simian virus 40 T antigen at amino- and carboxy-terminal sites." J Virol. 65(10): 5131-40.

Chia, W. and Rigby, P. W. (1981). "Fate of viral DNA in nonpermissive cells infected with simian virus 40." Proc Natl Acad Sci U S A. 78(11): 6638-42.

Choi, S., Gamper, A. M., White, J. S. and Bakkenist, C. J. (2010). "Inhibition of ATM kinase activity does not phenocopy ATM protein disruption: implications for the clinical utility of ATM kinase inhibitors." Cell Cycle. 9(20): 4052-7.

Chu, W. K. and Hickson, I. D. (2009). "RecQ helicases: multifunctional genome caretakers." Nat Rev Cancer. 9(9): 644-54.

Ciccia, A. and Elledge, S. J. (2010). "The DNA damage response: making it safe to play with knives." Mol Cell. 40(2): 179-204.

Cimprich, K. A. and Cortez, D. (2008). "ATR: an essential regulator of genome integrity." Nat Rev Mol Cell Biol. 9(8): 616-27.

Cohen, G. L., Wright, P. J., DeLucia, A. L., Lewton, B. A., Anderson, M. E. and Tegtmeyer, P. (1984). "Critical spatial requirement within the origin of simian virus 40 DNA replication." J Virol. 51(1): 91-6.

Cohen, M. M. and Simpson, S. J. (1980). "Growth kinetics of ataxia telangiectasia lymphoblastoid cells. Evidence for a prolonged S period." Cytogenet Cell Genet. 28(1-2): 24-33.

Cotsiki, M., Lock, R. L., Cheng, Y., Williams, G. L., Zhao, J., Perera, D., Freire, R., Entwistle, A., Golemis, E. A., Roberts, T. M., Jat, P. S. and Gjoerup, O. V. (2004). "Simian virus 40 large T antigen targets the spindle assembly checkpoint protein Bub1." Proc Natl Acad Sci U S A. 101(4): 947-52.

Couch, F. B., Bansbach, C. E., Driscoll, R., Luzwick, J. W., Glick, G. G., Betous, R., Carroll, C. M., Jung, S. Y., Qin, J., Cimprich, K. A. and Cortez, D. (2013). "ATR phosphorylates SMARCAL1 to prevent replication fork collapse." Genes Dev. 27(14): 1610-23.

Crouse, G. F. (2010). "An end for mismatch repair." Proc Natl Acad Sci U S A. 107(49): 20851-2.

Dahl, J., You, J. and Benjamin, T. L. (2005). "Induction and utilization of an ATM signaling pathway by polyomavirus." J Virol. 79(20): 13007-17.

Davies, S. L., North, P. S. and Hickson, I. D. (2007). "Role for BLM in replication-fork restart and suppression of origin firing after replicative stress." Nat Struct Mol Biol. 14(7): 677-9.

Debatisse, M., Le Tallec, B., Letessier, A., Dutrillaux, B. and Brison, O. (2012). "Common fragile sites: mechanisms of instability revisited." Trends Genet. 28(1): 22-32.

DeCaprio, J. A. (2009). "Does detection of Merkel cell polyomavirus in Merkel cell carcinoma provide prognostic information?" J Natl Cancer Inst. 101(13): 905-7.

DeCaprio, J. A. (2009). "How the Rb tumor suppressor structure and function was revealed by the study of Adenovirus and SV40." Virology. 384(2): 274-84.

DeCaprio, J. A. and Garcea, R. L. (2013). "A cornucopia of human polyomaviruses." Nat Rev Microbiol. 11(4): 264-76.

Deckbar, D., Jeggo, P. A. and Lobrich, M. (2011). "Understanding the limitations of radiation-induced cell cycle checkpoints." Crit Rev Biochem Mol Biol. 46(4): 271-83.

Dehe, P. M., Coulon, S., Scaglione, S., Shanahan, P., Takedachi, A., Wohlschlegel, J. A., Yates, J. R., 3rd, Llorente, B., Russell, P. and Gaillard, P. H. (2013). "Regulation of Mus81-Eme1 Holliday junction resolvase in response to DNA damage." Nat Struct Mol Biol. 20(5): 598-603.

Derheimer, F. A. and Kastan, M. B. (2010). "Multiple roles of ATM in monitoring and maintaining DNA integrity." FEBS Lett. 584(17): 3675-81.

DiMaio, D. and Liao, J. B. (2006). "Human papillomaviruses and cervical cancer." Adv Virus Res. 66: 125-59.

DiMaio, D. and Miller, G. (2006). "Thirty years into the genomics era: tumor viruses led the way." Yale J Biol Med. 79(3-4): 179-85.

Dornreiter, I., Erdile, L. F., Gilbert, I. U., von Winkler, D., Kelly, T. J. and Fanning, E. (1992). "Interaction of DNA polymerase alpha-primase with cellular replication protein A and SV40 T antigen." EMBO J. 11(2): 769-76.

Durkin, S. G., Arlt, M. F., Howlett, N. G. and Glover, T. W. (2006). "Depletion of CHK1, but not CHK2, induces chromosomal instability and breaks at common fragile sites." Oncogene. 25(32): 4381-8.

Duursma, A. M., Driscoll, R., Elias, J. E. and Cimprich, K. A. (2013). "A role for the MRN complex in ATR activation via TOPBP1 recruitment." Mol Cell. 50(1): 116-22.

Falck, J., Coates, J. and Jackson, S. P. (2005). "Conserved modes of recruitment of ATM, ATR and DNA-PKcs to sites of DNA damage." Nature. 434(7033): 605-11.

Fanning, E. (1994). "Control of SV40 DNA replication by protein phosphorylation: a model for cellular DNA replication?" Trends Cell Biol. 4(7): 250-5.

Fanning, E. and Knippers, R. (1992). "Structure and function of simian virus 40 large tumor antigen." Annu Rev Biochem. 61: 55-85.

Fanning, E. and Zhao, K. (2009). "SV40 DNA replication: from the A gene to a nanomachine." Virology. 384(2): 352-9.

Foster, S. S., Balestrini, A. and Petrini, J. H. (2011). "Functional interplay of the Mre11 nuclease and Ku in the response to replication-associated DNA damage." Mol Cell Biol. 31(21): 4379-89.

Fotedar, R. and Roberts, J. M. (1991). "Association of p34cdc2 with replicating DNA." Cold Spring Harb Symp Quant Biol. 56: 325-33.

Fradet-Turcotte, A., Bergeron-Labrecque, F., Moody, C. A., Lehoux, M., Laimins, L. A. and Archambault, J. (2011). "Nuclear accumulation of the papillomavirus E1 helicase blocks S-phase progression and triggers an ATM-dependent DNA damage response." J Virol. 85(17): 8996-9012.

Franchitto, A. and Pichierri, P. (2011). "Understanding the molecular basis of common fragile sites instability: role of the proteins involved in the recovery of stalled replication forks." Cell Cycle. 10(23): 4039-46.

Friedman, K. L. and Brewer, B. J. (1995). "Analysis of replication intermediates by two-dimensional agarose gel electrophoresis." Methods Enzymol. 262: 613-27.

Gamper, A. M., Choi, S., Matsumoto, Y., Banerjee, D., Tomkinson, A. E. and Bakkenist, C. J. (2012). "ATM protein physically and functionally interacts with proliferating cell nuclear antigen to regulate DNA synthesis." J Biol Chem. 287(15): 12445-54.

Garcia, V., Phelps, S. E., Gray, S. and Neale, M. J. (2011). "Bidirectional resection of DNA double-strand breaks by Mre11 and Exo1." Nature. 479(7372): 241-4.

Gillespie, K. A., Mehta, K. P., Laimins, L. A. and Moody, C. A. (2012). "Human papillomaviruses recruit cellular DNA repair and homologous recombination factors to viral replication centers." J Virol. 86(17): 9520-6.

Gjoerup, O. and Chang, Y. (2010). "Update on human polyomaviruses and cancer." Adv Cancer Res. 106: 1-51.

Goodarzi, A. A. and Jeggo, P. A. (2013). "The repair and signaling responses to DNA double-strand breaks." Adv Genet. 82: 1-45.

Guo, Z., Kozlov, S., Lavin, M. F., Person, M. D. and Paull, T. T. (2010). "ATM activation by oxidative stress." Science. 330(6003): 517-21.

Haince, J. F., McDonald, D., Rodrigue, A., Dery, U., Masson, J. Y., Hendzel, M. J. and Poirier, G. G. (2008). "PARP1-dependent kinetics of recruitment of MRE11 and NBS1 proteins to multiple DNA damage sites." J Biol Chem. 283(2): 1197-208.

Hanada, K., Budzowska, M., Davies, S. L., van Drunen, E., Onizawa, H., Beverloo, H. B., Maas, A., Essers, J., Hickson, I. D. and Kanaar, R. (2007). "The structure-specific endonuclease Mus81 contributes to replication restart by generating double-strand DNA breaks." Nat Struct Mol Biol. 14(11): 1096-104.

Hardcastle, I. R., Cockcroft, X., Curtin, N. J., El-Murr, M. D., Leahy, J. J., Stockley, M., Golding, B. T., Rigoreau, L., Richardson, C., Smith, G. C. and Griffin, R. J. (2005). "Discovery of potent chromen-4-one inhibitors of the DNA-dependent protein kinase (DNA-PK) using a small-molecule library approach." J Med Chem. 48(24): 7829-46.

Hashimoto, Y., Puddu, F. and Costanzo, V. (2012). "RAD51- and MRE11-dependent reassembly of uncoupled CMG helicase complex at collapsed replication forks." Nat Struct Mol Biol. 19(1): 17-24.

Hein, J., Boichuk, S., Wu, J., Cheng, Y., Freire, R., Jat, P. S., Roberts, T. M. and Gjoerup, O. V. (2009). "Simian virus 40 large T antigen disrupts genome integrity and activates a DNA damage response via Bub1 binding." J Virol. 83(1): 117-27.

Hickson, I., Zhao, Y., Richardson, C. J., Green, S. J., Martin, N. M., Orr, A. I., Reaper, P. M., Jackson, S. P., Curtin, N. J. and Smith, G. C. (2004). "Identification and characterization of a novel and specific inhibitor of the ataxia-telangiectasia mutated kinase ATM." Cancer Res. 64(24): 9152-9.

Hirt, B. (1967). "Selective extraction of polyoma DNA from infected mouse cell cultures." J Mol Biol. 26(2): 365-9.

Hoeijmakers, J. H. (2009). "DNA damage, aging, and cancer." N Engl J Med. 361(15): 1475-85.

Holloman, W. K. (2011). "Unraveling the mechanism of BRCA2 in homologous recombination." Nat Struct Mol Biol. 18(7): 748-54.

Huang, H., Weiner, B. E., Zhang, H., Fuller, B. E., Gao, Y., Wile, B. M., Zhao, K., Arnett, D. R., Chazin, W. J. and Fanning, E. (2010). "Structure of a DNA polymerase alpha-primase domain that docks on the SV40 helicase and activates the viral primosome." J Biol Chem. 285(22): 17112-22.

Huang, H., Zhao, K., Arnett, D. R. and Fanning, E. (2010). "A specific docking site for DNA polymerase {alpha}-primase on the SV40 helicase is required for viral primosome activity, but helicase activity is dispensable." J Biol Chem. 285(43): 33475-84.

Huertas, P. and Jackson, S. P. (2009). "Human CtIP mediates cell cycle control of DNA end resection and double strand break repair." J Biol Chem. 284(14): 9558-65.

Ilves, I., Tamberg, N. and Botchan, M. R. (2012). "Checkpoint kinase 2 (Chk2) inhibits the activity of the Cdc45/MCM2-7/GINS (CMG) replicative helicase complex." Proc Natl Acad Sci U S A. 109(33): 13163-70.

Iyama, T. and Wilson, D. M., 3rd (2013). "DNA repair mechanisms in dividing and non-dividing cells." DNA Repair (Amst).

Jazayeri, A., Balestrini, A., Garner, E., Haber, J. E. and Costanzo, V. (2008). "Mre11-Rad50-Nbs1-dependent processing of DNA breaks generates oligonucleotides that stimulate ATM activity." EMBO J. 27(14): 1953-62.

Jeggo, P. A., Geuting, V. and Lobrich, M. (2011). "The role of homologous recombination in radiation-induced double-strand break repair." Radiother Oncol. 101(1): 7-12.

Jiang, M., Zhao, L., Gamez, M. and Imperiale, M. J. (2012). "Roles of ATM and ATR-Mediated DNA Damage Responses during Lytic BK Polyomavirus Infection." PLoS Pathog. 8(8): e1002898.

Jiang, X., Klimovich, V., Arunkumar, A. I., Hysinger, E. B., Wang, Y., Ott, R. D., Guler, G. D., Weiner, B., Chazin, W. J. and Fanning, E. (2006). "Structural mechanism of RPA loading on DNA during activation of a simple pre-replication complex." EMBO J. 25(23): 5516-26.

Kadaja, M., Isok-Paas, H., Laos, T., Ustav, E. and Ustav, M. (2009). "Mechanism of genomic instability in cells infected with the high-risk human papillomaviruses." PLoS Pathog. 5(4): e1000397.

Kang, Y. H., Galal, W. C., Farina, A., Tappin, I. and Hurwitz, J. (2012). "Properties of the human Cdc45/Mcm2-7/GINS helicase complex and its action with DNA polymerase epsilon in rolling circle DNA synthesis." Proc Natl Acad Sci U S A. 109(16): 6042-7.

Kanu, N. and Behrens, A. (2007). "ATMIN defines an NBS1-independent pathway of ATM signalling." EMBO J. 26(12): 2933-41.

Kolas, N. K., Chapman, J. R., Nakada, S., Ylanko, J., Chahwan, R., Sweeney, F. D., Panier, S., Mendez, M., Wildenhain, J., Thomson, T. M., Pelletier, L., Jackson, S. P. and Durocher, D. (2007). "Orchestration of the DNA-damage response by the RNF8 ubiquitin ligase." Science. 318(5856): 1637-40.

Kumagai, A., Lee, J., Yoo, H. Y. and Dunphy, W. G. (2006). "TopBP1 activates the ATR-ATRIP complex." Cell. 124(5): 943-55.

Kunkel, T. A. (2004). "DNA replication fidelity." J Biol Chem. 279(17): 16895-8.

Kunkel, T. A. and Burgers, P. M. (2008). "Dividing the workload at a eukaryotic replication fork." Trends Cell Biol. 18(11): 521-7.

Lara-Gonzalez, P., Westhorpe, F. G. and Taylor, S. S. (2012). "The spindle assembly checkpoint." Curr Biol. 22(22): R966-80.

Lau, A., Swinbank, K. M., Ahmed, P. S., Taylor, D. L., Jackson, S. P., Smith, G. C. and O'Connor, M. J. (2005). "Suppression of HIV-1 infection by a small molecule inhibitor of the ATM kinase." Nat Cell Biol. 7(5): 493-500.

Laulier, C., Cheng, A. and Stark, J. M. (2011). "The relative efficiency of homology-directed repair has distinct effects on proper anaphase chromosome separation." Nucleic Acids Res. 39(14): 5935-44.

Le Tallec, B., Dutrillaux, B., Lachages, A. M., Millot, G. A., Brison, O. and Debatisse, M. (2011). "Molecular profiling of common fragile sites in human fibroblasts." Nat Struct Mol Biol. 18(12): 1421-3.

Leahy, J. J., Golding, B. T., Griffin, R. J., Hardcastle, I. R., Richardson, C., Rigoreau, L. and Smith, G. C. (2004). "Identification of a highly potent and selective DNA-dependent protein kinase (DNA-PK) inhibitor (NU7441) by screening of chromenone libraries." Bioorg Med Chem Lett. 14(24): 6083-7.

Letessier, A., Millot, G. A., Koundrioukoff, S., Lachages, A. M., Vogt, N., Hansen, R. S., Malfoy, B., Brison, O. and Debatisse, M. (2011). "Cell-type-specific replication initiation programs set fragility of the FRA3B fragile site." Nature. 470(7332): 120-3.

Levine, A. J. (2009). "The common mechanisms of transformation by the small DNA tumor viruses: The inactivation of tumor suppressor gene products: p53." Virology. 384(2): 285-93.

Levine, A. J. and Oren, M. (2009). "The first 30 years of p53: growing ever more complex." Nat Rev Cancer. 9(10): 749-58.

Li, J. J. and Kelly, T. J. (1984). "Simian virus 40 DNA replication in vitro." Proc Natl Acad Sci U S A. 81(22): 6973-7.

Li, J. J. and Kelly, T. J. (1985). "Simian virus 40 DNA replication in vitro: specificity of initiation and evidence for bidirectional replication." Mol Cell Biol. 5(6): 1238-46.

Li, S., Ting, N. S., Zheng, L., Chen, P. L., Ziv, Y., Shiloh, Y., Lee, E. Y. and Lee, W. H. (2000). "Functional link of BRCA1 and ataxia telangiectasia gene product in DNA damage response." Nature. 406(6792): 210-5.

Liao, H., Winkfein, R. J., Mack, G., Rattner, J. B. and Yen, T. J. (1995). "CENP-F is a protein of the nuclear matrix that assembles onto kinetochores at late G2 and is rapidly degraded after mitosis." J Cell Biol. 130(3): 507-18.

Liddington, R. C., Yan, Y., Moulai, J., Sahli, R., Benjamin, T. L. and Harrison, S. C. (1991). "Structure of simian virus 40 at 3.8-A resolution." Nature. 354(6351): 278-84.

Liu, P., Barkley, L. R., Day, T., Bi, X., Slater, D. M., Alexandrow, M. G., Nasheuer, H. P. and Vaziri, C. (2006). "The Chk1-mediated S-phase checkpoint targets initiation factor Cdc45 via a Cdc25A/Cdk2-independent mechanism." J Biol Chem. 281(41): 30631-44.

Liu, Q., Guntuku, S., Cui, X. S., Matsuoka, S., Cortez, D., Tamai, K., Luo, G., Carattini-Rivera, S., DeMayo, F., Bradley, A., Donehower, L. A. and Elledge, S. J. (2000). "Chk1 is an essential kinase that is regulated by Atr and required for the G(2)/M DNA damage checkpoint." Genes Dev. 14(12): 1448-59.

Lobrich, M., Shibata, A., Beucher, A., Fisher, A., Ensminger, M., Goodarzi, A. A., Barton, O. and Jeggo, P. A. (2010). "gammaH2AX foci analysis for monitoring DNA double-strand break repair: strengths, limitations and optimization." Cell Cycle. 9(4): 662-9.

Lopes, M., Cotta-Ramusino, C., Pellicioli, A., Liberi, G., Plevani, P., Muzi-Falconi, M., Newlon, C. S. and Foiani, M. (2001). "The DNA replication checkpoint response stabilizes stalled replication forks." Nature. 412(6846): 557-61.

Lucas, I., Germe, T., Chevrier-Miller, M. and Hyrien, O. (2001). "Topoisomerase II can unlink replicating DNA by precatenane removal." EMBO J. 20(22): 6509-19.

Lukas, J., Lukas, C. and Bartek, J. (2011). "More than just a focus: The chromatin response to DNA damage and its role in genome integrity maintenance." Nat Cell Biol. 13(10): 1161-9.

Lydeard, J. R., Lipkin-Moore, Z., Sheu, Y. J., Stillman, B., Burgers, P. M. and Haber, J. E. (2010). "Break-induced replication requires all essential DNA replication factors except those specific for pre-RC assembly." Genes Dev. 24(11): 1133-44.

Marteijn, J. A., Bekker-Jensen, S., Mailand, N., Lans, H., Schwertman, P., Gourdin, A. M., Dantuma, N. P., Lukas, J. and Vermeulen, W. (2009). "Nucleotide excision repair-induced H2A ubiquitination is dependent on MDC1 and RNF8 and reveals a universal DNA damage response." J Cell Biol. 186(6): 835-47.

Martin-Parras, L., Lucas, I., Martinez-Robles, M. L., Hernandez, P., Krimer, D. B., Hyrien, O. and Schvartzman, J. B. (1998). "Topological complexity of different populations of pBR322 as visualized by two-dimensional agarose gel electrophoresis." Nucleic Acids Res. 26(14): 3424-32.

Masai, H., Matsumoto, S., You, Z., Yoshizawa-Sugata, N. and Oda, M. (2010). "Eukaryotic chromosome DNA replication: where, when, and how?" Annu Rev Biochem. 79: 89-130.

Matos, J., Blanco, M. G., Maslen, S., Skehel, J. M. and West, S. C. (2011). "Regulatory control of the resolution of DNA recombination intermediates during meiosis and mitosis." Cell. 147(1): 158-72.

Matos, J., Blanco, M. G. and West, S. C. (2013). "Cell-cycle kinases coordinate the resolution of recombination intermediates with chromosome segregation." Cell Rep. 4(1): 76-86.

Matsuoka, S., Ballif, B. A., Smogorzewska, A., McDonald, E. R., 3rd, Hurov, K. E., Luo, J., Bakalarski, C. E., Zhao, Z., Solimini, N., Lerenthal, Y., Shiloh, Y., Gygi, S. P. and Elledge, S. J. (2007). "ATM and ATR substrate analysis reveals extensive protein networks responsive to DNA damage." Science. 316(5828): 1160-6.

McFadden, K. and Luftig, M. A. (2013). "Interplay between DNA tumor viruses and the host DNA damage response." Curr Top Microbiol Immunol. 371: 229-57.

McKinnon, P. J. (2012). "ATM and the molecular pathogenesis of ataxia telangiectasia." Annu Rev Pathol. 7: 303-21.

Mechali, M. (2010). "Eukaryotic DNA replication origins: many choices for appropriate answers." Nat Rev Mol Cell Biol. 11(10): 728-38.

Meek, K., Dang, V. and Lees-Miller, S. P. (2008). "DNA-PK: the means to justify the ends?" Adv Immunol. 99: 33-58.

Meek, K., Douglas, P., Cui, X., Ding, Q. and Lees-Miller, S. P. (2007). "trans Autophosphorylation at DNA-dependent protein kinase's two major autophosphorylation site clusters facilitates end processing but not end joining." Mol Cell Biol. 27(10): 3881-90.

Menear, K. A., Adcock, C., Boulter, R., Cockcroft, X. L., Copsey, L., Cranston, A., Dillon, K. J., Drzewiecki, J., Garman, S., Gomez, S., Javaid, H., Kerrigan, F., Knights, C., Lau, A., Loh, V. M., Jr., Matthews, I. T., Moore, S., O'Connor, M. J., Smith, G. C. and Martin, N. M. (2008). "4-[3-(4-cyclopropanecarbonylpiperazine-1-carbonyl)-4-fluorobenzyl]-2H-phthalazin- 1-one: a novel bioavailable inhibitor of poly(ADP-ribose) polymerase-1." J Med Chem. 51(20): 6581-91.

Moarefi, I. F., Small, D., Gilbert, I., Hopfner, M., Randall, S. K., Schneider, C., Russo, A. A., Ramsperger, U., Arthur, A. K., Stahl, H. and et al. (1993). "Mutation of the cyclin-dependent kinase phosphorylation site in simian virus 40 (SV40) large T antigen specifically blocks SV40 origin DNA unwinding." J Virol. 67(8): 4992-5002.

Moldovan, G. L. and D'Andrea, A. D. (2009). "How the fanconi anemia pathway guards the genome." Annu Rev Genet. 43: 223-49.

Moody, C. A. and Laimins, L. A. (2009). "Human papillomaviruses activate the ATM DNA damage pathway for viral genome amplification upon differentiation." PLoS Pathog. 5(10): e1000605.

Moody, C. A. and Laimins, L. A. (2010). "Human papillomavirus oncoproteins: pathways to transformation." Nat Rev Cancer. 10(8): 550-60.

Mordes, D. A., Glick, G. G., Zhao, R. and Cortez, D. (2008). "TopBP1 activates ATR through ATRIP and a PIKK regulatory domain." Genes Dev. 22(11): 1478-89.

Moynahan, M. E. and Jasin, M. (2010). "Mitotic homologous recombination maintains genomic stability and suppresses tumorigenesis." Nat Rev Mol Cell Biol. 11(3): 196-207.

Munoz-Galvan, S., Tous, C., Blanco, M. G., Schwartz, E. K., Ehmsen, K. T., West, S. C., Heyer, W. D. and Aguilera, A. (2012). "Distinct roles of Mus81, Yen1, Slx1-Slx4, and Rad1 nucleases in the repair of replication-born double-strand breaks by sister chromatid exchange." Mol Cell Biol. 32(9): 1592-603.

Murnane, J. P. and Painter, R. B. (1982). "Complementation of the defects of DNA synthesis in irradiated and unirradiated ataxia-telangiectasia cells." Proc Natl Acad Sci U S A. 79(6): 1960-3.

Nam, E. A. and Cortez, D. (2011). "ATR signalling: more than meeting at the fork." Biochem J. 436(3): 527-36.

Namiki, Y. and Zou, L. (2006). "ATRIP associates with replication protein A-coated ssDNA through multiple interactions." Proc Natl Acad Sci U S A. 103(3): 580-5.

Neal, J. A., Dang, V., Douglas, P., Wold, M. S., Lees-Miller, S. P. and Meek, K. (2011). "Inhibition of homologous recombination by DNA-dependent protein kinase requires kinase activity, is titratable, and is modulated by autophosphorylation." Mol Cell Biol. 31(8): 1719-33.

Neal, J. A. and Meek, K. (2011). "Choosing the right path: does DNA-PK help make the decision?" Mutat Res. 711(1-2): 73-86.

Neu, U., Stehle, T. and Atwood, W. J. (2009). "The Polyomaviridae: Contributions of virus structure to our understanding of virus receptors and infectious entry." Virology. 384(2): 389-99.

Nimonkar, A. V., Genschel, J., Kinoshita, E., Polaczek, P., Campbell, J. L., Wyman, C., Modrich, P. and Kowalczykowski, S. C. (2011). "BLM-DNA2-RPA-MRN and

EXO1-BLM-RPA-MRN constitute two DNA end resection machineries for human DNA break repair." Genes Dev. 25(4): 350-62.

Nitiss, J. L. (2009). "DNA topoisomerase II and its growing repertoire of biological functions." Nat Rev Cancer. 9(5): 327-37.

O'Driscoll, M., Ruiz-Perez, V. L., Woods, C. G., Jeggo, P. A. and Goodship, J. A. (2003). "A splicing mutation affecting expression of ataxia-telangiectasia and Rad3-related protein (ATR) results in Seckel syndrome." Nat Genet. 33(4): 497-501.

Okubo, E., Lehman, J. M. and Friedrich, T. D. (2003). "Negative regulation of mitotic promoting factor by the checkpoint kinase chk1 in simian virus 40 lytic infection." J Virol. 77(2): 1257-67.

Opresko, P. L., Sowd, G. and Wang, H. (2009). "The Werner syndrome helicase/exonuclease processes mobile D-loops through branch migration and degradation." PLoS One. 4(3): e4825.

Orba, Y., Suzuki, T., Makino, Y., Kubota, K., Tanaka, S., Kimura, T. and Sawa, H. (2010). "Large T antigen promotes JC virus replication in G2-arrested cells by inducing ATM- and ATR-mediated G2 checkpoint signaling." J Biol Chem. 285(2): 1544-54.

Otto, B. and Fanning, E. (1978). "DNA polymerase alpha is associated with replicating SV40 nucleoprotein complexes." Nucleic Acids Res. 5(5): 1715-28.

Painter, R. B. and Young, B. R. (1980). "Radiosensitivity in ataxia-telangiectasia: a new explanation." Proc Natl Acad Sci U S A. 77(12): 7315-7.

Petermann, E. and Helleday, T. (2010). "Pathways of mammalian replication fork restart." Nat Rev Mol Cell Biol. 11(10): 683-7.

Petermann, E., Orta, M. L., Issaeva, N., Schultz, N. and Helleday, T. (2010). "Hydroxyurea-stalled replication forks become progressively inactivated and require two different RAD51-mediated pathways for restart and repair." Mol Cell. 37(4): 492-502.

Pohlhaus, J. R. and Kreuzer, K. N. (2006). "Formation and processing of stalled replication forks--utility of two-dimensional agarose gels." Methods Enzymol. 409: 477-93.

Preiser, P. R., Wilson, R. J., Moore, P. W., McCready, S., Hajibagheri, M. A., Blight, K. J., Strath, M. and Williamson, D. H. (1996). "Recombination associated with replication of malarial mitochondrial DNA." EMBO J. 15(3): 684-93.

Psyrri, A. and DiMaio, D. (2008). "Human papillomavirus in cervical and head-and-neck cancer." Nat Clin Pract Oncol. 5(1): 24-31.

Pursell, Z. F. and Kunkel, T. A. (2008). "DNA polymerase epsilon: a polymerase of unusual size (and complexity)." Prog Nucleic Acid Res Mol Biol. 82: 101-45.

Radhakrishnan, S. K., Bebb, D. G. and Lees-Miller, S. (2013). "Targeting ataxia-telangiectasia mutated deficient malignancies with poly ADP ribose polymerase inhibitors." Transl Cancer Res. 2(3): 155-62.

Rass, E., Chandramouly, G., Zha, S., Alt, F. W. and Xie, A. (2013). "Ataxia telangiectasia mutated (ATM) is dispensable for endonuclease I-SceI-induced homologous recombination in mouse embryonic stem cells." J Biol Chem. 288(10): 7086-95.

Raveendranathan, M., Chattopadhyay, S., Bolon, Y. T., Haworth, J., Clarke, D. J. and Bielinsky, A. K. (2006). "Genome-wide replication profiles of S-phase checkpoint mutants reveal fragile sites in yeast." EMBO J. 25(15): 3627-39.

Ray Chaudhuri, A., Hashimoto, Y., Herrador, R., Neelsen, K. J., Fachinetti, D., Bermejo, R., Cocito, A., Costanzo, V. and Lopes, M. (2012). "Topoisomerase I poisoning results in PARP-mediated replication fork reversal." Nat Struct Mol Biol. 19(4): 417-23.

Reaper, P. M., Griffiths, M. R., Long, J. M., Charrier, J. D., Maccormick, S., Charlton, P. A., Golec, J. M. and Pollard, J. R. (2011). "Selective killing of ATM- or p53-deficient cancer cells through inhibition of ATR." Nat Chem Biol. 7(7): 428-30.

Riabinska, A., Daheim, M., Herter-Sprie, G. S., Winkler, J., Fritz, C., Hallek, M., Thomas, R. K., Kreuzer, K. A., Frenzel, L. P., Monfared, P., Martins-Boucas, J., Chen, S. and Reinhardt, H. C. (2013). "Therapeutic Targeting of a Robust Non-Oncogene Addiction to PRKDC in ATM-Defective Tumors." Sci Transl Med. 5(189): 189ra78.

Rigby, P. W. and Berg, P. (1978). "Does simian virus 40 DNA integrate into cellular DNA during productive infection?" J Virol. 28(2): 475-89.

Rohaly, G., Korf, K., Dehde, S. and Dornreiter, I. (2010). "Simian virus 40 activates ATR-Delta p53 signaling to override cell cycle and DNA replication control." J Virol. 84(20): 10727-47.

Rouleau, M., Patel, A., Hendzel, M. J., Kaufmann, S. H. and Poirier, G. G. (2010). "PARP inhibition: PARP1 and beyond." Nat Rev Cancer. 10(4): 293-301.

Rozenblatt-Rosen, O., Deo, R. C., Padi, M., Adelmant, G., Calderwood, M. A., Rolland, T., Grace, M., Dricot, A., Askenazi, M., Tavares, M., Pevzner, S. J., Abderazzaq, F., Byrdsong, D., Carvunis, A. R., Chen, A. A., Cheng, J., Correll, M., Duarte, M., Fan, C., Feltkamp, M. C., Ficarro, S. B., Franchi, R., Garg, B. K., Gulbahce, N., Hao, T., Holthaus, A. M., James, R., Korkhin, A., Litovchick, L., Mar, J. C., Pak, T. R., Rabello, S., Rubio, R., Shen, Y., Singh, S., Spangle, J. M., Tasan, M., Wanamaker, S., Webber, J. T., Roecklein-Canfield, J., Johannsen, E., Barabasi, A. L., Beroukhim, R., Kieff, E., Cusick, M. E., Hill, D. E., Munger, K., Marto, J. A., Quackenbush, J., Roth, F. P., DeCaprio, J. A. and Vidal, M. (2012). "Interpreting cancer genomes using systematic host network perturbations by tumour virus proteins." Nature. 487(7408): 491-5.

Ruthenburg, A. J., Li, H., Patel, D. J. and Allis, C. D. (2007). "Multivalent engagement of chromatin modifications by linked binding modules." Nat Rev Mol Cell Biol. 8(12): 983-94.

Sakakibara, N., Mitra, R. and McBride, A. A. (2011). "The papillomavirus E1 helicase activates a cellular DNA damage response in viral replication foci." J Virol. 85(17): 8981-95.

Sarkaria, J. N., Busby, E. C., Tibbetts, R. S., Roos, P., Taya, Y., Karnitz, L. M. and Abraham, R. T. (1999). "Inhibition of ATM and ATR kinase activities by the radiosensitizing agent, caffeine." Cancer Res. 59(17): 4375-82.

Sartori, A. A., Lukas, C., Coates, J., Mistrik, M., Fu, S., Bartek, J., Baer, R., Lukas, J. and Jackson, S. P. (2007). "Human CtIP promotes DNA end resection." Nature. 450(7169): 509-14.

Schlacher, K., Christ, N., Siaud, N., Egashira, A., Wu, H. and Jasin, M. (2011). "Double-strand break repair-independent role for BRCA2 in blocking stalled replication fork degradation by MRE11." Cell. 145(4): 529-42.

Schneider, C., Weisshart, K., Guarino, L. A., Dornreiter, I. and Fanning, E. (1994). "Species-specific functional interactions of DNA polymerase alpha-primase with

simian virus 40 (SV40) T antigen require SV40 origin DNA." Mol Cell Biol. 14(5): 3176-85.

Schneider, J. and Fanning, E. (1988). "Mutations in the phosphorylation sites of simian virus 40 (SV40) T antigen alter its origin DNA-binding specificity for sites I or II and affect SV40 DNA replication activity." J Virol. 62(5): 1598-605.

Schwarz, E., Freese, U. K., Gissmann, L., Mayer, W., Roggenbuck, B., Stremlau, A. and zur Hausen, H. (1985). "Structure and transcription of human papillomavirus sequences in cervical carcinoma cells." Nature. 314(6006): 111-4.

Shi, Y., Dodson, G. E., Shaikh, S., Rundell, K. and Tibbetts, R. S. (2005). "Ataxia-telangiectasia-mutated (ATM) is a T-antigen kinase that controls SV40 viral replication in vivo." J Biol Chem. 280(48): 40195-200.

Shibata, A., Conrad, S., Birraux, J., Geuting, V., Barton, O., Ismail, A., Kakarougkas, A., Meek, K., Taucher-Scholz, G., Lobrich, M. and Jeggo, P. A. (2011). "Factors determining DNA double-strand break repair pathway choice in G2 phase." EMBO J. 30(6): 1079-92.

Shiotani, B., Nguyen, H. D., Hakansson, P., Marechal, A., Tse, A., Tahara, H. and Zou, L. (2013). "Two Distinct Modes of ATR Activation Orchestrated by Rad17 and Nbs1." Cell Rep. 3(5): 1651-62.

Shuda, M., Feng, H., Kwun, H. J., Rosen, S. T., Gjoerup, O., Moore, P. S. and Chang, Y. (2008). "T antigen mutations are a human tumor-specific signature for Merkel cell polyomavirus." Proc Natl Acad Sci U S A. 105(42): 16272-7.

Singh, T. R., Ali, A. M., Busygina, V., Raynard, S., Fan, Q., Du, C. H., Andreassen, P. R., Sung, P. and Meetei, A. R. (2008). "BLAP18/RMI2, a novel OB-fold-containing protein, is an essential component of the Bloom helicase-double Holliday junction dissolvasome." Genes Dev. 22(20): 2856-68.

Sogo, J. M., Lopes, M. and Foiani, M. (2002). "Fork reversal and ssDNA accumulation at stalled replication forks owing to checkpoint defects." Science. 297(5581): 599-602.

Sowd, G., Li, N. and Fanning, E. (2013). "ATM and ATR Activities Maintain Replication Fork Integrity during SV40 Chromatin Replication." PLoS Pathog. 9(4): e1003283.

Sowd, G. A. and Fanning, E. (2012). "A Wolf in Sheep's Clothing: SV40 Co-opts Host Genome Maintenance Proteins to Replicate Viral DNA." PLoS Pathog. 8(11): e1002994.

Stehle, T., Gamblin, S. J., Yan, Y. and Harrison, S. C. (1996). "The structure of simian virus 40 refined at 3.1 A resolution." Structure. 4(2): 165-82.

Stiff, T., Reis, C., Alderton, G. K., Woodbine, L., O'Driscoll, M. and Jeggo, P. A. (2005). "Nbs1 is required for ATR-dependent phosphorylation events." EMBO J. 24(1): 199-208.

Stillman, B. W. and Gluzman, Y. (1985). "Replication and supercoiling of simian virus 40 DNA in cell extracts from human cells." Mol Cell Biol. 5(8): 2051-60.

Stracker, T. H. and Petrini, J. H. (2011). "The MRE11 complex: starting from the ends." Nat Rev Mol Cell Biol. 12(2): 90-103.

Stucki, M., Clapperton, J. A., Mohammad, D., Yaffe, M. B., Smerdon, S. J. and Jackson, S. P. (2005). "MDC1 directly binds phosphorylated histone H2AX to regulate cellular responses to DNA double-strand breaks." Cell. 123(7): 1213-26.

Su, R. T. and DePamphilis, M. L. (1976). "In vitro replication of simian virus 40 DNA in a nucleoprotein complex." Proc Natl Acad Sci U S A. 73(10): 3466-70.

Sundin, O. and Varshavsky, A. (1980). "Terminal stages of SV40 DNA replication proceed via multiply intertwined catenated dimers." Cell. 21(1): 103-14.

Sundin, O. and Varshavsky, A. (1981). "Arrest of segregation leads to accumulation of highly intertwined catenated dimers: dissection of the final stages of SV40 DNA replication." Cell. 25(3): 659-69.

Tang, Q., Bell, P., Tegtmeyer, P. and Maul, G. G. (2000). "Replication but not transcription of simian virus 40 DNA is dependent on nuclear domain 10." J Virol. 74(20): 9694-700.

Tapper, D. P., Anderson, S. and DePamphilis, M. L. (1979). "Maturation of replicating simian virus 40 DNA molecules in isolated nuclei by continued bidirectional replication to the normal termination region." Biochim Biophys Acta. 565(1): 84-97.

Tapper, D. P., Anderson, S. and DePamphilis, M. L. (1982). "Distribution of replicating simian virus 40 DNA in intact cells and its maturation in isolated nuclei." J Virol. 41(3): 877-92.

Tapper, D. P. and DePamphilis, M. L. (1978). "Discontinuous DNA replication: accumulation of Simian virus 40 DNA at specific stages in its replication." J Mol Biol. 120(3): 401-22.

Tapper, D. P. and DePamphilis, M. L. (1980). "Preferred DNA sites are involved in the arrest and initiation of DNA synthesis during replication of SV40 DNA." Cell. 22(1 Pt 1): 97-108.

Toledo, L. I., Murga, M. and Fernandez-Capetillo, O. (2011). "Targeting ATR and Chk1 kinases for cancer treatment: a new model for new (and old) drugs." Mol Oncol. 5(4): 368-73.

Toledo, L. I., Murga, M., Zur, R., Soria, R., Rodriguez, A., Martinez, S., Oyarzabal, J., Pastor, J., Bischoff, J. R. and Fernandez-Capetillo, O. (2011). "A cell-based screen identifies ATR inhibitors with synthetic lethal properties for cancer-associated mutations." Nat Struct Mol Biol. 18(6): 721-7.

Tomimatsu, N., Mukherjee, B. and Burma, S. (2009). "Distinct roles of ATR and DNA-PKcs in triggering DNA damage responses in ATM-deficient cells." EMBO Rep. 10(6): 629-35.

Uematsu, N., Weterings, E., Yano, K., Morotomi-Yano, K., Jakob, B., Taucher-Scholz, G., Mari, P. O., van Gent, D. C., Chen, B. P. and Chen, D. J. (2007). "Autophosphorylation of DNA-PKCS regulates its dynamics at DNA double-strand breaks." J Cell Biol. 177(2): 219-29.

Veuger, S. J., Curtin, N. J., Richardson, C. J., Smith, G. C. and Durkacz, B. W. (2003). "Radiosensitization and DNA repair inhibition by the combined use of novel inhibitors of DNA-dependent protein kinase and poly(ADP-ribose) polymerase-1." Cancer Res. 63(18): 6008-15.

Virshup, D. M., Russo, A. A. and Kelly, T. J. (1992). "Mechanism of activation of simian virus 40 DNA replication by protein phosphatase 2A." Mol Cell Biol. 12(11): 4883-95.

Waga, S., Bauer, G. and Stillman, B. (1994). "Reconstitution of complete SV40 DNA replication with purified replication factors." J Biol Chem. 269(14): 10923-34.

Waga, S. and Stillman, B. (1994). "Anatomy of a DNA replication fork revealed by reconstitution of SV40 DNA replication in vitro." Nature. 369(6477): 207-12.

Waga, S. and Stillman, B. (1998). "The DNA replication fork in eukaryotic cells." Annu Rev Biochem. 67: 721-51.

Wallace, N. A., Robinson, K., Howie, H. L. and Galloway, D. A. (2012). "HPV 5 and 8 E6 abrogate ATR activity resulting in increased persistence of UVB induced DNA damage." PLoS Pathog. 8(7): e1002807.

Wang, J., Gong, Z. and Chen, J. (2011). "MDC1 collaborates with TopBP1 in DNA replication checkpoint control." J Cell Biol. 193(2): 267-73.

Wang, Y., Zhou, X. Y., Wang, H., Huq, M. S. and Iliakis, G. (1999). "Roles of replication protein A and DNA-dependent protein kinase in the regulation of DNA replication following DNA damage." J Biol Chem. 274(31): 22060-4.

Wang, Z., Wang, F., Tang, T. and Guo, C. (2012). "The role of PARP1 in the DNA damage response and its application in tumor therapy." Front Med. 6(2): 156-64.

Wechsler, T., Newman, S. and West, S. C. (2011). "Aberrant chromosome morphology in human cells defective for Holliday junction resolution." Nature. 471(7340): 642-6.

Weisshart, K., Taneja, P., Jenne, A., Herbig, U., Simmons, D. T. and Fanning, E. (1999). "Two regions of simian virus 40 T antigen determine cooperativity of double-hexamer assembly on the viral origin of DNA replication and promote hexamer interactions during bidirectional origin DNA unwinding." J Virol. 73(3): 2201-11.

Weitzman, M. D., Lilley, C. E. and Chaurushiya, M. S. (2010). "Genomes in conflict: maintaining genome integrity during virus infection." Annu Rev Microbiol. 64: 61-81.

Weitzman, M. D., Lilley, C. E. and Chaurushiya, M. S. (2011). "Changing the ubiquitin landscape during viral manipulation of the DNA damage response." FEBS Lett. 585(18): 2897-906.

Weller, S. K. (2010). "Herpes simplex virus reorganizes the cellular DNA repair and protein quality control machinery." PLoS Pathog. 6(11): e1001105.

Weterings, E. and Chen, D. J. (2007). "DNA-dependent protein kinase in nonhomologous end joining: a lock with multiple keys?" J Cell Biol. 179(2): 183-6.

Woodman, C. B., Collins, S. I. and Young, L. S. (2007). "The natural history of cervical HPV infection: unresolved issues." Nat Rev Cancer. 7(1): 11-22.

Wright, J. A., Keegan, K. S., Herendeen, D. R., Bentley, N. J., Carr, A. M., Hoekstra, M. F. and Concannon, P. (1998). "Protein kinase mutants of human ATR increase sensitivity to UV and ionizing radiation and abrogate cell cycle checkpoint control." Proc Natl Acad Sci U S A. 95(13): 7445-50.

Wu, L. and Hickson, I. D. (2003). "The Bloom's syndrome helicase suppresses crossing over during homologous recombination." Nature. 426(6968): 870-4.

Xu, D., Guo, R., Sobeck, A., Bachrati, C. Z., Yang, J., Enomoto, T., Brown, G. W., Hoatlin, M. E., Hickson, I. D. and Wang, W. (2008). "RMI, a new OB-fold complex essential for Bloom syndrome protein to maintain genome stability." Genes Dev. 22(20): 2843-55.

Yajima, H., Lee, K. J. and Chen, B. P. (2006). "ATR-dependent phosphorylation of DNA-dependent protein kinase catalytic subunit in response to UV-induced replication stress." Mol Cell Biol. 26(20): 7520-8.

Yang, L., Wold, M. S., Li, J. J., Kelly, T. J. and Liu, L. F. (1987). "Roles of DNA topoisomerases in simian virus 40 DNA replication in vitro." Proc Natl Acad Sci U S A. 84(4): 950-4.

Yaniv, M. (2009). "Small DNA tumour viruses and their contributions to our understanding of transcription control." Virology. 384(2): 369-74.

Yardimci, H., Wang, X., Loveland, A. B., Tappin, I., Rudner, D. Z., Hurwitz, J., van Oijen, A. M. and Walter, J. C. "Bypass of a protein barrier by a replicative DNA helicase." Nature. 492(7428): 205-9.

Yin, J., Sobeck, A., Xu, C., Meetei, A. R., Hoatlin, M., Li, L. and Wang, W. (2005). "BLAP75, an essential component of Bloom's syndrome protein complexes that maintain genome integrity." EMBO J. 24(7): 1465-76.

You, Z., Bailis, J. M., Johnson, S. A., Dilworth, S. M. and Hunter, T. (2007). "Rapid activation of ATM on DNA flanking double-strand breaks." Nat Cell Biol. 9(11): 1311-8.

Yun, M. H. and Hiom, K. (2009). "CtIP-BRCA1 modulates the choice of DNA double-strand-break repair pathway throughout the cell cycle." Nature. 459(7245): 460-3.

Zhao, X., Madden-Fuentes, R. J., Lou, B. X., Pipas, J. M., Gerhardt, J., Rigell, C. J. and Fanning, E. (2008). "Ataxia telangiectasia-mutated damage-signaling kinase- and proteasome-dependent destruction of Mre11-Rad50-Nbs1 subunits in Simian virus 40-infected primate cells." J Virol. 82(11): 5316-28.

Zhou, B., Arnett, D. R., Yu, X., Brewster, A., Sowd, G. A., Xie, C. L., Vila, S., Gai, D., Fanning, E. and Chen, X. S. (2012). "Structural basis for the interaction of a hexameric replicative helicase with the regulatory subunit of human DNA polymerase alpha-primase." J Biol Chem. 287(32): 26854-66.

Zhu, X., Mancini, M. A., Chang, K. H., Liu, C. Y., Chen, C. F., Shan, B., Jones, D., Yang-Feng, T. L. and Lee, W. H. (1995). "Characterization of a novel 350-kilodalton nuclear phosphoprotein that is specifically involved in mitotic-phase progression." Mol Cell Biol. 15(9): 5017-29.

Ziv, Y., Bielopolski, D., Galanty, Y., Lukas, C., Taya, Y., Schultz, D. C., Lukas, J., Bekker-Jensen, S., Bartek, J. and Shiloh, Y. (2006). "Chromatin relaxation in response to DNA double-strand breaks is modulated by a novel ATM- and KAP-1 dependent pathway." Nat Cell Biol. 8(8): 870-6.

Zou, L., Cortez, D. and Elledge, S. J. (2002). "Regulation of ATR substrate selection by Rad17-dependent loading of Rad9 complexes onto chromatin." Genes Dev. 16(2): 198-208.

Zou, L. and Elledge, S. J. (2003). "Sensing DNA damage through ATRIP recognition of RPA-ssDNA complexes." Science. 300(5625): 1542-8.